REGULATION OF UREA CYCLE RELATED ENZYMES IN RESPONSE TO FREEZING IN THE WOOD FROG, *RANA SYLVATICA*

By

Stuart R. Green

B.Sc. (Hons.), 2015

A Thesis Submitted to the Faculty of Graduate Studies and Research in partial fulfillment of the requirements for the degree of

Master of Science

Department of Biology

Carleton University

Ottawa, Ontario, Canada

The undersigned hereby recommend to the Faculty of Graduate Studies and Research acceptance of this thesis

"REGULATION OF UREA CYCLE RELATED ENZYMES IN RESPONSE TO FREEZING IN THE WOOD FROG, *RANA SYLVATICA*"

submitted by

Stuart R. Green

In partial fulfillment of the requirements for the degree of Master of Science

_____

Chair, Department of Biology

_____

Thesis Supervisor

Carleton University

ABSTRACT

The North American wood frog, *Rana sylvatica*, is one of the few vertebrate species that is capable of surviving freezing. Prevention of intracellular ice formation and maintenance of osmotic balance is facilitated by the production of large concentrations of urea during freezing in the liver. The regulatory roles of three enzymes critical to production of urea; glutamate dehydrogenase (GDH), carbamoyl phosphate synthetase I (CPS1), and ornithine transcarbamylase (OTC), were investigated in the liver in response to freezing. Freeze-exposed GDH had heightened substrate affinity and higher maximal activity than the control. Freeze-exposed GDH also had decreased acetylation and ADP-ribosylation. CPS1 from frozen frogs was demonstrated to have a higher affinity for ammonium and decreased lysine glutarylation relative to the control. Freeze-exposed OTC demonstrated improved affinity for ornithine and increased serine phosphorylation. Taken together, the results suggest that urea production is sustained in the liver of the wood frog during freezing.

ACKNOWLEDGEMENTS

The number of people who have helped me to make it this far in my studies is too long to list so I apologize in advance to anyone whom I will inevitably forget to mention. First, I must thank my parents and my brothers for all of the love, support and guidance they have given me over the years, and for reminding me to have some balance in life outside of university.

I cannot thank Dr. Ken and Jan Storey enough for all of the effort they put into training me, both in lending me invaluable insight in conducting experiments and also teaching me how to properly write scientific literature. Their dedication to all the students in the lab is astounding. Then there are the numerous mentors from the Storey lab both past and present that have sacrificed their time in helping me to learn new techniques or procedures. I am particularly grateful to Neal and Ryan B. for teaching me the basics back in my undergrad and also Christie and Bryan for encouraging me to try new techniques.

Over the years at Carleton, I have had many friends who have helped me get through the hectic journey of going through undergrad and grad school. I would like to thank Tom and Trong for the many study sessions in undergrad and for helping to lead our softball team (even if the score didn't always turn out great). I would like to thank everyone whose desk is near mine for putting up with my questions and the sound of crunching sunflower seeds. Lastly, I must thank all of the professors and teachers who have taught me over the years through their seemingly tireless effort and commitment.

TABLE OF CONTENTS

LIST OF ABBREVIATIONS

α-KG	α ketoglutaric acid
ATP	adenosine triphosphate
ADP	adenosine diphosphate
BSA	bovine serum albumin
CM	carboxymethyl sepharose (cation exchange material)
CP	Carbamoyl phosphate
CPS1	carbamoyl phosphate synthetase 1 (ammonia consuming)
DEAE	diethylaminoethanol Sepharose (anion exchange material)
DSF	differential scanning fluorimetry
DTT	dithiothreitol
E_a	activation energy
ECL	enhanced chemiluminescence
EDTA	Ethylene diaminetetraacetic acid
EGTA	Ethylene glycol tetraacetic acid

GDH	glutamate dehydrogenase
GTP	guanosine triphosphate
I_{50}	half maximal inhibitory concentration
INP	Ice Nucleating Protein
K_A	half maximal activator concentration
KDa	kilodalton
K_M	Michaelis-Menten Constant (half maximal substrate concentration)
MS/MS	tandem mass spectrometry
NAD^+	oxidized nicotinamide adenine dinucleotide
NADH	reduced nicotinamide adenine dinucleotide
NAG	N-acetylglutamate
NAGS	N-acetylglutamate synthase
OTC	ornithine transcarbamylase
P_i	inorganic phosphate

PMSF	Phenyl methyl sulfonyl fluoride
PVDF	polyvinylidene difluoride
SDS	sodium dodecyl sulfate
SDS-PAGE	sodium dodecyl sulfate polyacrylamide gel electrophoresis
SEM	standard error of the mean
TBS	Tris buffered saline
TBST	Tris buffered saline Tween-20
TCA Cycle	Tricarboxylic acid cycle
Tris	Tris[hydroxymethyl]aminomethane
T_m	melting temperature
V_{max}	maximal enzyme velocity

LIST OF TABLES

LIST OF FIGURES

Chapter 1

General Introduction

Animal Overwintering Strategies

Freezing temperatures during the winter in temperate climates pose a challenge to many animals. Even endothermic animals such as mammals and birds are not immune to the effects of winter since their high metabolic rate and homeothermic nature requires great quantities of food that are often unavailable to them, and thus forces them to either reduce their metabolic rate in the case of hibernating species, or to find food elsewhere in the case of migrating species. This problem also exists for ectothermic animals such as the wood frog, but being unable to maintain an elevated body temperature, they must find ways to not only reduce their metabolic rate, but also survive freezing temperatures. This challenge is one of the main reasons why biodiversity of cold-blooded vertebrates is comparatively low relative to warm-blooded vertebrates in habitats with freezing winter conditions (Pincheira-Donoso et al., 2013). Those species that are capable of surviving such conditions either avoid freezing altogether or, in some cases tolerate the freezing of much of their body water.

Avoidance of freezing conditions often takes the form of animals hiding at the bottom of lakes that almost never freeze completely due to the insulation afforded by ice on the surface. This is common amongst many species of frogs such as the leopard frog (*Rana pipiens*), bullfrog (*Rana catesbeiana*), and also aquatic turtles (Tattersall and Ultsch, 2008). For species that winter on land, forming burrows can help reptiles prevent freezing by finding underground shelter from the cold (Ultsch, 2006). Certain species of insects can also avoid freezing completely despite deep subzero temperatures through the accumulation of cryoprotectants; for example, glycerol concentrations can increase up to

2030 μmol/g wet weight in the larvae of the goldenrod gall moth (*Epiblema scudderiana*) (Kelleher et al., 1987).

Other species have developed the amazing ability to endure the freezing of large percentage of their body water. Freeze tolerance in nature often involves survival of an accumulation of 50-65% of total body water as extracellular ice. Strong freeze tolerance among reptiles is limited mostly to several species of turtle hatchlings but also the European common lizard (*Zootoca vivipara,* AKA *Lacerta vivipara*) and adult box turtles (*Terrapene carolina*), although several other species can endure short periods of freezing at higher temperatures (Storey and Storey, 2017; Ultsch, 2006). Freezing in amphibians occurs among several species of frogs that overwinter under leaf litter on the forest floor including the wood frog (*Rana sylvatica*), the spring peeper (*Pseudacris crucifer*), the chorus frog (*Pseudacris triseriata*), the gray tree frog (*Hyla versicolor*) and the closely related Cope's gray tree frog (*Hyla chrysoscelis*) (Storey and Storey, 1992). Freeze tolerance in salamanders is not common and has not been thoroughly researched, although it has been reported to be well developed in the Siberian salamander (*Salamandrella keyserlingii*) and the Schrenck newt (*Salamandrella schrenckii*) with both species capable of surviving extreme temperatures down to -30°C (Berman and Meshcheryakova, 2012; Berman et al., 1984; Berman et al., 2010) .

Survival of freezing in animals typically involves several physiological strategies: dehydration of internal organs, the accumulation of metabolites in cells that prevent the formation of intracellular ice, and controlling the location and mechanisms of ice formation to avoid damage to tissues. Dehydration of tissues and organs helps to depress the freezing point of the cytosol and thereby prevent the formation of intracellular ice that

would cause irreversible damage to tissue. This strategy is seen in a wide variety of organisms and is notable as an important strategy to survive freezing conditions in organisms ranging from the Antarctic nematode *Panagrolaimus davidii* (Wharton et al., 2003) to the wood frog (Churchill and Storey, 1993). The accumulation of metabolites that reduce the freezing point, called cryoprotectants, is also seen in numerous organisms and works in conjunction with dehydration to prevent damage to cells and organs. The identity of the cryoprotectants varies between frog species but the main cryoprotectants are usually glycerol, as in the case of *H. versicolor* and *H. chrysoscelis* (Layne and Jones, 2001), and glucose in others like the wood frog or the *Pseudacris* species, as will be discussed in more detail later. Similar mechanisms exist in response to freezing in hatchlings of the freshwater turtle species *Chrysemys picta* that spend their first winter on land; increases in blood glucose (3 fold), glycerol (3 fold) and amino acids (2.25 fold) have been measured with about half of the increase in amino acids being taurine (Storey et al., 1988). Ice nucleating proteins, INPs, are present in several freeze tolerant animal species and these help to induce ice crystallization at higher subzero temperatures and minimize supercooling. This is known to play an important role in freeze-tolerant insects whose hemolymph freezes at relatively high temperatures due to the INPs. During INP induced ice nucleation, solutes are excluded from the forming ice crystals and thereby this increases the osmolality of the hemolymph and helps to dehydrate the cells (Duman, 2001). Antifreeze proteins (AFPs) are commonly found in freeze-tolerant species and, while seemingly a contradiction, it has recently been shown that a primary function of AFPs in freeze tolerant animals is actually to minimize ice recrystallization (Duman, 2001; Yu et al., 2010). Recrystallization occurs when smaller less energetically

favourable ice crystals gradually are replaced by fewer larger crystals which can cause structural damage to tissue (Martino and Zaritzky, 1989). AFPs help to prevent recrystallization by binding to ice crystals to prevent their growth thereby ensuring that they remain relatively small (Gupta and Deswal, 2014; Olijve et al., 2016). Together these strategies aid animals in survival of whole body freezing, allowing them to colonize northern habitats.

Freeze Tolerance in *Rana sylvatica*

The wood frog (*Rana sylvatica*) is found widely distributed across the boreal forests of North America ranging from northern Georgia to Alaska. In order to cope with harshness of freezing winters experienced in many regions of its range, the wood frog goes through remarkable physiological and biochemical transformations. The most notable among these is the ability to freeze solid during the winter. During bouts of freezing the wood frog ceases to have a heartbeat, does not breathe, and shows no brain activity but manages to revive itself during the springtime. Freeze tolerance is relatively rare among vertebrates and represents one of the most extreme hypometabolic conditions in nature (Storey and Storey, 1988). To survive these conditions, in addition to finding shelter under leaf litter (Storey and Storey, 1984), the wood frog reworks much of its internal biochemical processes to reduce metabolic expenditure during extended periods of time without feeding and produces metabolites which act as cryoprotectants to help prevent damage to the frog's cellular components and internal organs (Storey and Storey, 1986).

The most important metabolic cryoprotectant generated by the wood frog in order to survive bouts of freezing is glucose. Glucose-loaded wood frogs have been shown to

have considerably increased survival rates at low temperatures that would normally be fatal, thus supporting the role of glucose as a cryoprotectant (Costanzo et al., 1993). Glucose levels rise rapidly during the early hours of freezing and help to prevent the intracellular space from freezing and resist excessive water loss into extracellular ice masses. Inside the wood frog's liver glucose is rapidly generated through greatly increased glycogenolysis and is transported throughout the body to provide protection from freezing (Storey, 1987). During freezing the water in the animal's body cavity and other extracellular spaces freezes, resulting in approximately 65% of the total body water of the frog existing as extracellular ice (Storey and Storey, 1988). Glucose levels in frozen wood frogs may increase to levels far exceeding those seen under normal conditions, up to approximately 400 μmol/gram wet weight in the liver of frozen frog compared to normal concentrations of about 1-5 μmol/g (Storey and Storey, 1984).

Formation and management of extracellular ice is understood to be controlled through the action of ice nucleating agents (e.g. bacteria on skin or gut often trigger the freezing), or the production of INPs and AFPs or ice restructuring proteins in the wood frog. FR10 is a freeze responsive protein found in the wood frog that appears to be an AFP. The protein shows strong structural homology with the AFP of a marine fish and its heterologous expression in insect cells conferred improved freeze survivability (Biggar et al., 2013). Wood frog blood is also known to have ice nucleating activity, although the identity of the protein component responsible is not known (Storey et al., 1992; Wolanczyk et al., 1990).

While the importance of the glucose in the wood frog is well understood, more recently research has begun to shed light on the relevance of urea in wood frog survival

responses. Due to the highly permeable nature of their skin, amphibians are prone to loss of water and can utilize urea as an osmoprotectant in the event of dehydrating conditions or elevated salinity (Jørgensen, 1997). Maintenance of a high concentration of urea to aid in osmotic balance is not a solution unique to amphibians facing dehydration. High urea is also a well-documented part of normal elasmobranch (sharks and rays) physiology in order to counter the strong osmolality of their marine environment with urea concentrations in their tissues being kept up to 400 mM (Zeidel et al., 2005). During freezing, the wood frog can lose much of its body's water like many other amphibians and also accumulates large amounts of urea in its body. Critical internal organs such as the liver are particularly dehydrated and may lose around 25% of their water content to form ice in the body cavity (Costanzo et al., 1993). The urea is thought to play two overlapping roles in the survival of the wood frog as both a cryoprotectant and an osmoprotectant during freezing. One study has demonstrated that over a 48 hour freezing period livers of wood frogs from Ohio showed a 40% increase in urea levels compared to unfrozen livers from the same population whereas Alaskan wood frogs demonstrated an 80% increase in urea (Costanzo et al., 2013). This study suggests that the increase in urea is important for members of this species in freeze survival since the Alaskan populations are capable of surviving lower freeze-inducing temperatures. The study also demonstrated that the Alaskan population had a significantly higher activity of glutamate dehydrogenase (GDH) within skeletal muscle in the glutamate consuming direction during winter acclimation (Costanzo et al., 2013). This suggests one way in which the organism may increase its urea levels prior to and during freezing since release of ammonium ion from skeletal muscle could be metabolized in the liver in order to

generate higher levels of urea. Urea functions as a cryoprotectant on several levels in that it has been shown to significantly reduce damage to organs (heart and muscle) during freezing in the wood frog and improve viability of erythrocytes (Costanzo and Lee, 2005; Costanzo and Lee, 2008). The mechanism behind this cryoprotection is at least partly due to simple osmotic effects owing to the high intracellular concentration thereby helping to avoid excessive organ dehydration due to extracellular ice (Bakhach, 2009), however urea also has been shown to have a concentration independent cryoprotective effect between 40 and 80 mM for wood frog erythrocytes, implying another mechanism exists (Costanzo and Lee, 2005).

Nitrogen Metabolism

Nitrogen metabolism in many animals is focused on ameliorating the consequences of harmful or toxic byproducts of protein catabolism. Ammonia is thought to be toxic to neural cells because it leads to excessive glutamate levels that acts a neurotransmitter. This causes inappropriate NMDA receptor activation and downstream reduction of phosphorylation by protein kinase C that activates Na^+/K^+ATPase in the cell membrane and depletes cellular ATP levels (Felipo et al., 1994; Martinelle and Häggström, 1993). Aquatic animals simply release the dilute ammonia directly into their surroundings often via their gills (Regnault, 1987; Van Waarde, 1983). However, terrestrial animals cannot afford to waste valuable water supplies in association with excreting ammonia and therefore they convert ammonia into a less toxic metabolite that can be accumulated to higher concentrations before excretion. In most mammalian and amphibian species (Balinsky, 1981) this metabolite is urea while in avian and reptilian species it is usually uric acid (Jackson et al., 1986). Terrestrial invertebrates typically

produce uric acid as a waste. Some pulmonate gastropods, such as the land snail *Otala lactea*, produce urea (Linton and Campbell, 1962) whereas insects usually excrete uric acid through their respective excretory organs: the malpighian tubules (Wigglesworth, 1987). Because of the reduced toxicity of these metabolites, the animal can accumulate larger concentrations of these waste products before discarding them, thereby allowing them to conserve water. Production of uric acid occurs in all animals to a certain degree as it is a catabolic product of purine degradation and is excreted in human urine due to a lack of the uricase gene whose protein product allows for further oxidation of uric acid to allantoin in most mammals (Kratzer et al., 2014). Despite uric acid being energetically expensive to produce via purine metabolism, uric acid has a low solubility in water, allowing organisms to excrete it as a solid precipitate to reduce water loss greatly (Wright, 1995).

The urea cycle is a central feature of nitrogenous waste metabolism in many animals. The urea cycle is composed of a five-enzyme process and involves both cytosolic and mitochondrial compartments (Fig. 1.1.). Through this process ammonium is trapped by the ATP-dependent enzyme carbamoyl phosphate synthetase I (CPS1) to form carbamoyl phosphate (CP) which is then ligated to ornithine inside the mitochondria by ornithine transcarbamylase (OTC) to form the amino acid citrulline (Jackson et al., 1986). Citrulline is then transported outs of the mitochondria where it is linked to aspartate via the ATP-dependent reaction catalyzed by argininosuccinate synthetase (ASS). Argininosuccinate is then is acted upon by argininosuccinate lyase (ASL) to form fumarate (a TCA cycle intermediate) and arginine which can then be used to regenerate ornithine through the release of a urea molecule via arginase. This can then be taken up

by the mitochondria to participate in the cycle again. Glutamate dehydrogenase plays an important role in fueling the urea cycle by mediating the mitochondrial levels of free ammonium for CPS1 activity. Another variant of CPS, CPS2, exists in the cytosol and differs functionally from CPS1 by utilizing glutamine as an ammonia donor. CPS2 does not participate in the urea cycle due to its location in the cytosol since OTC is lacking there but instead plays an important early step in pyrimidine biosynthesis and is held within a single protein containing two other enzymatic activities: aspartate carbamoyltransferase and dihydroorotase (referred to as the CAD protein) (Ben-Sahra et al., 2013).

Regulation of the urea cycle is commonly thought to be focused at the level of CPS1. CPS1 is reliant upon the allosteric activator N-acetyl glutamate (NAG) which is produced by N-acetylglutamate synthase (NAGS) (Beliveau Carey et al., 1993). Due to the importance of NAG in activating CPS1, it is thought that the regulation of enzymes related to the supply of this activator such as glutaminase (produces glutamate from glutamine) and more directly NAGS may also be important in regulating urea cycle activity (Brosnan and Brosnan, 2002). However, evidence has shown that regulation of CPS1 occurs at more than just the level of allosteric activation and it has been demonstrated that fatty acylation at the active site with a palmitate group can inhibit its activity in rat liver (Corvi et al., 2001). Regulation of other enzymes in the urea cycle is not fully understood, although lysine acetylation has been associated with OTC control in humans (Yu et al., 2009).

Many of the intermediates of the urea cycle may also be utilized in competing pathways. For example, both arginine and ornithine can undergo decarboxylation

reactions to feed into polyamine synthesis via agmatine and putrescine, respectively (Regunathan and Reis, 2000). Arginine serves as a branch point in metabolism as it can contribute to the production of both nitrous oxide (NO), an important small signaling molecule and creatine (important for formation of the phosphagen phosphocreatine) (Morris, 2002). Due to the importance of many of the urea cycle intermediates in other pathways, it is likely that regulation of these pathways may have effects on the urea production capacity of the liver.

Protein Post-translation Modifications

Surviving extreme conditions such as freezing in the wood frog and other hypometabolic states requires tight control over metabolic pathways in order to both conserve energy and, in the case of the wood frog, maintain high levels of osmoprotectants and cryoprotectants. In order to cope with rapid freezing the metabolic pathways of the wood frog need to be able to respond in a quick and efficient manner to avoid damage due to freezing. While control over enzymatic activities may be accomplished by coarse controls such as translating additional copies of the enzyme or targeting existing enzyme for destruction by the proteasome, this requires large amounts of ATP energy that may not be available under hypometabolic conditions. Instead, fine controls on enzyme function such as by various types of post-translational modifications (PTMs) are an attractive option for modulating the activities of specific enzymes to tailor the metabolic processes to cope with environmental conditions (Lant and Storey, 2010). The addition or removal of a small PTM such as a phosphate group is ATP-inexpensive and can be reversed easily by an appropriate phosphatase or kinase should the environmental conditions alter again. Whereas reversible protein phosphorylation has

been shown to be a common motif in regulating enzymatic activity, many other PTMs also exist that may act independently or in conjunction with phosphorylation (Karve and Cheema, 2011). New PTMs are being discovered all the time, although whether or not specific enzymes exist which regulate their addition or removal and whether their presence/absence has regulatory effects on enzyme function is sometimes unknown (Khater and Mohanty, 2015). Studies from our own lab have demonstrated the versatility of PTMs in modulating enzymatic activity. One such study revealed that acetylation can regulate the activity of lactate dehydrogenase in the red eared slider, *Trachemys scripta elegans*, in response to anoxic conditions (Xiong and Storey, 2012).

PTMs are hypothesized to play a major role in helping to regulate the wood frogs metabolic pathways in response to freezing or other environmental insults, since these environmental changes can often occur rapidly, leading to the necessity of a quick metabolic response in order to survive freezing. One study has suggested that *R. sylvatica* can undergo a reduction in lactate dehydrogenase (LDH) acetylation in response to dehydration and can thereby confer altered kinetic parameters to the enzyme (Abboud and Storey, 2013). Regulation of glycogen metabolism has been a perennial focus of freeze tolerance research in the wood frog and has been shown to be strongly regulated by phosphorylation of glycogen synthase kinase 3 (GSK3) during bouts of freezing in multiple tissues with the active phosphorylated form being particularly abundant in frozen frogs (Dieni et al., 2012). With increased activity of GSK3, glycogen synthase is phosphorylated and inactivated thereby reducing the level of glycogen synthesis, and facilitating the catabolism of glycogen by glycogen phosphorylase to produce free glucose as a cryoprotectant (Russell and Storey, 1995). Protein kinase C (PKC), an

important regulatory enzyme involved in targeting other proteins for phosphorylation at serine and threonine residues, has been shown to be less phosphorylated (and less active) in liver and kidney tissue in the wood frog as a response to freeze exposure (Dieni and Storey, 2014). This implies that reversible protein phosphorylation may serve as a general regulatory response for making changes to enzymes/pathways during freezing. With these examples already present in the literature concerning the regulation of enzymes involved in glucose metabolism by PTMs in wood frog, the question remains as to whether enzymes related to other processes such as nitrogen metabolism are regulated through similar mechanisms.

Many enzymes involved in regulation of nitrogen metabolism (eg. GDH, CPSI, OTC) are found within the mitochondria where the local topography of PTMs may differ greatly from that of the cytosol. Regulation of mitochondrial proteins in animals by acetylation is commonly known to occur, although the mechanism by which proteins become acetylated is unclear as there is no clear candidate for acetyltransferase activity within the mitochondria themselves (Ghanta et al., 2013). While the mechanism behind the acetylation in currently unknown, up to 63% of mitochondrial proteins have been recorded to be affected by acetylation (Baeza et al., 2016) thereby making it likely that acetylation contributes greatly to regulation in mitochondrial processes. This is further supported by the presence of three members of the sirtuin family of deacetylases, sirtuins 3-5, that are present in mitochondria. Sirtuins play an important role in modulating the removal not only of acetyl groups but also of more exotic PTMs that are currently less well-understood such as malonyl, succinyl and glutaryl groups from lysine residues (Du et al., 2011; Tan et al., 2014).

Objectives and Hypotheses

Wood frog survival of freezing has multiple aspects including production of cryoprotectants, dehydration of internal organs and metabolic rate depression. Urea is an important metabolite produced in the liver of the wood frog that plays a role in maintaining osmotic balance during the dramatic physiological changes accompanying freezing and thawing. It is known that urea levels continue to rise in the liver during freezing despite overall decreases in metabolic rate. This thesis seeks to understand the regulation of the urea cycle by investigating key enzymes that are associated with its activity in liver through determining the functional parameters associated with these enzymes. In order to determine the regulation of the urea cycle during freezing three enzymes will be examined:

1. Chapter 2: Glutamate dehydrogenase. GDH, while not being a part of the urea cycle proper, contributes greatly to the urea cycle by providing ammonium for CPS1 since both are in localized within the mitochondria in the liver. Glutamate is an important product of protein catabolism and can be directed into the Krebs cycle by GDH through the following reaction:

   $$\text{L-glutamate} + NAD^+ + H_2O \leftrightarrow \alpha\text{-ketoglutarate} + NH_4^+ + NADH + H^+$$

2. Chapter 3: Ornithine transcarbamylase. OTC is the second urea cycle enzyme and is found in the mitochondria. OTC utilizes the important metabolite ornithine that is also used competitively for polyamine synthesis. OTC uses carbamoyl phosphate to generate citrulline in the following reaction:

   $$\text{L-ornithine} + \text{carbamoyl phosphate} \leftrightarrow \text{L-citrulline} + P_i$$

3. Chapter 4: Carbamoyl phosphate synthetase I. CPS1 is the first urea cycle enzyme and catalyzes the rate limiting step of the urea cycle in the mitochondria utilizing two molecules of ATP for every molecule of carbamoyl phosphate produced. This essentially irreversible step of the urea cycle requires the presence of the obligate activator N-acetylglutamate to catalyze the following reaction:

$$2\ ATP + NH_4^+ + bicarbonate \rightarrow 2\ ADP + carbamoyl\ phosphate + Pi$$

The enzymatic parameters of these enzymes are hypothesized to alter in response to freezing in the wood frog liver to help maintain urea production during freezing. In the context of the enzymes, this is likely to manifest as a lower K_M for substrates, a higher V_{max} and increased I_{50} of effective inhibitors of the enzymes.

Owing to the rapid nature of freezing and reduced metabolic nature during freezing it is also hypothesized that changes posttranslational modifications (PTMs) will be responsible for alterations in the enzyme function. These PTMs could take a variety of different forms including phosphorylation and acylation events but in any case, they are desirable for the frog since the use of PTMs is an energetically efficient way to alter the flux through a particular enzymatic reaction (Prabakaran et al., 2012).

These enzymes are also hypothesized to be optimized to function under conditions faced by the wood frog during freezing such as hyperglycemia, and low temperature. The freeze-exposed version of the enzyme is anticipated to be more active under these conditions than the control version in order to continue production urea needed to avoid freeze damage and mediate osmotic balance.

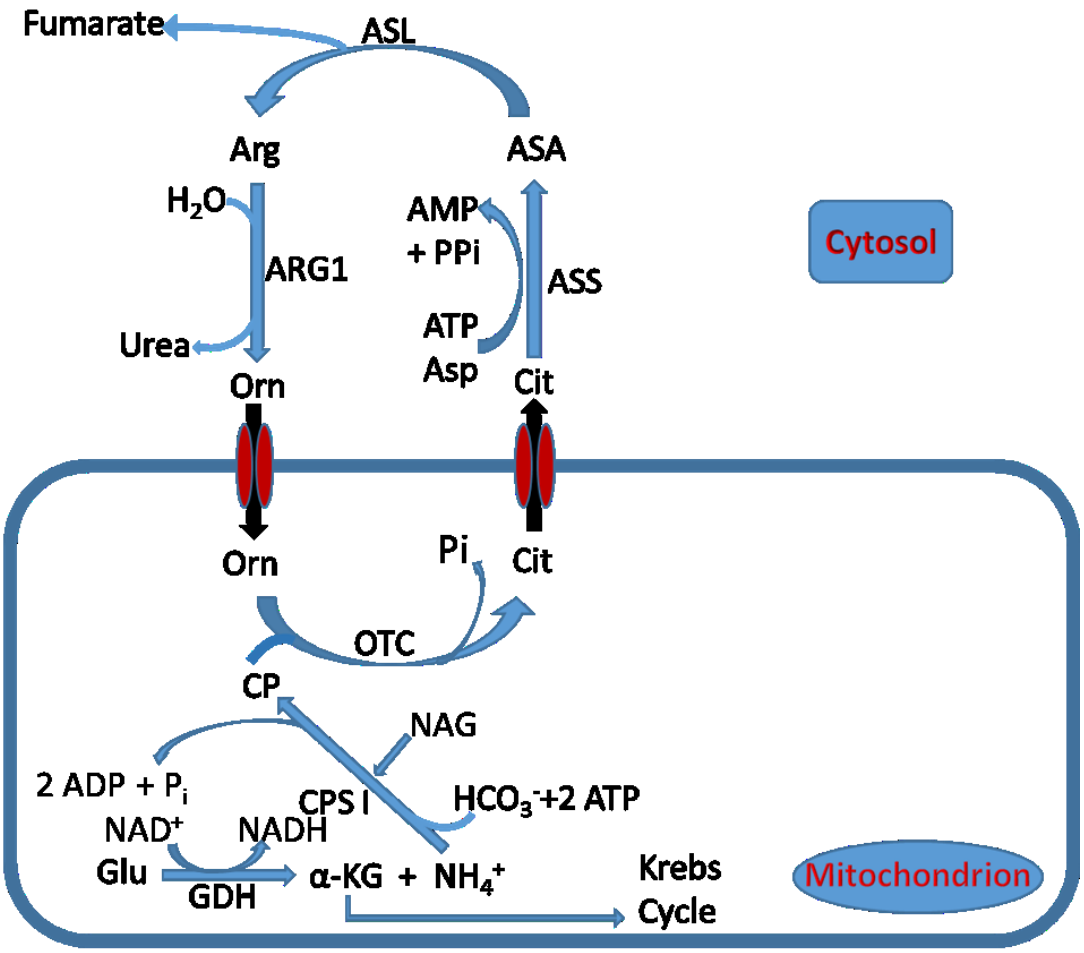

Fig. 1.1. The urea cycle is divided between cytosolic and mitochondrial compartments. Glutamate dehydrogenase (GDH) generates free ammonia through oxidation in the mitochondria as well as producing α-ketoglutarate (α-KG) that can enter the Krebs cycle. The ammonia generated can be condensed with carbonate ions through the consumption of 2 ATP in order to generate carbamoyl phosphate (CP) through the action of carbamoyl phosphate synthetase I (CPS1). Ornithine transcarbamylase (OTC) utilizes the CP to produce citrulline (Cit). This is then transported out of the mitochondria where it is combined with aspartate (Asp), and consuming ATP, generates argininosuccinate (ASA) via argininosuccinate synthase (ASS). Argininosuccinate lyase (ASL) cleaves argininosuccinate to produce fumarate and arginine (Arg). Arginase 1 (ARG1) then cleaves arginine to release free urea and regenerates ornithine that can then travel back into the mitochondria to complete the cycle.

Chapter 2

Regulation of glutamate dehydrogenase in the freeze tolerant wood frog

Introduction

During the winter months when air temperatures drop below freezing, the biochemical pathways in the wood frog undergo large-scale changes in order to alter the production of metabolites needed for survival of freezing. Understanding the function of glutamate dehydrogenase (GDH) in response to hypometabolic and freezing conditions is important since this enzyme is key to connecting carbohydrate and amino acid metabolism as well as producing mitochondrial ammonium ion, a substrate needed for the urea cycle enzyme CPS1. GDH carries out this role though oxidative deamination of glutamate (referred to as the forward reaction) through the use of either NAD^+ or $NADP^+$ to generate α-ketoglutaric acid (α-KG) accompanied by the release of ammonium ion. GDH can also catalyze the reverse reaction to incorporate ammonium ions into the synthesis of glutamate. However, this is not commonly seen under most physiological conditions since the concentration of ammonium ion needed to cause a substantial reaction rate in this direction could result in cellular toxicity due to the high K_M NH_4^+ (Li et al., 2009). Certain groups of hepatocytes in the mammalian liver are known to produce glutamate in this way for use in the formation of glutamine via the transamination reaction (Spanaki and Plaitakis, 2012). Production of α-KG from glutamate can, in turn, be used to generate cellular energy since α-KG is an intermediate in the TCA cycle and can be oxidized. Alternatively, the addition of substrates for the TCA cycle can be used to feed into gluconeogenesis in the liver in order to generate glucose (Brosnan, 2000).

Prior to experiencing freezing temperatures in the winter, the wood frog ceases to eat in early autumn and suppresses many metabolically demanding processes such as protein synthesis. At this point, wood frogs may begin to engage in proteolysis of skeletal

muscle, liberating glutamate and other amino acids that results in an increase in the amount of nitrogenous waste being produced and the flow of materials into the TCA cycle via GDH (Costanzo et al., 2015). The concentration of ammonium in wood frog livers also increases during freezing by almost three-fold with a considerable decrease in the concentration of glutamate, suggesting that GDH remains active during freezing (Storey and Storey, 1986). While GDH is important in regulating influx of materials through the citric acid cycle, the production of ammonium ions via the forward GDH reaction can lead to cellular toxicity (Katunuma et al., 1966). To cope with this, many terrestrial animals sequester excess ammonium by incorporating it into urea via the urea cycle which spans both mitochondrial and cytosolic spaces (Morris, 2002).

GDH is a homohexamer composed of subunits that have a molecular weight of approximately 56 kDa (Smith et al., 2002). GDH has allosteric sites which help to regulate its activity in response to GTP/ATP and GDP/ADP concentrations (Fang et al., 2002). Because high concentrations of GTP and ATP are indications of an abundance of cellular energy, these molecules act as potent inhibitors of GDH activity to reduce flux of α-KG into the TCA cycle (Li et al., 2009). Conversely ADP has been shown to be an allosteric activator of GDH due to its role in signaling low cellular energy (Banerjee et al., 2003). Expression of GDH can be found in many organs of the body, but the liver expresses large quantities of the enzyme and due to its role in urea metabolism (Morris, 2002), it was of particular interest in studying GDH regulation. A previous study from our lab showed that GDH is regulated in a mammalian hibernator, the Richardson's ground squirrel (*Spermophilus richardsonii*), to cope with hypometabolic conditions placed on the animal. The study showed that a reduction in K_M for substrates in both

directions of the reaction were present concurrently with a reduction in GDH phosphorylation in the hibernating animal suggesting that GDH is more active during hibernation (Bell and Storey, 2010). Wood frog GDH has also been explored in relation to differences between geographically distinct populations. The results of the study demonstrated that an Alaskan population had a significantly higher activity of GDH within skeletal muscle in the glutamate consuming direction compared to GDH from an Ohio population of wood frogs during winter acclimation. This suggested that catabolism of muscle tissue may be of increasing importance in more northern populations in preparation for winter to increase ammonium ion available for urea production in the liver (Costanzo et al., 2013).

Due to the importance of urea as both a cryoprotectant and an osmoprotectant to reduce freezing and/or dehydration stress on cells (Costanzo and Lee, 2005), it was hypothesized that GDH is regulated in wood frog tissues in order to favour production of urea to benefit freezing survival. The research in this chapter investigates the regulation of GDH in wood frog liver to identify the molecular mechanism that can promote this GDH function.

Materials and Methods

Animals and Chemicals

The chemicals used to perform the experiments described here were purchased from BioShop (Burlington, ON), or from Sigma Chemical Company (St. Louis, MO) unless otherwise stated. Water used in all experiments was distilled water filtered with a Milli-Q (Millipore Corporation) water purifier.

Male wood frogs, *Rana sylvatica*, were collected from spring breeding ponds in the Ottawa area. Animals were first washed in a tetracycline bath and then held for two weeks at 5ºC in moist containers with sphagnum moss to help simulate the natural environment. The control group was subjected to these conditions until they were euthanized by pithing. For freezing exposure, groups of frogs were placed inside containers lined with damp paper toweling and cooled in an incubator set to -3ºC to induce freezing. Ice formation on the paper toweling triggered nucleation of frog body fluids and then and then frogs were left at -3 °C for 24 hours prior to euthanasia by pithing. The animals were dissected quickly and their tissues of interest, including liver, were frozen in liquid nitrogen and then transferred to -72ºC for storage until use. The treatment of the animals was approved by the Carleton University Animal Care Committee (protocol 13683) under the guidelines set out by the Canadian Council on Animal Care.

Enzyme Purification

Liver samples were quickly weighed (usually 0.15-0.2g) and homogenized in a 1:9 w:v ratio with homogenate buffer A (50 mM MES buffer, 2 mM EDTA, 2 mM EGTA, 25 mM β-GP, 10 mM β-mercaptoethanol, 10% glycerol v:v, pH 6.2) with several crystals of PMSF serine protease inhibitor. Samples were kept cool on ice while being homogenized in order to prevent excessive heating and loss of enzymatic activity. The samples were then centrifuged in an Eppendorf 5810R tabletop centrifuge cooled to 4ºC at 13,500 x g for 30 minutes. The supernatant was carefully removed and the volume was measured. The pellet was discarded.

A CM Sepharose cation exchange chromatography column was prepared and equilibrated with 15 mL of buffer A at pH 6.2. The crude enzyme sample was then loaded onto the column and washed using 20 mL of buffer A to remove any unbound protein. GDH was eluted from the column using a pH gradient ranging from a pH of 6.2 to a pH of 8.0. The gradient was created by using 20 mL of buffer A pH 6.2 and 20mL of buffer B (same components as buffer A but with 50 mM Tris instead of MES) at pH 8.0. GDH activity was measured in the glutamate-consuming direction and the top 8 fractions containing GDH activity were pooled and saved for the next step of the purification.

A GTP-agarose affinity column (Sigma chemical company) was prepared using 4.5 mL of the material that was then equilibrated by running in 15 mL of homogenate buffer B at pH 7.5 through the column. The sample was then loaded and allowed to run through after which 15 mL of additional buffer B at pH 7.5 was run through the column to remove any unbound protein. GDH was eluted from the GTP-agarose column using a 30 mL linear gradient of 0-2 M KCl prepared in buffer B at the same pH. The top 6 fractions containing GDH activity were pooled and were determined to be pure. Samples from each step in the purification were run on an SDS-PAGE gel (sodium dodecyl sulfate – polyacrylamide gel electrophoresis) to ensure the purity of the sample. The gels were stained using a silver staining protocol (Gromova and Celis, 2006). Gels were first immersed in fixing solution (50% methanol, 12% acetic acid, 0.05% formalin) for 2 hours to ensure protein bands did not diffuse through the gel. Gels were washed 3 times 7 min each using 20% methanol to ensure acid was removed from the gel. Gels were then sensitized to the silver stain for 2 min using a 0.02% w/v sodium thiosulfate solution. Sensitizing solution was disposed and the gels were rinsed twice for a minute each time

with water. Silver stain (0.6% w/v silver nitrate, 0.076% formalin) was applied to the gel for 20 minutes and then disposed. Gels were washed with water 30 s and developing solution (6% w/v sodium carbonate, 0.04% w/v sodium thiosulfate, 0.05% formalin) was added to the gel until good protein bands became distinctly visible on the gel. The reaction was then ended by adding 12% acetic acid solution.

Enzymatic Assays and Determination of Kinetic Parameters

Enzymatic reactions in the forward direction, arbitrarily defined as the glutamate oxidizing direction, were performed by using a 50 mM Tris buffer at pH 8.0 in the presence of 4 mM NAD^+ and 40 mM glutamate. These conditions were determined to be sufficient to elicit maximal velocity of the enzymatic reaction in this direction. The absorbance of individual wells was read every 21 seconds for 40 times at 340 nm using a Thermo Scientific Multiskan Spectrum microplate reader to determine the activity of GDH since the NADH produced by this reaction absorbs strongly at this wavelength. The reverse reaction, the α-KG reducing direction, was carried out in a 50 mM HEPES buffer at pH 7.2. Enzymatic substrates were prepared in the buffer and then pH adjusted to ensure they remained at pH 7.2. Standard assay conditions used 0.2 mM NADH, 0.8 mM α-KG, and 240 mM NH_4^+. Assays were performed at 22ºC unless otherwise stated.

K_M values for the different substrates were determined by varying the substrate concentration and holding the cosubstrate concentration constant at optimal levels and measuring the relative activity. Using an enzyme kinetic analysis program, Kinetics v.3.5.1 (Brooks, 1992), the K_M values for each substrate were determined. The I_{50} of GTP was determined by increasing concentrations of the inhibitor under optimal

substrate concentrations; stock GTP was prepared as a 1:2 molar mixture of GTP: $MgCl_2$. Determination of K_A values for ADP was performed using optimal substrate concentrations and varying ADP concentrations. Relative ratios between the unactivated GDH and GDH activated by the presence of 1 mM ADP were also determined at optimal substrate concentrations. V_{max} was determined by measuring the activity of the enzyme at optimal substrate concentrations and are expressed per mg purified protein.

Protein concentration was determined in the enzyme samples by using the Bio-Rad protein assay reagent. Bovine serum albumin (BSA) was used as a protein standard and sample absorbances were read at 595 nm using a BioTek microplate reader.

Low Temperature Enzyme Kinetics and Arrhenius Plots

In order to analyze the kinetic parameters of GDH in the forward and reverse direction at 5°C, the spectrophotometer was cooled inside a Precision 815 low temperature incubator (Thermo Scientific) set at 5°C. Microplates were also prechilled to 5°C using an Echotherm heating/cooling plate (Torrey Pines Scientific, USA) before assay. Prior to adding purified GDH to initiate the reaction the temperature of a blank well was measured using a thermistor to ensure that the temperature was within 2°C of the target temperature and this was also repeated immediately after the assay.

Arrhenius plots were constructed by measuring maximal GDH velocity in the forward direction at 4 different temperatures from 5°C to 37°C. Temperatures lower than room temperature were obtained using the method described above, while the internal heating block in the spectrophotometer was used to heat the plate to 37°C. As before, the temperature of wells was confirmed both before and after the assay.

Western Blots for Post-Translational Modifications

Determination of the relative levels of GDH PTMs was performed using a western blotting method on a partially purified sample obtained by using enzyme from the first CM chromatography step, as described earlier. Samples were prepared for SDS-PAGE by mixing them 1:1 v/v in SDS-PAGE loading buffer (100 mM Tris, 4% w/v SDS, 20% v/v glycerol, 0.2% bromophenol blue, 10% v/v β-mercaptoethanol, pH 6.8) and boiling for 5 minutes to ensure denaturation of proteins. The samples were stored at -20°C until use. Samples were electrophoresed on a 10% polyacrylamide gel (with a 5% stacking gel) in running buffer (25 mM Tris-base, 250 mM glycine. 0.1% w/v SDS, pH 8.0-8.3) at 180 V for 45 minutes to separate the protein bands by molecular weight. The proteins in the gels were then transferred to PVDF membranes at 300 mA for 90 minutes while being immersed in transfer buffer (20% v/v methanol, 200 mM glycine, 25 mM Tris-base). Following transfer the blots were washed in TBST (20 mM Tris base, 140 mM NaCl, 0.05% Tween-20, pH 7.6). Membranes were probed with primary antibodies specific to PTMs of interest overnight on a rocker in a refrigerator. All antibodies used were obtained from rabbits except the antibody specific to phosphorylated-tyrosine residues that was from mouse. The antibodies used in the experiments were diluted 1:1000 in TBST and are listed as follows:

1. Anti-phosphorylated tyrosine: Invitrogen # 13-6600
2. Anti-phosphorylated serine: Invitrogen # 61-8100
3. Anti-phosphorylated threonine: Invitrogen # 71-8200
4. Anti-methylated lysine: StressMarq Biosciences Inc. # SPC-158F
5. Anti-mono and dimethylated arginine: CovaLab # mab0002

6. Anti-nitrosylated cysteine: abcam # ab50185
7. Anti-pan acetylated: Santa Cruz Biotechnology # SC-8663

In addition to these antibodies, an ADP-ribose binding reagent conjugated to the Fc portion of rabbit IgG was used to probe the proteins for mono- and poly-ADP ribosylation in the same manner as the antibodies diluted 1:1000 in TBST (EMD Millipore, MABE1016).

Following incubation with the primary antibody the membranes were washed for 3 x 5 min in TBST to remove any non-specific bound antibody. The appropriate horseradish peroxidase conjugated secondary antibody (anti-rabbit IgG or anti-mouse IgG) was then applied in a dilution of 1:2000 v:v and incubated for at least 1 hour. After this, the secondary antibody was removed and the membrane was washed again for 3 x 5 min. Then an enhanced chemiluminescence (ECL) protocol was used to determine the signal strength of the PTM in question and the blots were imaged using a ChemiGenius Bioimaging System (Syngene, Frederick, MD, USA). ECL protocol consisted of mixing equal volumes of a luminol solution (2.5 mM luminol,0.4 mM p-coumaric acid, 100 mM Tris pH 8.8) with hydrogen peroxide (0.0186% H_2O_2, 100 mM Tris pH 8.8) and distributing evenly on the surface of the membrane. The raw values were then standardized to the amount of protein present in the GDH bands after staining the membrane with Coomassie brilliant blue stain (0.25% w/v Coomassie Brilliant Blue R in 50% v/v methanol, 7.5% v/v acetic acid) and quantifying Relative signal intensities of the Coomassie bands using GeneTools software (v3.00.02).

Differential Scanning Fluorimetry

Differential scanning fluorimetry (DSF) is a fluorescent dye-based technique that is used to measure the melting point of a protein that can be performed in a PCR machine (Biggar et al., 2012; Niesen et al., 2007). This technique is based upon a fluorescent dye (SYPRO orange) that is strongly quenched in an aqueous environment but can have its fluorescent properties restored upon adsorption to a hydrophobic entity. In this case, the fluorescent properties can be amplified in the presence of the hydrophobic amino acid residues that become exposed during thermal denaturation of a protein. Purified GDH (concentration of 0.04 mg/mL) in DSF buffer (100 mM potassium phosphate buffer, pH 7.0, 150 mM NaCl) and 40x concentrated SYPRO orange reagent were mixed in the wells of a thin-walled PCR plate and brought to a final volume of 20 µL with DSF buffer and then a transparent adhesive film was used to cover the plate. The plate was placed in a Bio-Rad iQ5 PCR machine set to increase temperature by 1°C every 30 seconds from 15°C to 93°C. Fluorescence intensity (excitation wavelength of 485 nm, emission wavelength of 575 nm) of SYPRO orange was measured at every 1°C increment. Due to the high concentrations of urea that can be experienced in liver cells during freezing in the wood frog, the effects of urea were also studied on the thermal stability of GDH. This effect of urea was assessed by addition of 100 mM urea (prepared in the DSF buffer) to the wells in the PCR plates. The fluorescence increase was modelled using a Boltzmann distribution curve (using OriginPro 8.5), with the protein melting temperature (T_m) determined as the temperature that resulted in half-maximal fluorescence.

Statistical Analysis

The K_M values for substrates of purified liver GDH were calculated using a nonlinear least squares regression computer program, Kinetics 3.5.1 (Brooks, 1992).

Enzyme activity was determined using a Microplate Analysis Program (Brooks, 1994). To assess statistical significance between the control and freeze-exposed parameters, the Student's t-test was used and differences were considered significant when $p < 0.05$. As needed, graphing used RBioplot statistical software employing one way ANOVAs and Tukey's post hoc test to assess statistical differences (Zhang and Storey, 2016).

Results

Enzyme Purification

GDH from wood frog liver was purified to homogeneity in a two-step chromatographic process. The first step, elution of GDH from CM using a pH gradient from 6.3 to 8.0, was effective at removing many of the impurities and resulted in a 4.7 fold purification with 62% activity retained. The second column step, binding the GDH to GTP agarose and eluting using a 0-2 M KCl gradient, was effective at removing the remaining impurities resulting in a fold purification for the step of about 10 and approximately 50% yield of enzymatic activity. Altogether, the full procedure yielded 31% of the original enzymatic activity and a 47-fold purification with a final specific activity for GDH of 3320 mU/mg (Table 2.1). Using SDS-PAGE followed by staining with silver demonstrated that the GDH was purified to homogeneity. A standard commercially obtained bovine liver GDH (Sigma Aldrich) was run alongside the wood frog GDH samples to act as a molecular weight standard. Both the control and frozen wood frog liver GDH were found to be around the same molecular weight as bovine hepatic GDH and wood frog GDH was calculated to be 58 kDa based on electrophoretic mobility compared to the protein standards loaded (expected to be 56 kDa, see Fig. 2.1).

Enzyme Kinetics

Enzymatic parameters were measured in both the forward and reverse direction of the enzymatic reaction using purified GDH from control and freeze-exposed frogs. The enzymes differed in multiple kinetic parameters (Table 2.2). At 22ºC under standard assay conditions, the K_M for glutamate of the freeze-exposed enzyme was significantly lower than the control, 1.24 mM compared to 2.1 mM, respectively. This trend also occurred for the K_M of NAD^+ with the frozen parameter being 0.84 mM compared to the control value of 1.39 mM. In addition to an increase in affinity being associated with the frozen state for the substrates in the forward direction of the reaction, the V_{max} value for frozen GDH was significantly greater than the control at 3320 mU/mg compared to 2390 mU/mg in the control. A 1:2 molar ratio of GTP to Mg^{2+} was shown to be very effective at inhibiting both the control and freeze-exposed enzyme in the forward direction. The GTP I_{50} for the freeze-exposed GDH was higher at 0.44 μM GTP versus 0.122 μM in the control (Table 2.2).

The α-KG consuming direction of the reaction also showed differences in kinetic parameters between the control and stress conditions with the affinity for ammonium ion being lower in the control (K_M 35 mM) compared to the freeze-exposed GDH (K_M 11 mM). Enzyme affinity for the control and frozen enzyme for α-KG was also significantly different with the control showing a lower affinity for the substrate (0.33 mM) than the freeze-exposed (0.179 mM).

ADP is widely known to be an activator of GDH activity. The K_A, the concentration of activator that causes a half-maximal increase in enzymatic activity, was not significantly different between the control and frozen GDH in either the forward or

reverse direction of the GDH reaction, where it was determined to be approximately 30 μM in all cases (Table 2.2). The concentration of activator that causes a half-maximal increase in the activity of an enzyme is not the only factor that influences its potency as an activator however, and the ratio of the maximal velocity with allosteric activator saturation relative to the activity without the activator is also important. In the forward direction of the reaction, the addition of ADP had approximately the same effect on the control and frozen GDH activity (Table 2.2). The relative increase in activity upon the addition of 1 mM ADP was more noticeable in the forward direction of the reaction with the activity being approximately doubled in the presence of ADP. The reverse direction demonstrated a lower effect of ADP activation with the relative increase in GDH activity in the presence of 1 mM ADP being 1.33 fold for control GDH and 1.56 fold for frozen GDH.

The effects of ADP on GDH affinity for its substrates was also investigated. The results showed that addition of 1 mM ADP to the forward direction significantly increased the glutamate K_M for both control and frozen GDH, retaining the approximate relative difference between the control and frozen in the absence of ADP (Fig. 2.2). Interestingly the K_M for NAD^+ did not change with the addition of ADP to the control enzyme but it greatly increased the affinity of frozen GDH for NAD^+. In the reverse direction, it was noted that ADP had a similar effect upon the α-KG K_M compared to the glutamate K_M in that it lowered the affinity for substrate (ie. K_M rose) whereas ADP had no significant effect on the NH_4^+ K_M of frozen GDH, although it did slightly lower the NH_4^+ K_M of the control counterpart but control GDH still had a lower affinity for the substrate than the frozen enzyme.

The effects of urea and glucose on the activity and affinity of GDH for its substrates were also investigated. Both forms of GDH appeared to have lower K_M values for glutamate in the presence of 100 mM urea although the difference for the frozen K_M values was not significant. Interestingly, the K_M for glutamate decreased in the presence of urea in both forms of GDH while the NAD^+ K_M increased greatly for the frozen enzyme and no significant change was noted for the control (Fig. 2.2). In the reverse direction, urea had no effect on the K_M of NH_4^+ for the frozen, though it decreased it slightly for the control. Urea had no effect on the K_M of α-KG in either the control or the freeze-exposed GDH. In the forward direction of the reaction, urea had a slightly lower I_{50} for the frozen (0.54 M) compared to control (0.67 M) (Table 2.2). Glucose greatly lowered the K_M of the control GDH for glutamate while the freeze-exposed enzyme remained approximately the same. The addition of glucose did not appear to have any effect on the NAD^+ K_M for either the control or freeze-exposed. The presence of 400 mM glucose in the reverse direction of the reaction resulted in a substantial increase in the K_M for NH_4^+ in the frozen GDH, with a slight decrease in the K_M for the control value. Glucose did not result in a significant changes in the K_M for α-KG in the control or frozen form of GDH.

All the aforementioned assays were performed at room temperature (~22°C) which is different from the conditions that a wood frog would face during the winter. Hence, assays at 5°C were also performed to examine substrate affinities at a lowered temperature (Table 2.2). In the forward direction, there was no significant difference in the affinities for glutamate at 5°C for control or frozen GDH. However, the NAD^+ K_M decreased at the lower temperature to 0.68 mM ± 0.01 for control GDH and 0.66 ± 0.07

for frozen GDH. While no differences were seen in the substrate affinities at 5°C, in the forward direction, the maximal enzyme activity was significantly higher in the frozen than in the control (1580 ± 10 versus 1170 ± 20 mU/mg respectively) with both control and frozen GDH activities approximately halved from the respective 22°C values. In the reverse direction the K_M for ammonium ion did not change significantly between the two temperatures, with K_M NH_4^+ being lower for frozen GDH than for control (p=0.0509) similar to what was also seen at 22°C. The K_M for α-KG at 5°C was significantly lower for the frozen than for the control (0.27 ± 0.02 versus 0.36 ± 0.02 mM). The V_{max} in the reverse direction was significantly higher at 22°C for the freeze-exposed enzyme compared to the control, however this trend was not seen at 5°C since the activity fell more in the frozen from 22°C than the control.

Western Blots to Assess Posttranslational Modifications

Western blots specific for various posttranslational modifications demonstrated that both control and freeze-exposed wood frog liver GDH had comparable levels of most PTMs (ie. phosphorylation at serine, threonine or tyrosine residues, as well as methyl-arginine and nitrosylation). However, acetylation was higher for control GDH than the frozen enzyme, with the control form having 1.2 times higher relative signal intensity (Fig. 2.3). The frozen form of the enzyme also demonstrated lowered ADP-ribosylation compared to the control with control displaying 1.12 times more luminescence than the frozen. In contrast, frozen GDH showed a significantly higher ($p = 0.046$) degree of lysine methylation compared to the control enzyme. A similar trend for arginine methylation was seen but was not significantly different.

Differential Scanning Fluorimetry

Differential scanning fluorimetry is a sensitive method for determining the thermal stability of purified globular proteins. This method demonstrated that control liver GDH had a significantly higher unfolding temperature (T_m) than the freeze-exposed counterpart (58.0 ± 0.1°C versus 55.9 ± 0.1 °C)(Fig. 2.4). Due to the high concentration of urea in the frozen frog, the effects of 100mM urea on the thermal stability of GDH were also investigated. Both forms of GDH responded similarly to the urea treatments, with a slight decrease in the T_m value of the protein (Fig. 2.4).

Arrhenius Plots

Arrhenius plots serve as a way to determine the activation energy of an enzymatic reaction by plotting the inverse temperature (in Kelvin) against the logarithm of the V_{max}. The Arrhenius plot was constructed for purified control and freeze-exposed GDH by varying the assay temperature and measuring activity in the forward direction under saturating substrate conditions (Fig. 2.5). The parallel slopes of the Arrhenius plots demonstrate that the activation energy was the same for control and the freeze-exposed GDH at 29-30 kJ/mol (Table 2.2).

Table 2.1. Representative purification of GDH from liver from freeze-exposed wood frogs. Two steps were used: (a) CM Sepharose column chromatography with elution using a pH gradient, and (b) affinity chromatography on a GTP agarose column with elution using a 0-2 M KCl gradient. Activities are measured in the forward (glutamate oxidizing direction of the reaction).

Step	Total Protein (mg)	Total Activity (mU)	% Yield	Fold Purification	Specific Activity (mU/mg)
Crude	18.72	1331	-	-	71.1
CM Sepharose	2.47	823	61.8	4.68	333.1
GTP Agarose	0.12	412	31.0	46.71	3322.3

Table 2.2. Kinetic parameters for the forward and reverse reaction of purified *R. sylvatica* liver GDH taken from control and freeze-exposed animals. K_M values were determined using saturating conditions of co-substrate(s). Data are means ± SEM, n = 4 determinations except where noted. Assays were performed at pH 8.0 for the glutamate-consuming direction and pH 7.2 for the α-KG consuming direction and at 22°C except as noted.

	Control	Frozen
Forward reaction		
K_M Glutamate (mM)	2.1 ± 0.2	1.24 ± 0.09**
K_M NAD^+ (mM)	1.39 ± 0.03	0.84 ± 0.03**
I_{50} GTP, Mg^{2+} (1:2) (μM)	0.122 ± 0.009	0.44 ± 0.01**
I_{50} Urea (M)	0.67 ± 0.01	0.54 ± 0.02**
K_A ADP (μM)	32 ± 2	29 ± 1
(V_{max} 1 mM ADP)/(V_{max} unactivated)	2.02 ± 0.07	1.90 ± 0.03
V_{max} forward direction 22°C (mU/mg)	2390 ± 70	3320 ± 50**
K_M Glutamate 5°C (mM)	2.17 ± 0.06	2.10 ± 0.14[a]
K_M NAD^+ 5°C (mM)	0.68 ± 0.07[a]	0.66 ± 0.07
V_{max} forward direction 5°C (mU/mg)	1170 ± 20[a]	1580 ± 10**[a]
Activation Energy (kJ/mol)	29 ± 1	29.7 ± 0.7
Reverse reaction		
K_M NH_4^+ (mM)	35 ± 2	11 ± 1**
K_M α-KG (mM)	0.33 ± 0.04	0.179 ± 0.009*
K_a ADP (μM)	31 ± 4 (n=3)	34 ± 5
(V_{max} 1 mM ADP)/(V_{max} unactivated)	1.33 ± 04	1.56 ± 0.05*
V_{max} Reverse direction 22°C (mU/mg)	16900 ± 750	20600 ± 700**
K_M NH_4^+ 5°C (mM)	29 ± 3 (n=3)	16 ± 1 (p=0.0509)
K_M α-KG 5°C (mM)	0.36 ± 0.02	0.27 ± 0.02*[a]
V_{max} reverse direction 5°C (mU/mg)	8400 ± 590[a]	8300 ± 500[a]

* Significantly different from the corresponding control value, $p < 0.05$; ** $p < 0.01$.

[a] indicates the parameter is significantly different from the corresponding parameter at 22°C, $p < 0.05$

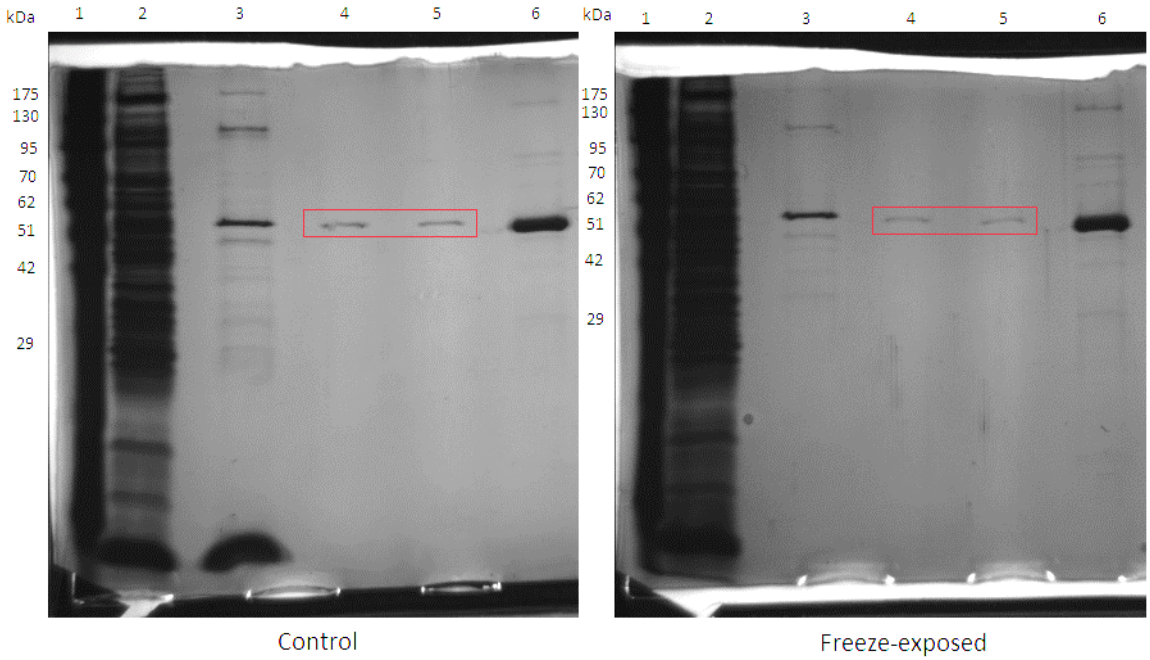

Fig. 2.1. SDS-PAGE gel electrophoresis showing the purification of GDH to homogeneity from liver of control and freeze-exposed wood frogs in a two-step process; silver-staining was used to visualize protein. The left gel shows GDH from control liver while the right gel shows GDH from liver of freeze-exposed frogs. Lanes are as follows; 1. Molecular weight ladder (GeneDirex 10.5-175kDa) with molecular weights labeled on the left; 2. 20X diluted crude liver homogenate; 3. Pooled samples from CM pH gradient elution; 4-5. Pooled samples from the 0-2M KCl elution from GTP agarose; 6. Commercial bovine liver GDH. Some of the lower molecular weight bands are not visible in the ladder.

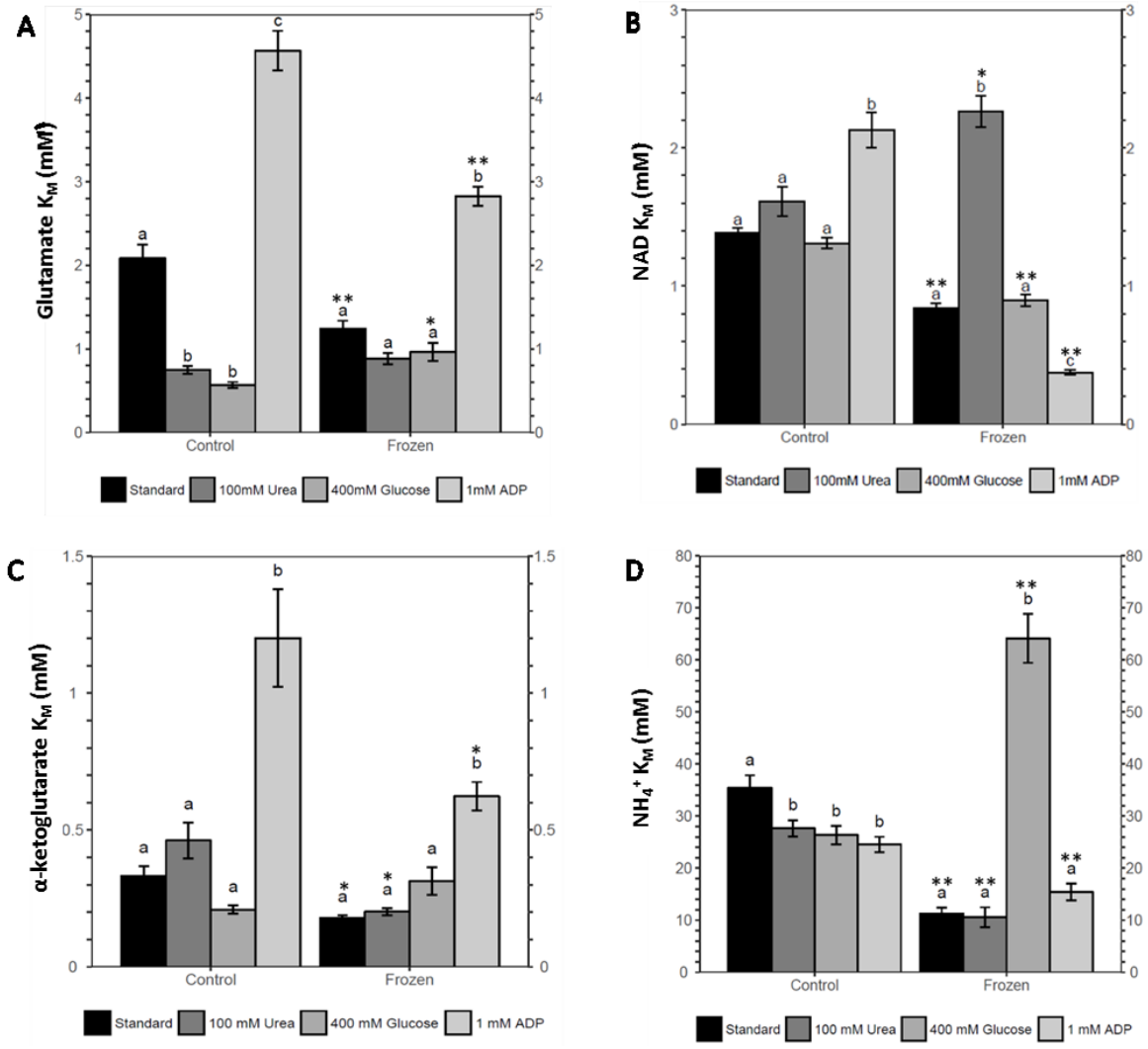

Fig. 2.2. The effects of metabolites on the affinity of purified control and frozen *R. sylvatica* liver GDH for A) glutamate, B) NAD, C) α-KG, and D) NH_4^+ substrates, comparing control to freeze-exposed. Data are mean ± SEM, n = 4. Statistical analysis used one-way ANOVAs and Tukey's post hoc tests for each form of GDH (control and frozen) to compare the effects of different additives on the K_M; data were considered significantly different when $p < 0.05$ (represented by the letters a, b, c above the bars). T-tests were used to compare the control GDH parameters to the respective freeze-exposed GDH parameters. '*' indicates the frozen parameter is different from the control $p<0.05$ and '**' indicates $p<0.01$. All assay were performed at 22°C.

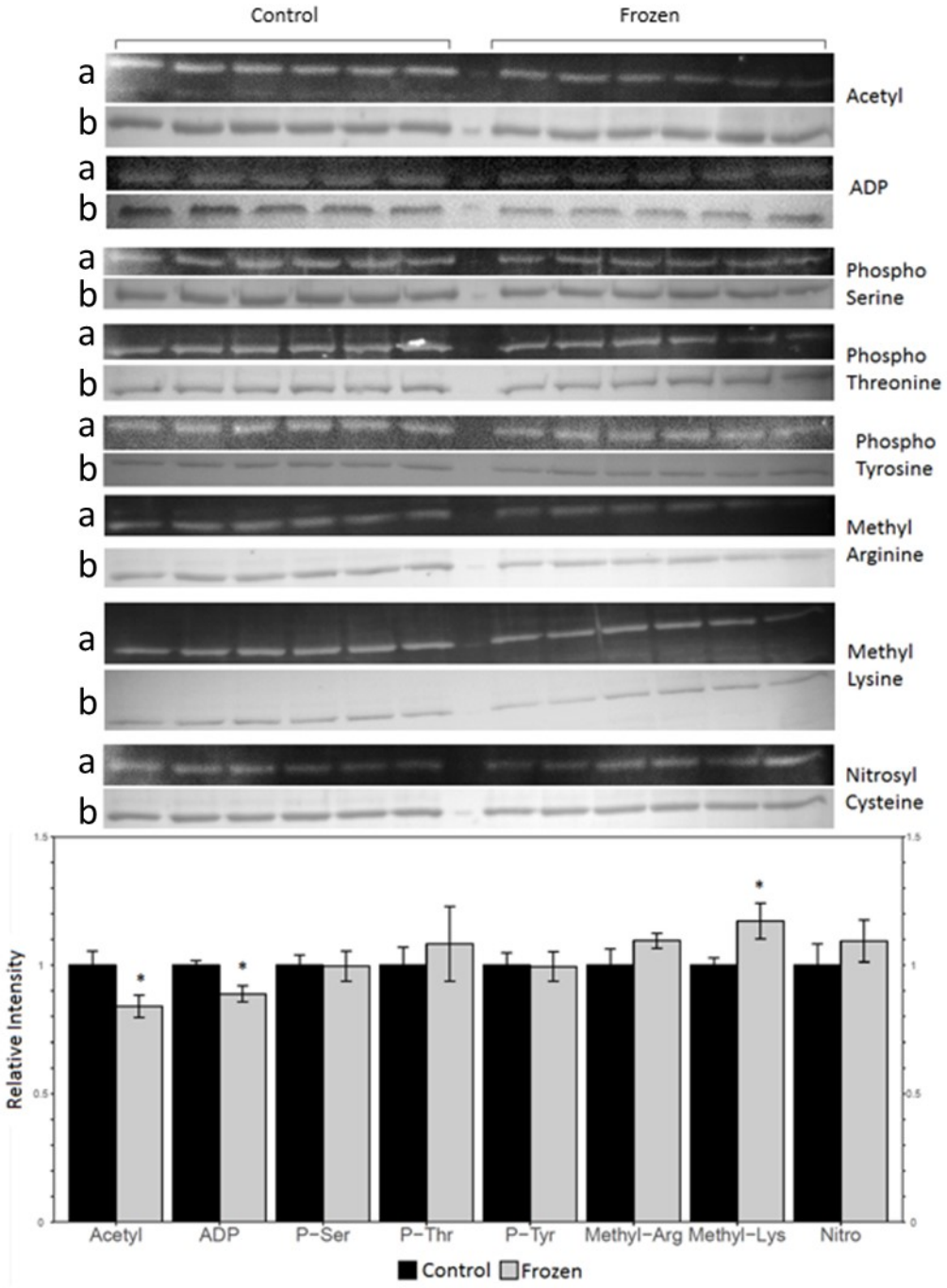

Fig. 2.3. Summary of the Western blots performed to ascertain the differences in posttranslational modifications of partially purified *R. sylvatica* liver from control and stress. The relative band intensity refers to the quotient of the intensity of the chemiluminescent signal (labeled 'a') divided by the band intensity observed after staining with Coomassie brilliant blue (labeled 'b'). '*' indicates that the frozen is significantly different from the control for a given PTM, Student's t-test $p<0.05$. All conditions were found to have equal variance by Bartlett's test ($p>0.05$) so homoscedastic t-tests were used.

A

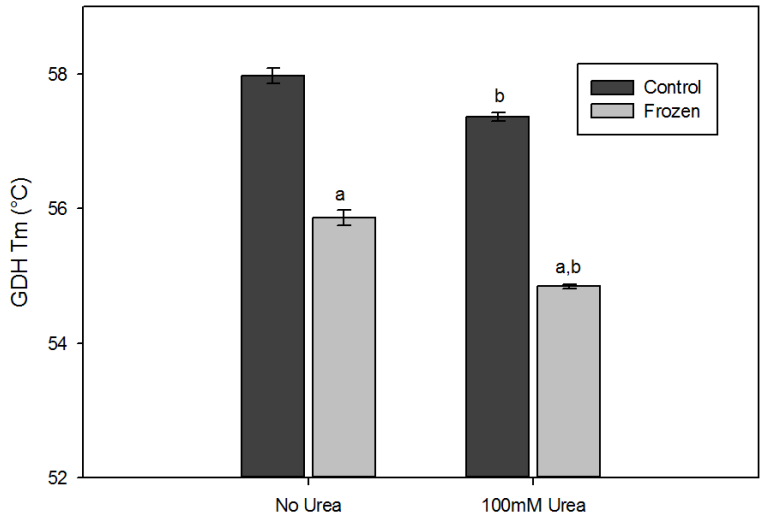

B

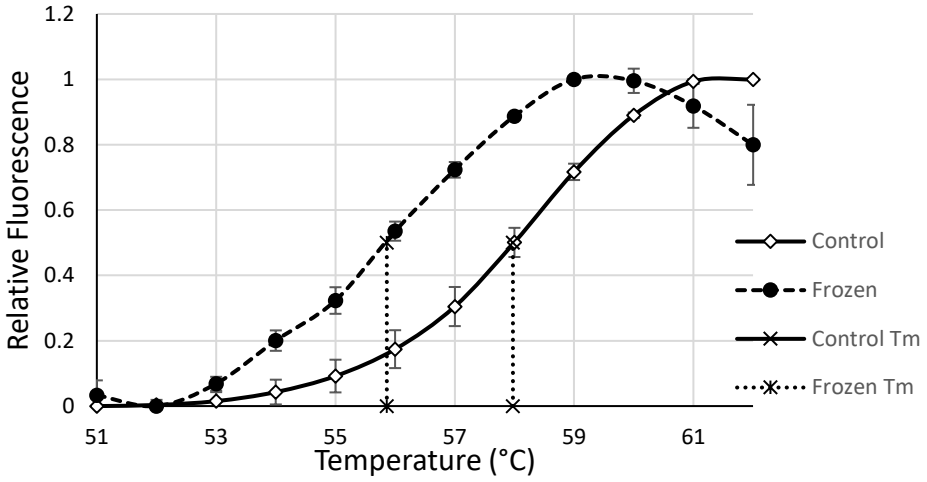

Fig. 2.4. Differential scanning fluorimetry analysis of the relative thermal stability of GDH purified from control and frozen frogs and the influence of 100 mM urea on the melting temperature of the protein at pH 7.0. Determinations were performed with a concentration of 0.04 mg/mL purified GDH in each assay well. **A)** T_m values for control and frozen with and without 100 mM urea. 'a' indicates that the frozen T_m is significantly different from the control (Student's t-test, $p<0.05$). 'b' indicates that the T_m in the presence of 100 mM urea was significantly different from the same parameter without urea. Data are means ± SEM, n=3-4. **B**) Demonstrating relationship of temperature, relative fluorscence and T_m with fluorescence adjusted to 1 at maximum and 0 at minimum. Data represents GDH trials performed without 100 mM urea.

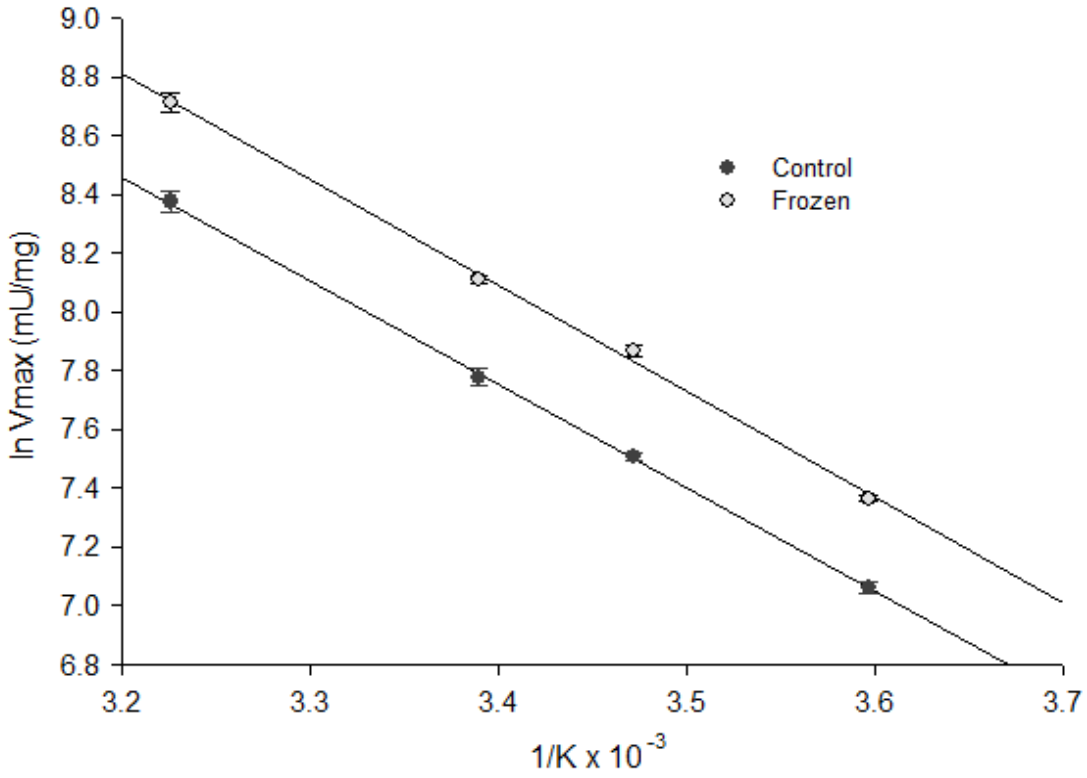

Fig. 2.5. Arrhenius plot showing the lack of difference in activation energy between purified GDH from freeze-exposed and control wood frogs. Maximal activities in the forward direction were measured at 4 different temperatures between 5°C between 37°C. Data are mean ± SEM, n=4.

Discussion

Frigid winter conditions are often a barrier for many species in colonizing northern habitats. These problems are particularly exacerbated in species unable to regulate their internal body temperature such as the wood frog. While finding shelter under leaf litter can help insulate the frog's body from direct exposure to the elements, the temperature can still drop to levels that result in freezing of the animal's body water. Production of cryoprotectants in the form of glucose and urea are known to help prevent damage to the animal's internal organs by preventing intracellular ice formation and limiting the extent of cell volume reduction due to water exiting cells due to extracellular ice crystals (do Amaral et al., 2013). Most of the research into the alteration of the wood frog's biochemical pathways in response to freeze-exposure has been aimed at understanding its carbohydrate metabolism, with a particular focus on understanding how it creates and maintains large quantities of glucose to act as a cryoprotectant (Storey and Storey, 2017). Urea has been experimentally shown to be an important metabolite that can act as both a cryoprotectant and an osmoprotectant, however to date little research has been targeted at understanding how nitrogen metabolism is regulated in response to freezing (Costanzo and Lee, 2005). Glutamate dehydrogenase is a mitochondrial enzyme with an important role in amino acid metabolism, including a crucial role in deaminating amino acids and providing ammonium ions for mitochondrial carbamoyl phosphate synthase I, the first step of the urea cycle.

Analysis of GDH kinetic parameters showed that the enzyme from liver of freeze-exposed wood frogs showed higher affinity for all substrates under standard conditions.

However, the K_M for ammonium ion is very high compared to the other substrates, meaning that activity in the glutamate producing direction is likely low in the wood frog liver as is also seen in mammalian species (Li et al., 2009). The increase in substrate affinities therefore suggests that the regulation of wood frog GDH likely results in an increase in flux in the glutamate consuming direction in the frozen animal. Increasing the affinity for glutamate and NAD^+ could result in more ammonium ion being released and an increase in the available materials for the Krebs cycle and urea cycle. This increase in ammonium ion could fuel an increase in the amount of urea being produced, particularly because GDH is localized in the mitochondria along with CPS1, the enzyme that utilizes ammonium ion to catalyze the first step of the urea cycle (Struck et al., 2005). An increased GDH activity in the glutamate consuming direction also suggests that the wood frog may be catabolizing proteins at an increased rate during freezing, possibly to supplement energy supply. The GTP inhibition measured in the presence of Mg^{2+} is consistent with this idea since lower I_{50} values were associated with the control state. GTP is produced in the Krebs cycle and acts as a potent inhibitor of GDH. In the control state smaller amounts of GTP are needed to induce a 50% reduction in GDH activity in the glutamate consuming direction than in the freeze-exposed condition. This supports previous data showing that freezing favors consumption of glutamate and release of ammonium ion that could be used to generate urea (Storey and Storey, 1986).

The addition of metabolites commonly encountered by the wood frog during freezing to the GDH assay caused a variety of different effects. Urea at 100 mM had the effect of decreasing the affinity of frozen GDH for its substrate in the forward direction relative to the control. Urea in this regard may act as a feedback regulator to inhibit

overproduction of NH_4^+ ions during freezing, particularly important to frozen frogs since they cannot dispose of nitrogenous wastes from tissues due to their blood being frozen (Storey et al., 1992). Alterations in the reverse direction in the presence of urea were not as noticeable. Glucose is an important cryoprotectant in the wood frog and is found in very high concentrations during freezing in order to prevent damage to cellular components. The effects of glucose on GDH are not entirely clear and seem to be somewhat inconsistent between substrates. In the forward direction, the presence of glucose resulted in a higher K_M glutamate for the enzyme from frozen frogs than the control (although glucose suppressed the K_M in both instances as compared with the values in the absence of glucose). By contrast, the K_M NAD^+ for control GDH remained higher than the frozen value in both the presence or absence of glucose.

Due to the role of GDH in supplementing the Krebs cycle with additional fuel by producing α-KG from glutamate, GDH is sensitive to indicators of both abundance and depletion of cellular energy. GTP is produced in the Krebs cycle and so helps to serve as a mechanism of feedback inhibition on the production of α-KG when mitochondrial energy status is high. Conversely, low cellular energy is signaled by elevated ADP levels and therefore ADP often serves as an allosteric modulator of many enzymes related to energy production, including GDH (Bell et al., 2012). The forward reaction maximal velocity of wood frog GDH increased by about 2 fold and the reverse increased about 1.3 times for the control and about 1.6 times for frozen GDH. For all substrates, the frozen GDH had a higher affinity for its substrates in the presence of 1 mM ADP relative to the controls. The higher affinity for glutamate by frozen GDH is likely significant in maintaining activity despite reductions in amount of substrate available since it is known

that glutamate concentrations in wood frog liver fall from approximately 3.4 to 1.4 μmol/g wet weight during freezing (Storey and Storey, 1986). The K_m of frozen GDH for NAD^+ decreased markedly in the presence of ADP contrasting greatly to the increase in K_m under the same conditions noted for the control. This further suggests that the freeze-exposed form of GDH is modified in the liver of the wood frog to promote catabolism of glutamate.

At 22°C, both the forward and reverse reactions of GDH also demonstrated higher V_{max} values for the frozen enzyme than the control. This emphasizes that control of GDH is being inhibited in some way. At 5°C in the forward direction, a similar trend was seen, with the V_{max} being significantly higher for liver GDH from frozen frogs compared with controls, despite the substrate affinities for glutamate and NAD^+ being approximately the same at this temperature. The higher affinity of frozen, versus control, GDH for both NAD^+ and glutamate at higher temperatures may be important in cases of brief periods of thawing during the winter since wood frogs typically experience multiple freeze-thaw cycles over the winter (Larson and Barnes, 2016). During these instances, it may be important for the frog to catabolize glutamate as a substrate for energy production in the mitochondria in order to reduce dependency on carbohydrate fuels that may be reserved for a more important job of producing glucose cryoprotectant. The higher affinity for glutamate under these circumstances could prove important since glutamate levels in the liver are typically reduced following freezing (Storey and Storey, 1986). This would also help to generate more urea to act as a cryo/osmo-protectant in preparation for potential refreezing. Affinities in the reverse direction appear to be similar at 5°C in that control GDH still retains a higher K_M for both ammonium ion and α-KG.

The activity in the reverse direction was noted to be higher for the freeze-exposed GDH at 22°C than the control, although this trend was not seen at 5°C. During freezing, glucose levels increase considerably and it was noted that glucose significantly increased the ammonium ion K_M for frozen GDH. This is an interesting finding since it is known that ammonium ion levels increase dramatically in wood frog liver (up to about 7.5 μmol/g wet weight) during freezing so it may be that glucose may alter the affinity of the freeze-exposed GDH for ammonium ion to prevent backflow and reformation of glutamate (Storey and Storey, 1986). The parameters in the reverse direction along with those in the forward help to indicate that a difference exists between liver GDH from 5°C controls and -3°C frozen animals.

The differences in the kinetic parameters of the control and freeze-exposed GDH suggested that there are structural differences between the two forms of the enzyme. To see if the differences in kinetic parameters were related to a change in the overall structure of the enzyme, DSF was employed. DSF is a fluorimetric method that utilizes a qRT-PCR machine to measure the unfolding of a protein in real-time with the use of a fluorophore (in this case SYPRO-orange) that can bind to hydrophobic regions of proteins (Biggar et al., 2012; Niesen et al., 2007). The results (Fig. 2.3) showed that control GDH from wood frog liver was significantly more stable than the frozen form with or without the presence of 100 mM urea. This means that the frozen version of GDH is less resistant to thermal denaturation. This would be advantageous to the wood frog since the frozen GDH would be exposed to lower temperatures in the animal and would therefore likely need to be more flexible in order to stay functional at these lower temperatures. Sacrificing thermal stability in order to maintain biological function of

proteins is a well-known phenomenon in organisms that live permanently in frigid conditions (known as psychrophiles) (Feller, 2010). However, alteration of enzymes, possibly through PTMs, to accommodate varying temperatures is less well understood. As such, the discovery that GDH from a freeze-exposed wood frog liver has a lower thermal stability offers evidence that some ectotherms are capable of modifying their existing proteins to retain function at lower temperatures.

The differences in kinetic parameters observed between the purified control and freeze exposed GDH suggested that the enzyme is being regulated in some way at the molecular level. Changes in PTMs on the enzyme was considered as a way to explain the changes in enzyme activity. Typically phosphorylation is the PTM that is most often considered when dealing with reversible changes that can be utilized for modulating enzyme activity and properties since there exists a diverse repertoire of regulatory protein kinases (Cohen, 2000; Dephoure et al., 2013). However, analysis of global changes in the amounts of phosphorylated serine, threonine and tyrosine (the commonly phosphorylated residues on proteins) on wood frog GDH showed no significant changes between the control and freeze states. Additional Western blots revealed that for most of the other PTMs probed there were also no statistically significant changes between the control and stress conditions. However, control GDH showed a significantly higher relative intensity when probed for acetylated amino acid residues and ADP-ribosylation. Changes in acetylation of GDH have been reported before and it has been shown that a decrease in acetylation of human GDH due to exogenous sirtuin 3 *in vitro* mediated deacetylation can result in an increase in GDH activity, thereby suggesting that acetylation serves to inhibit GDH activity (Schlicker et al., 2008). ADP-ribosylation of arginine and lysine residues is

also known to be important in the regulation of GDH with increased mono-ADP-ribosylation being associated with a decrease in GDH activity (Herrero-Yraola et al., 2001). ADP ribosylation may play an important role in modulating the metabolic activity of mitochondrial enzymes and it is promoted by the action of sirtuin 4 (Haigis et al., 2006). Thus, the decrease in acetylation noted for frozen GDH is possibly due to a promotion of sirtuin 3 activity and the decrease in ADP-ribosylation may be due to an inhibition of sirtuin 4 activity, although an increase in the activity of enzymes removing ADP-ribosyl attachments could also be possible (Kim et al., 2012). The significance of the slight increase in methylation on lysine residues is unknown, and may not be important since this PTM does not have a previously established role in modulating GDH activity. Although several confirmed and putative mitochondrial protein methyltransferases have been identified, it is unclear as to whether this modification plays a role in mitochondrial metabolism (Carilla-Latorre et al., 2010; Małecki et al., 2015). The higher affinity of frozen, versus control, GDH for its various substrates (described earlier) and the relief of GTP inhibition may be explained by the changes in PTMs associated with GDH during freezing. PTMs provide a rapid and energy-inexpensive means of changing enzyme properties and acetylation of proteins is beginning to be better understood as a regulatory mechanism for many proteins involved in central metabolic roles. In the case of frog GDH changes in enzyme acetylation may provide a rapid way to increase flux through the Krebs cycle by increasing GDH affinity for its substrates and maximal activity as well as elevating available ammonium ion for urea production in response to freezing.

Chapter 3

Regulation of ornithine transcarbamylase in the freeze tolerant wood frog

Introduction

To cope with periods of whole body freezing, the wood frog must generate high concentrations of intracellular metabolites to act as a defense to freezing. While glucose has been extensively studied in this regard, urea is another metabolite that plays a role in helping amphibians survive the winter by helping to prevent ice-damage to cellular components. Urea is elevated in the wood frog during freezing through its accumulation during the fall and winter (Costanzo et al., 2013) as well as ongoing production in the liver tissue during the course of freezing (Costanzo et al., 2015). Elevated urea and glucose concentrations help to decrease the freezing point of the intracellular fluid thereby avoiding intracellular ice formation. However, urea has also been demonstrated to have cryoprotective effects that are not dependent upon concentration possibly suggesting an additional cryoprotective mechanism (Costanzo and Lee, 2005). Extracellular ice formation can also result in indirect damage due to cellular dehydration since solutes are excluded from growing ice crystals leading to an imbalance in solute concentration between the exterior and interior of cells (Bakhach, 2009). Urea is therefore not only important as a cryoprotectant but also as an osmoprotectant in that elevated concentrations of urea help to prevent excessive organ dehydration during freezing (Costanzo and Lee, 2005). Urea is known to be used by a wide variety of amphibians to survive periods of drought by acting as an osmoprotectant thereby helping the animal retain water, suggesting it serves a similar purpose in the wood frog during freezing (Jørgensen, 1997).

The urea cycle is needed for production of urea in ureotelic animals, however its regulation is not well understood in terms of reduced metabolic states and freezing in the

wood frog. The urea cycle comprises a five-enzyme process divided between the cytosol and the mitochondria. Ornithine transcarbamylase (OTC) is one of the two mitochondrial enzymes involved in the urea cycle as it catalyzes the addition of a carbamoyl phosphate molecule (generated by another enzyme, CPSI) to the non-proteinogenic amino acid ornithine to form citrulline. Ornithine is located at the intersection of several pathways in the metabolism of the liver. Ornithine can be consumed by ornithine decarboxylase (ODC) to produce putrescine and carbon dioxide in the first step of polyamine synthesis (Emmerson et al., 1997). Ornithine is also involved in the production of the proteinogenic amino acids glutamate and proline through the formation of the intermediate pyrroline-5-carboxylate by the action of the mitochondrial enzyme ornithine amino transferase (Jones, 1985; Wu and Morris Jr., 1998). The existence of competing pathways for ornithine suggests that enzymes consuming this substrate are regulated to control its metabolic fate.

OTC is a homotrimer with three active sites located at the intersection between the individual polypeptides (Tuchman et al., 1998). Regulation of nitrogenous waste in anuran species has been an area of interest in terms of gene expression relating to urea cycle enzymes since they begin life as ammonotelic tadpoles and then transition to more terrestrial adult frogs that are ureotelic. It has been demonstrated that bull frog (*Rana catesbeiana*) OTC and CPSI mRNAs are upregulated downstream of the action of thyroid hormones during the onset of metamorphosis and thereby help to facilitate the transition to ureotelic metabolism (Helbing et al., 1992). While transcriptional regulation of the urea cycle is certainly a fascinating aspect of frog development, in the course of freezing it is less likely that the wood frog would undergo large-scale changes in terms of gene

expression since it would be more efficient to modify existing enzyme molecules to cope with physiological changes. Few PTMs are known to be associated with regulation of OTC, although it is known that acetylation on a lysine residue on OTC is involved in lowering its affinity for carbamoyl phosphate (CP) in response fluctuations in glucose or amino acid metabolism (Yu et al., 2009). This finding suggests that urea production is controlled at least in part by OTC regulation and therefore may have a role in the wood frog response to freezing.

Methods

Chemicals and Animals

The chemicals used in the following experiments were obtained from the same sources as described in chapter 2 unless otherwise stated. Wood frogs were divided into control groups and dissected in the same manner as described in chapter 2.

Enzyme Purification

Liver samples were removed from storage in a -72ºC freezer and placed in liquid nitrogen. These samples were then quickly weighed and homogenized 1:9 w/v with a couple of crystals of PMSF in homogenate buffer at a pH of 6.3 (25 mM HEPES, 1 mM EDTA, 1mM EGTA, 1 mM DTT, 10 mM NaF, 20% glycerol v/v). Samples were homogenized by use of a Janke & Kunkel IKA-Werk Ultra Turrax homogenizer and were kept cool with ice throughout the homogenization process. Homogenized samples were then centrifuged in an Eppendorf 5810R tabletop centrifuge pre-chilled to 4ºC at 13,500 x g for 30 minutes. Following centrifugation, samples were carefully pipetted out of the test tube and the pellet was discarded.

Homogenized samples were loaded onto a carboxymethyl sepharose (CM Sephadex™) bed measuring 3 cm high by 1 cm in diameter equilibrated in 15 mL of homogenate buffer at pH 6.3. The column was then subsequently washed with 30 mL of the homogenate buffer at pH 6.3 to remove any unbound protein. The OTC was then eluted in fractions of ~1.3 mL each using a 30 mL 0-300mM sodium monobasic phosphate gradient also at pH 6.3. OTC activity was tested in the gradient and the first three fractions with high activity were pooled for the next step.

The pooled sample from the phosphate gradient elution was de-salted via a spin column procedure using 5 mL of Sephadex™ G-25 for every 0.5 mL of pooled CM sample. In this procedure, 5 mL of Sephadex™ G-25 were loaded into syringes stopped at the bottom with glass wool and placed in 15 mL plastic test tubes. Each syringe centrifuged at 2500 RPM in a VWR Clinical 50 benchtop centrifuge for 2 minutes to remove water. These were then filled with 5 mL of homogenate buffer and centrifuged again for the same time and speed. Finally, each syringe was loaded with 0.5 mL of protein sample and centrifuged for 1 minute. The desalted samples were collected from the bottom of the test tubes. The collected desalted samples then had their pH changed slowly to 8.0 using drops of 1 M NaOH with constant stirring. These were loaded onto a diethylaminoethanol-Sepharose (DEAE Sephadex™ A-25, GE Healthcare) anion exchange resin measuring 3 cm in length by 1cm in diameter pre-equilibrated in 15 mL of homogenate buffer at pH 8.0. Washing the column with homogenate buffer resulted in most of the OTC activity being removed from the column. The fractions (~2 mL each) with the 4 highest OTC activities were pooled for analysis of the purity and study of kinetic parameters. These fractions were subjected to SDS-PAGE and were stained using

silver staining (see Chapter 2 methods) to demonstrate that the fractions were partially pure OTC.

Citrulline Detection Assay

Citrulline detection assays were performed in a non-binding 96 well microplate (Cellstar®, Sigma-Aldrich) using the method described by Knipp and Vašák (Knipp and Vasák, 2000). Enzymatic reactions were run at saturating conditions using 10 mM carbamoyl phosphate and 10mM ornithine in a total reaction volume of 60 µL for 15 minutes in a 50 mM Tris assay buffer brought to a pH of 8.5. Reactions were typically performed with 10µL of sample except for crude homogenates which used only 5 µL. Enzymatic reactions were terminated with the addition of 200 µL of the colour-developing reagent (COLDER) described by Knipp and Vašák as this is highly acidic. COLDER consists of a mixture prepared immediately before use of 1 part solution A (80 mM butanedione monoxime, 2 mM thiosemicarbazide) with 3 parts solution B (3 M H_3PO_4, 6 M H_2SO_4, 2 mM $NH_4Fe(SO_4)_2$). Solution B could be stored indefinitely at 4°C, but solution A could be stored only for a month at 4°C and was kept in the dark at all times. The plate was subsequently heated to 95ºC for 15 minutes to allow the formation of the dye to occur (Knipp and Vasák, 2000) Heating was performed using a Torrey Pines Scientific EchoTherm™ cooling/heating plate in a fume hood while the plate was covered in aluminum foil to reduce exposure to light. Following development of the coloured product in the microplate, the absorbance of the wells was measured at 540 nm using a Thermo Scientific Multiskan Spectrum microplate reader. A standard curve of citrulline detection using this assay was performed using citrulline concentrations ranging from 0-400 µM at pH 8.5 in 50mM Tris buffer using 4 replicates. One unit of OTC

activity in this study was defined as the activity that produced 1 μmol of citrulline per minute at pH 8.5 at 22°C. A linear relationship between absorbance at 540 nm and citrulline concentration was observed up to 400 μM (Appendix II Fig. A.2.1).

Determination of Kinetics Parameters

Determination of the K_M values for CP and ornithine was performed by measuring the activity of the partially purified enzyme with saturating concentrations of one substrate (10mM in both cases) at six different concentrations of the other substrate (including 0mM). The reaction was terminated with the addition of COLDER at 4 different time points (0, 5, 10, and 20 minutes). Using the absorbance data at 540 nm the concentration of citrulline was determined in each well from a standard curve and the activities could be calculated.

Protein Concentration Assay

Protein concentration was determined using the Bio-Rad protein assay as described in chapter 2 with BSA as the protein standard.

Western Blots

Following a partial purification, two bands were visible in the SDS-PAGE gel using Coomassie stain. Western blotting was used to identify which band was responsible for the OTC activity (Fig. 2). A rabbit polyclonal anti-OTC antibody was obtained from GeneTex (GTX105140) and diluted 1:1000 in TBST for western blotting. Samples were concentrated 4× and were mixed 1:1 with 2× SDS loading buffer. Western blotting procedures were the same as in Chapter 2.

Western blots were also used to determine if OTC was post-translationally modified in response to the freezing conditions. The antibodies used were diluted 1:1000 from their stock concentrations and about 5 mL of this was used to probe the OTC bands for specific PTMs. The antibodies used are described in Chapter 2.

Visualization using ECL as described in Chapter 2 was performed and the blots were then stained with Coomassie brilliant blue to adjust for OTC in each lane relative to the chemiluminescent signal.

Mass Spectrometry

To further confirm the identity of OTC from the partially purified sample, the two main protein bands found were cut from an SDS-PAGE gel after staining with Coomassie Brilliant blue and were analyzed using the Proteomics Platform at the Quebec Genomics center at Laval University (Quebec City, Canada). Further confirmation was desirable since certainty of the identity of the band was crucial for performing western blots targeted at specific posttranslational modifications on OTC. Tandem mass spectrometry (MS/MS) was performed by the Quebec Genomics center on a trypsin digest of the protein. The resulting mass spectra generated were analyzed by performing a search on the TAX_ranidea_8397_20150318 database with Mascot version 2.5.1 software (Matrix Science, London UK). Tolerances for the fragment ions and parent ions were set to 0.100 Da. Carbamidomethyl cysteine was a fixed modification since these residues were alkylated to prevent cysteine crosslinking. The resulting data was interpreted using Scaffold 4.4.6 proteomics software (Proteome Software Inc., Portland Oregon). Peptide identification was accepted if higher than 95% probability and protein identification was

accepted for higher than a 95% probability and with 2 peptides matched to the protein (Nesvizhskii et al., 2003).

Statistical Analysis

To determine the K_M values for CP and ornithine from the activities obtained during the kinetics assays, a nonlinear least squares regression computer program, Kinetics 3.51, was used (Brooks, 1992). Rate of enzyme activity was determined from the microplate raw data using a Microplate Analysis program (Brooks, 1994). Student's t-tests were used to compare control to frozen data with differences considered significant when $p<0.05$.

Results

Purification

A partial purification was performed on both control and freeze-exposed OTC. Using a phosphate gradient at pH 6.3, OTC was eluted from a CM cation-exchange column. This column yielded 39% activity from the crude homogenate. OTC did not bind to the DEAE column at pH 8.0. This step of the procedure resulted in greater activity being returned than was in the eluate from the CM column. Using SDS-PAGE, the purity of the sample was visualized and shown to be partially pure, with two major protein bands seen in the gel following silver staining (Fig. 3.1). The partially pure sample of OTC had a final specific activity of 874mU/mg (Table 3.1).

Kinetic Parameters

The affinity of OTC for ornithine was higher in the freeze-exposed OTC than the control. The K_M for ornithine in the control was found to be 0.25 ± 0.02 mM compared to

the frozen counterpart that was only about half that at 0.13 ± 0.01. The CP affinity remained unchanged between the control and the freeze-exposed forms of the enzyme with both of them having a K_M at about 0.22 ± 0.02 mM (Table. 3.2). No significant differences were seen in OTC activity under saturated substrate concentrations for the control and freeze-exposed crude liver extracts when normalized for total protein content (control 50 ± 5, frozen 46.2 ± 1.2 mU/mg).

OTC Identification and Mass Spectrometry

The results of the Western blot done with a rabbit anti-OTC antibody demonstrated that the upper band in the SDS-PAGE gel (around 40kDa) was OTC (Fig. 3.2). This was further confirmed using the proteomics platform of the Quebec Genomics Center (Quebec City, Canada) which showed that the sequence similarity of the band at 40kDa closely matched that of *Rana catesbeiana* (the American bullfrog) (see Appendix I Fig. A.1.1). The contaminant band (lower molecular weight) was shown to be glyceraldehyde-3-phosphate dehydrogenase through the use of MS/MS (Fig. 3.2). Hereafter the band at 40kDa was known to be OTC and this band was used for all of the additional Western blots performed to quantify post-translational modifications.

Western Blots for Posttranslational Modifications

The Western blots performed on the partially purified OTC revealed an increase of 1.64× in the relative levels of phosphorylation on the serine residues from the freeze-exposed liver relative to the control (Fig. 3.3). Phosphorylation in threonine and tyrosine residues did not show any significant difference nor were there any other differences

between the control and stress in cysteine nitrosylation, lysine methylation, or lysine acetylation.

Table 3.1. Representative two-step partial purification of OTC from freeze-exposed *Rana sylvatica* liver. The first step used a phosphate gradient to elute OTC from a CM cation exchange column at pH 6.3. This was followed with an elution of the OTC from DEAE at pH 8.0.

Step	Total Protein (mg)	Total Activity (mU)	Yield (% activity)	Fold Purification	Specific Activity (mU/mg)
Crude	25.3	1637	NA	NA	64.7
CM^-	3.85	636	38.9	2.56	165.4
$DEAE^+$	1.01	887	54.2	13.5	874.7

Table 3.2. Comparison of the substrate affinity for OTC from partially pure control and freeze exposed wood frog liver, n=4. OTC activity from control and frozen crude liver extracts was normalized to the total protein amount from the extracts, n =3. Data was compared using Student's t-test and was determined to be significantly different when $p < 0.05$ indicated by '*'. All assays were performed at 22°C in pH 8.5 50 mM Tris buffer.

	Control	Frozen
K_M ornithine (mM)	0.25 ± 0.02	0.13 ± 0.01*
K_M carbamoyl phosphate (mM)	0.22 ± 0.04	0.22 ±0.02
Crude OTC (mU/mg protein)	50 ± 5	46 ± 1

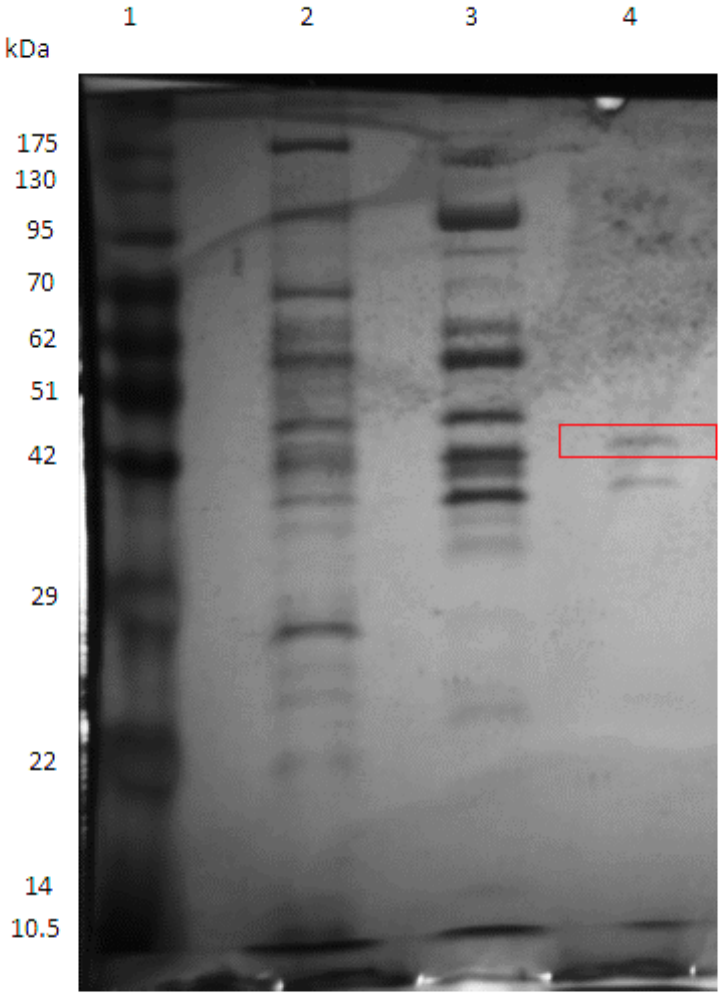

Fig. 3.1. Silver stained SDS-PAGE gel demonstrating partial purification of the control OTC from *Rana sylvatica* liver. Lane 1: GeneDirex PiNK Plus prestained 10.5-175kDa protein ladder. Lane 2: 20 × diluted crude liver extract. Lane 3: Pooled fractions from CM eluted with phosphate gradient at pH 6.3. Lane 4: Pooled fractions from filtration through DEAE at pH 8.0. The box shows the protein band determined to be the OTC, which was confirmed via western blotting.

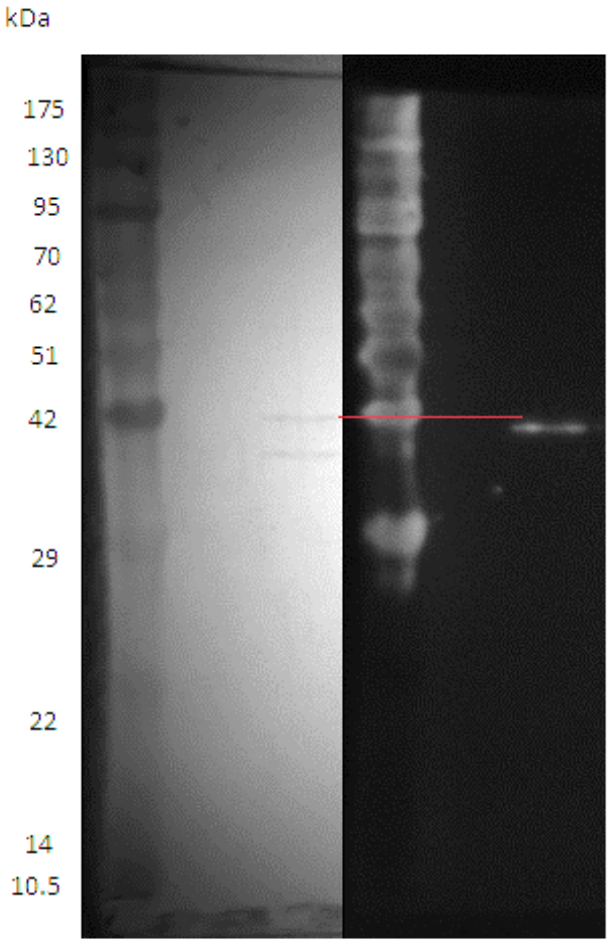

Fig 3.2. Western blot using OTC antibody for identification of the protein band corresponding to OTC in a partially pure control sample from wood frog liver. The left image shows the blot stained with Coomassie brilliant blue while the right blot shows the same blot during enhanced chemiluminescence with the blot probed using the OTC antibody. The two blots were aligned using the closest marker in the ladder (42kDa) to the bands visible in the Coomassie stained image. The line demonstrates that the higher molecular weight protein cross-reacted with the OTC antibody.

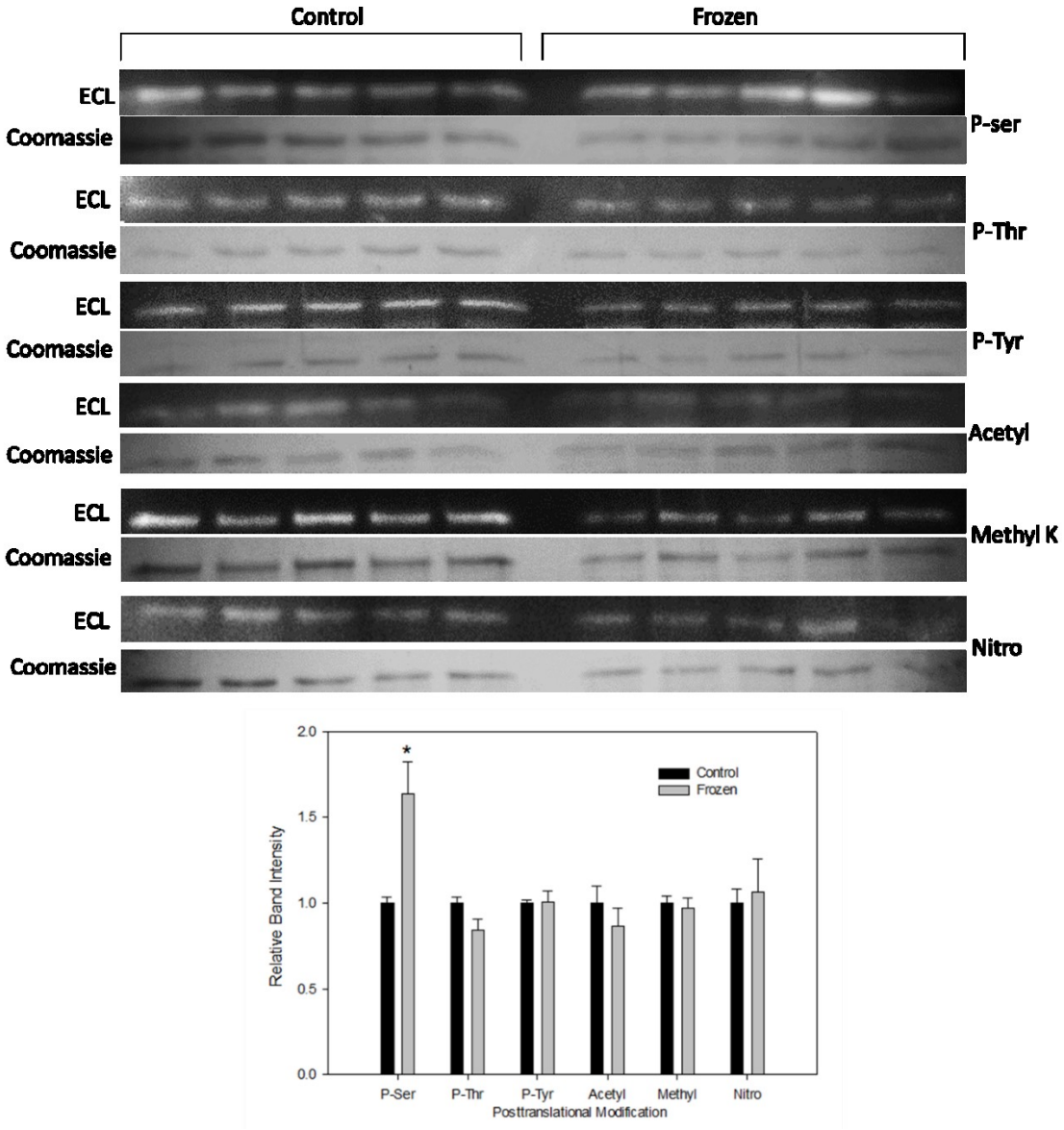

Fig. 3.3. Visual and graphical representation of western blots probing for various PTMs of OTC performed on a partially purified sample. Control bands are shown on the left and freeze-exposed OTC is on the right with the chemiluminescent images shown above the corresponding Coomassie brilliant blue stained blot. The bar chart demonstrates the relative band intensity of the PTM in the control compared to the frozen. '*' indicates a significantly different parameter between the control and stress using Student's t-test, $p<0.05$.

Discussion

Production of urea in the liver of the wood frog is elevated during the late fall and early winter to prepare the wood frog for freezing. Freezing can be dangerous for the frog due to the possibility of damaging ice formation in the cells. Freezing can also cause indirect damage to the wood frogs cells by inducing cellular dehydration (Bakhach, 2009). Elevated levels of urea and glucose combat these effects by increasing osmolality and reducing the freezing point of the cytosol (Costanzo and Lee, 2005). Urea as a chaotrope disrupts the hydrogen bonds between water molecules and therefore can help to prevent ice nucleation (Russo, 2007; Zolles et al., 2015). It has been noted before that the wood frog can maintain high levels of CPSI activity during freezing despite reduction in overall metabolic rate, although the nature of changes to the protein was not explored (Schiller et al., 2008). This leads to the question as to whether other urea cycle enzymes might be potentially regulated to facilitate increased production capacity during freezing.

OTC has not been widely studied with regards to metabolic regulation since CPSI is commonly assumed to be the main regulatory step of the urea cycle due to it being close to irreversible. However, it is possible that in response to extreme conditions faced by the wood frog that there may be a generalized increase in the activity of many of the enzymes in the urea cycle. This could be to increase or to stabilize the production capacity of urea in spite of the overall reduced metabolic rate associated with freezing. Another anuran species, the African clawed frog (*Xenopus laevis*), can increase the activity of multiple urea cycle related enzymes, including OTC to about 3 fold higher, in response to elevated salinity (Lee et al., 1982). Both freezing and elevated salinity are stresses related to the risk of cellular dehydration so the ability to increase intracellular

urea concentrations is a common response among amphibians to maintain osmotic balance. This suggests that urea cycle enzymes in certain frog species undergo robust regulatory changes in response to environmental stress.

Partial purification of OTC from wood frog liver resulted in an increase in activity following the DEAE elution. This suggests that there could be an endogenous inhibitor present in the partially pure sample until that point, although the identity of this inhibitor is unknown. Several studies in other vertebrates have demonstrated that various amino acids; valine, histidine, glycine, methionine, leucine, isoleucine, and alanine all have some degree of inhibition (Lusty et al., 1979; Marshall and Cohen, 1972). Alternatively, it is possible that the addition of phosphate, used to elute the OTC from the CM chromatography column may have been inhibiting it since it is known that phosphate can act as a competitive inhibitor against CP for OTC (Cohen et al., 1992; Xiong and Anderson, 1989). In either, case the DEAE sephadex column subsequently used would remove any small molecules present thus relieving inhibition.

The affinity for ornithine was higher in the freeze-exposed variant of the enzyme than the control (Table. 3.2). This suggests that the freeze-exposed variant of the wood frog's liver OTC can run at relatively higher rates of activity in the presence of lower amounts of ornithine. OTC activity of the crude liver samples seems comparable when adjusted for total protein concentration. The significance of this finding is not entirely certain in regards to the functional parameters of the OTC enzyme itself since this finding did not take into account the amount of OTC specifically, but it does suggest that similar maximal rates of OTC activity occur in both the control and freeze-exposed liver. Increased affinity of OTC for ornithine without a change in maximal velocity may be

relevant in preventing alternative metabolic pathways from consuming ornithine. This would then commit more ornithine to urea production during freezing. Ornithine can also be utilized by ornithine decarboxylase, to catalyze the first step of polyamine synthesis, and by ornithine aminotransferase, to consume ornithine in the production of the amino acid proline (Emmerson et al., 1997; Morris, 2002). The increased affinity of OTC for ornithine in response to freezing may therefore be important in encouraging urea production by restricting the utilization of ornithine into alterative pathways.

To determine the potential mechanism of the kinetic change between the control and freeze-exposed OTC, western blotting was used to determine the relative change in different PTMs. Before this could be done however, the identity of the band of the OTC band needed to be confirmed and so a preliminary western blot was performed using an antibody targeting OTC (Fig. 3.2). After it was determined that the higher molecular weight protein corresponded to the OTC monomer, the sample was analyzed with mass spectrometry for further confirmation that it was OTC. The confirmation afforded by the mass spectrometry then allowed the determination of PTM states on the protein band known to be OTC. These western blots showed that the two proteins were similar in PTMs except for phosphorylated serine residues. The freeze-exposed wood frog OTC was shown to have a higher (~1.6 fold) relative signal intensity than the control. This suggests that phosphorylation of serine residues serves as a way for the frog to regulate the functional parameters of OTC during freezing.

Regulation of OTC activity has been studied at the level of transcription and has been shown to have increased mRNA expression in rats fed a high protein diet (Wraight and Hoogenraad, 1988). The increased OTC expression under these conditions is

important in maximizing efficiency in processing nitrogenous wastes to accommodate and increased consumption of amino acids. However, in instances of greatly reduced metabolic rate, increasing expression of mRNA as a sole method in increasing OTC activity would not be preferred as transcription and translation are very energetically expensive processes. In addition to this, the onset of freezing can occur rapidly and in various bouts meaning that the response to freezing must also be able to occur in a quick and reversible manner. PTMs provide an ideal way in which existing protein molecules can be regulated to respond to rapidly changing conditions. One study has reported in humans that OTC activity is regulated in response to carbohydrate and amino acid availability via another PTM, acetylation of a lysine residue which decreases OTC activity (Yu et al., 2009). Although acetylation was examined in this study (Fig. 3.3), no difference was seen between the control and freeze-exposed OTC. Phosphorylation of serine/threonine residues on OTC has been reported to alter in mammalian hibernators in response to seasonal cues, and was proposed to play a role in enabling consumption of amino acids during states of reduced carbohydrate consumption occurring during hibernation by increasing capacity to generate urea (Chung et al., 2013). While regulation of OTC is not completely understood, it has become more apparent that OTC may be regulated through PTMs and play a significant role in regulating the production of wastes in ureotelic animals. Various mitochondrial specific protein kinases and phosphatases exist providing a mechanism for the change between phosphorylation states seen in OTC (Hofer and Wenz, 2014) and also some cytosolic protein kinases can be translocated into the mitochondria to regulate key metabolic enzymes (Horbinski and Chu, 2005). Taken

together the results presented here suggest that wood frog OTC is altered in response to freezing to encourage continued urea cycle metabolism.

Chapter 4

Regulation of carbamoyl phosphate synthetase I in the freeze tolerant wood frog

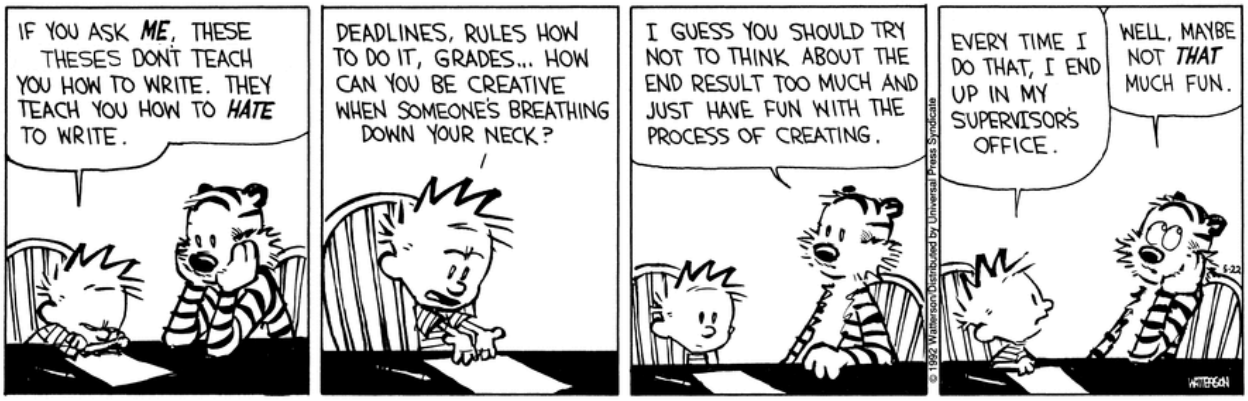

Introduction

Carbamoyl phosphate synthetase I (CPS1) is a ligase found in the mitochondria of many terrestrial vertebrates, playing a vital role in the urea cycle by mediating the entrance of nitrogen in the form of free ammonia into organic compounds that ultimately produce urea. The reaction catalyzed by this enzyme is complex and accordingly, the CPS1 molecule is a large protein (approximately 165 kDa for each of the two monomers) with multiple active sites and allosteric binding sites. Bicarbonate phosphorylation occurs at the first active site resulting in an activated carbamate intermediate that is transported via a tunnel in the enzyme to a second active site where ammonia replaces the phosphate group through a nucleophilic substitution and the molecule is subsequently phosphorylated again to form carbamoyl phosphate (CP) (de Cima et al., 2015). The overall reaction consumes two molecules of ATP, one ammonium ion, and one bicarbonate to generate one molecule of CP, 2 molecules of ADP and 1 molecule of P_i. This differs from carbamoyl phosphate synthetase II which is a cytosolic enzyme that utilizes glutamine as a nitrogen donor and is part of a large trifunctional enzyme encoded by the CAD gene that catalyzes the first three committed steps of *de novo* pyrimidine synthesis (Iwahana et al., 1996). A third CPS gene is also present in fish which utilizes glutamine for amine transfer (Chew et al., 2003). The CPS enzymes together represent an interesting protein family since they are capable of catalyzing carboxylation reactions without need of a biotin coenzyme.

Since CPS1 consumes two ATP, it represents a control point for regulation of the urea cycle since the reaction is essentially irreversible. Activity of CPS1 is tightly regulated by the presence of the obligate activator N-acetyl glutamate (NAG). NAG

synthase (NAGS) is responsible for the production of the activator using acetyl-CoA and glutamate. NAGS activity increases with levels of glutamate and therefore the concentration of NAG can serve as signal for excess amino acids in order to increase the activity of the urea cycle to accommodate increased nitrogen waste (Tuchman and Holzknecht, 1990). Structural studies have shown that NAG interacts with the C-terminal domain of the CPS1 enzyme inducing a conformational change that is necessary for both phosphorylation events as well as the formation of the tunnel to transport the carbamate intermediate between active sites (de Cima et al., 2015).

In addition to NAG as an allosteric activator, CPS1 is regulated in other ways such as post-translational modifications. Some studies have shown that deacetylation by sirtuin 5, plays an important role in activating CPS1 in response to starvation in mice (Guan and Xiong, 2011; Ogura et al., 2010). Other less well-understood PTMs have also been implicated in the regulation of CPS1 in addition to acetylation providing a complex means of regulating ureagenesis. Indeed, the role of sirtuin 5 in regulating the activity of CPS1 and other mitochondrial enzymes is not simply limited to acetylation, but other various protein acylations have been associated with alterations in CPS1 activity. Lysine succinylation and malonylation are reversible PTMs associated with CPS1 and their presence inhibits CPS1 activity (Du et al., 2011; Lin et al., 2012). Fatty acylation of the active site has been demonstrated to play a role in inactivation of CPS1 in rat liver (Corvi et al., 2001). To date CPS1 activity in amphibians has been researched in a few species including the crab-eating frog (*Fejervarya cancrivora*), a frog that can live for extended periods in brackish water. This study demonstrated that exposure to a saline environment resulted in increased hepatic CPS1 activity and an increase in plasma urea levels to help

the frog manage osmotic stress (Wright et al., 2004). Since osmotic stress is a critical feature of freezing, it follows that a similar regulation of CPS1 would be required in the wood frog.

Regulation of the urea cycle in the wood frog in response to freezing is poorly understood, although these animals are known to maintain elevated levels of urea throughout the winter period. Urea serves as a cryoprotectant in maintaining osmotic balance preventing cellular damage during freezing when present at elevated levels (Costanzo and Lee, 2005; Jørgensen, 1997). Studies have shown that CPS1 activity is maintained during the winter months, a time of general reduced metabolic expenditure, in spite of CPS1 and urea cycle activity being an energetically expensive process and an overall reduction in hepatic levels of CPS1 (Kiss et al., 2011; Schiller et al., 2008). The maintenance of CPS1 activity in the face of lowered levels of the enzyme suggests that the wood frog enhances the activity of existing enzyme molecules during the winter months via alterations in PTMs in order to maintain high levels of urea to help it to survive freezing and thawing (Kiss et al., 2011).

To understand fully the nature of regulation of the urea cycle in response to freezing in the wood frog it is necessary to evaluate the kinetic parameters of CPS1. Since this enzyme is known to be highly regulated, it is hypothesized that CPS1 in the freeze exposed frog liver will show differences in the kinetic parameters between the control and freeze-exposed forms of the enzyme. This regulation will then allow for compensation due to lower metabolic expenditure such that urea will be maintained at elevated concentrations during freezing.

Materials and Methods

Chemicals and Animals

The chemicals used in the following experiments were obtained from the same sources described in chapter 2 unless otherwise stated. NAG was obtained from TCI America (Portland, OR). Wood frogs were divided into control and frozen groups and dissected in the same manner described in chapter 2.

Enzyme Purification

Liver samples were removed from storage in a -72°C freezer and kept frozen by immersion in liquid nitrogen. Livers were quickly weighed and homogenized 1:9 w/v with a couple of crystals of PMSF in homogenate buffer A at a pH of 6.0 (50 mM HEPES, 2 mM EDTA, 2 mM EGTA, 10 mM β-mercaptoethanol, 25 mM β-glycerophosphate, 10% glycerol v/v). Samples were homogenized while being chilled with ice. Homogenized samples were then centrifuged in an Eppendorf 5810R tabletop centrifuge, pre-chilled to 4ºC, at 13,500 × g for 30 minutes. Following centrifugation, the supernatant was removed and saved while the pellet was discarded.

After centrifugation, the samples were desalted using G-25 column as described in Chapter 3 with homogenate buffer A. This was done to remove any small metabolites from the liver tissue that might interfere with the assay. Homogenized samples were loaded onto a CM bed measuring 2 cm high by 1 cm in diameter equilibrated in 15 mL of homogenate buffer at pH 6.0. The column was then washed with 15 mL of pH 6.0 buffer and fractions were collected with a fractionator at 2 mL per test tube. These fractions were tested for CPS1 activity and the highest 4 fractions were pooled and used in the next step.

A hydroxyapatite column 1.5 cm high by 1 cm wide was prepared and equilibrated in 15 mL of pH 7.4 homogenate buffer B (25 mM imidazole, 2 mM EDTA, 2 mM EGTA, 10mM β-mercaptoethanol, 20 mM β-glycerophosphate, 10% glycerol v/v). The pooled samples collected from the CM column were then applied to the hydroxyapatite surface and allowed to flow through. The hydroxyapatite column was then washed using 15 mM homogenate buffer B at pH 7.4 while collecting 2 mL fractions. CPS1 was then eluted by increasing phosphate concentration across a linear gradient from 0-500 mM (40 mL total) of phosphate in homogenate buffer B. The fractions were then assayed for CPS1 activity and the five most active fractions were pooled.

The pooled fractions were subjected to the same desalting procedure described before, eluting the protein into homogenate buffer B at pH 7.4. A Cibacron blue column was prepared (3 cm high by 1 cm in diameter) and this was equilibrated using 15 mL of homogenate buffer B. The desalted samples were allowed to flow into the column and then the column was washed with 15 mL of homogenate buffer B while collecting 2 mL fractions. CPS1 was eluted from the Cibacron blue column by a linear gradient of increasing KCl concentrations from 0-2 M with a total of 30 mL of elution while collecting 1.3 mL per tube. All the fractions were assayed for CPS1 activity and the fractions with the top five fractions pooled.

SDS-PAGE with an 8% polyacrylamide resolving gel was used to determine the purity of the sample and to demonstrate visually the efficacy of the purification protocol described. Gels were run for 45 minutes at 180V. A silver staining procedure was performed on the gel as described in Chapter 2.

CPS1 Assay

The CPS1 assay performed in the experiments was based upon a previously described enzyme coupling assay method (Kamau Machua et al., 2014). This method was altered somewhat due to the finding that Tris buffer interferes with the assay resulting in the detection of activity in the absence of ammonium and so 50 mM imidazole buffer was used instead since this did not have any non-specific background activity. This assay couples the production of ADP by CPS1 to the conversion of NAD^+ to NADH, which absorbs strongly at 340 nm. Assays were performed in clear 96 well microplates with the absorbance at 340 nm read every 21 seconds for 80 reads using a Thermo Scientific Multiskan Spectrum microplate reader. Standard assay concentrations for evaluating maximal activity are as follows: 0.3 mM NADH, 3 mM NH_4Cl, 20 mM $KHCO_3$, 5 mM NAG, 10 mM ATP-Mg^{2+}, 10 mM phosphoenolpyruvate. Each well contained 1U of pyruvate kinase (rabbit muscle, Sigma-Aldrich: P9136) and 1U of lactic acid dehydrogenase (porcine heart, Lee Biosolutions: 350-90) and 50 mM imidazole buffer at pH 7.4 and 22°C. All wells in the microplate were filled to 200 µL (Appendix II Fig. A.2.2).

Protein concentrations were determined using the Bio-Rad protein assay described in Chapter 2.

Mass Spectrometry

To ensure that the protein band purified corresponded to CPS1 the proteomics platform of the Quebec Genomics Center (Quebec City, Canada) analyzed samples obtained through SDS-PAGE of the purified protein. The purified protein band from the

control wood frog liver around 165 kDa in the 8% gel after Coomassie staining was excised using a razor blade and destained overnight to remove any excess Coomassie stain. This gel sample was sent to the proteomics platform of the Quebec Genomics proteomic analysis. Data was analyzed in the same way as in Chapter 3.

Western Blots

Western blotting procedures were performed according to the procedures described in Chapter 2 to identify the relative levels of different PTMs on CPS1. In addition to the antibodies described in Chapter 2 several other antibodies were used diluted 1:2000 in TBST as follows:

1. Anti-succinyllysine (PTM Biolabs, PTM-401)
2. Anti-malonyllysine (PTM Biolabs, PTM-901)
3. Anti-glutaryllysine (PTM Biolabs, PTM-1151)
4. Anti-glutathione (Santa Cruz, sc-52399)

Differential Scanning Fluorimetry

Differential scanning fluorimetry was performed in the same manner as described in Chapter 2. Concentrations of 0.03 mg/mL of purified CPS1 were used for both the control and frozen trials.

Results

Purification

Purification was performed in a three-step process that gave a 25.7% yield of CPS1 activity. The first step was using a CM cation exchange column to remove

positively charged proteins from the crude. This step returned all of the CPS1 activity and removed numerous other proteins resulting in a 1.56 fold purification from the crude (Table 4.1). The next step of the purification used a hydroxyapatite column and an elution with increasing phosphate concentration. This step yielded about 50% of the activity from the previous step but removed considerable amounts of impurities as seen in an SDS-PAGE gel (Fig. 4.1). Following desalting of the CPS1 sample, it was applied to a Cibacron blue column and eluted by increasing KCl concentration from 0-2 M. The whole purification had a fold purification of 4.85 times (Table 4.1). Using an SDS-PAGE gel, it was demonstrated that the enzyme was purified to homogeneity (Fig. 4.1).

Kinetics

Assaying purified CPS1 demonstrated several differences between the control and freeze-exposed enzyme. The freeze-exposed form of the enzyme demonstrated a higher V_{max} than the control versions of the enzyme (1.26 fold difference, Table 4.2). Analysis of the affinities of the control and frozen enzyme revealed several differences. The K_M for ammonium was lower in the frozen under standard assay conditions as well as in the presence of 100 mM urea. The frozen K_M for ammonium in the presence of glucose was not statistically different from the control, but this may be due to higher error seen here since overall urea and glucose did not seem to have any effect on the K_M for ammonium. (Fig 4.2). The K_M for ATP was the same under standard conditions between the control and frozen CPS1, however the addition of glucose resulted in a decrease in the ATP K_M for both the control and frozen CPS1. This decrease in K_M was more pronounced in the frozen enzyme, which resulted in the control and the frozen K_M values being significantly different in the presence of glucose (Fig. 4.2). Similarly, the K_M for bicarbonate was

shown to be similar between the control and the stress CPS1. The addition of urea increased the K_M for the control CPS1, but not for the frozen CPS1. The presence of urea thereby resulted in a difference between the K_M bicarbonate of control and the stress CPS1. NAG is an obligate activator for CPS1 and is therefore critical in regulating the activity of the enzyme. The activator constant K_A is the concentration of the activator that results in half-maximal activity. This value was the same for the control and the freeze-exposed enzyme under standard conditions, however the addition of 400 mM glucose significantly lowered the amount of activator needed to reach half-maximal activity for both conditions. This effect however, was more drastic for the frozen CPS1 than the control CPS1 and resulted in the frozen K_A being significantly lower than the control in the presence of glucose.

Two TCA cycle intermediates were noted to be inhibitors of CPS1 at high concentrations. The I_{50} values for both succinate and malate were noted to be lower in the control than the frozen, meaning that less of these metabolites would be needed to cause a reduction in the activity of CPS1. The effects of urea on CPS1 activity was also noted. The I_{50} for control (0.94 M) was noticeably higher than the frozen (0.65 M).

Mass Spectrometry

The identity of the protein band in the purified control and frozen sample was determined to be CPS1 using mass spectroscopy. Using the Mascot search engine on the peptide fragments generated showed 48% coverage of the bullfrog (*Rana catesbeiana*) CPS1 sequence for the control and 47 % for the frozen. The molecular weight of the CPS1 monomer is approximately 164 kDa. (Appendix I: Fig. A.1.2.).

PTM Western Blots

Analysis of relative levels of various PTMs through western blots using antibodies specific for PTMs demonstrated that the control CPS1 had a significantly higher degree (1.42 fold) of glutarylation on lysine residues than the frozen CPS1 (Fig. 4.3).

Differential Scanning Fluorimetry

Use of differential scanning fluorimetry on the purified CPS1 from the control and freeze-exposed wood frog livers demonstrated that the unfolding temperature (T_m: the temperature causing half-maximal fluorescence) was significantly lower in the frozen than in the control wood frog (control T_m = 54.4 ± 0.2 °C, frozen T_m = 52.9 ± 0.2 °C, Fig. 4.4). The addition of 100 mM urea significantly lowered the thermal stability of the control enzyme down to the same stability as the freeze-exposed CPS1 without urea. Addition of 100 mM urea to the freeze-exposed enzyme did not significantly change the thermal stability of the enzyme.

Table 4.1. Representative purification scheme of CPS1 from the liver of a control wood frog in three steps. The first step used the cation exchange column CM to act as a filter removing positively charged proteins at pH 6.0. The second step used hydroxyapatite at pH 7.4 and was eluted by increasing phosphate concentrations from 0-500 mM. The third step used a Cibacron blue column where CPS1 was eluted with 0-2 M KCl.

Step	Total Protein (mg)	Total Activity (mU)	Yield (% activity)	Fold Purification	Specific Activity (mU/mg)
Crude	9.03	218.6	NA	NA	24.2
CM	4.07	154.3	70.5	1.56	37.9
Hydroxyapatite	1.13	63.3	28.9	2.30	55.7
Cibacron Blue	0.480	56.3	25.7	4.85	117.3

Table 4.2. Comparison of the inhibitory effects of urea, succinate, and malate on the activity and the maximal velocity of purified CPS1 from control and frozen *Rana sylvatica* liver. All assays were performed at 22°C in pH 7.4 50 mM imidazole buffer. Data represent the means, n=4 ± SEM. '*' indicates significantly different from control where $p < 0.05$ in Student's t-test.

	Control	Frozen
V_{max} (mU/mg)	117.3 ± 5.0	148.5 ± 2.8*
Succinate I_{50} (mM)	63 ± 5	88 ± 4*
Malate I_{50} (mM)	55 ± 9	101 ± 7*
Urea I_{50} (M)	0.94 ± 0.06	0.652 ± 0.008 *

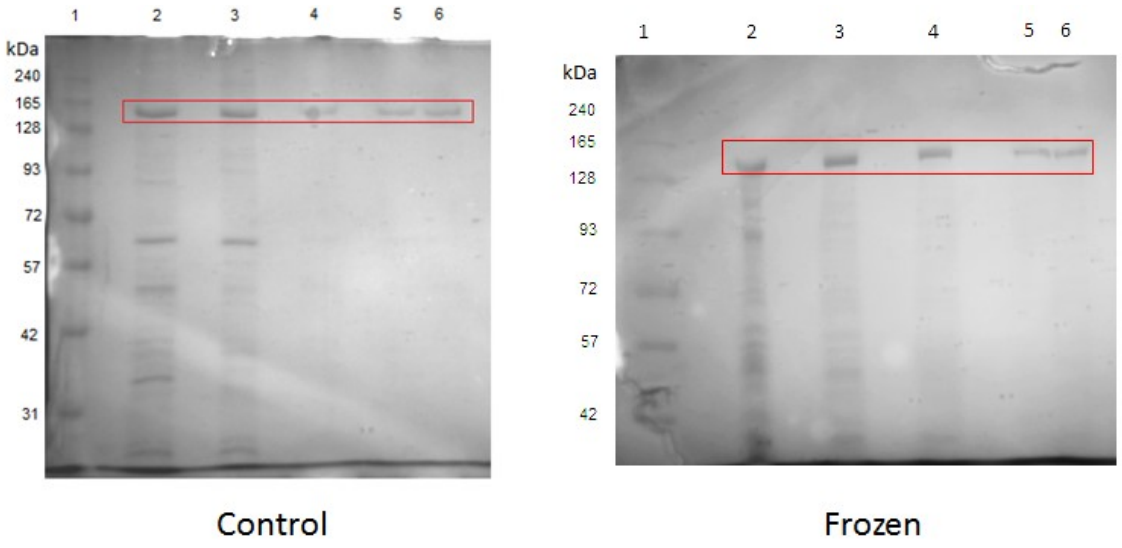

Fig. 4.1. Silver stained SDS-PAGE gel demonstrating purification of CPS1 from control and frozen wood frog liver. Lanes are as follows: 1: Genedirex BLUelf protein ladder 3-240 kDa, 2: Wood frog liver 5x diluted, 3: filtration through CM at pH 6.0, 4: elution from hydroxyapatite using 0-500mM phosphate, 5-6: elution from Cibcaron blue using 0-2 M KCl. 10 µL of sample were loaded into each well of the gel. The protein band in the box represents the CPS1 monomer.

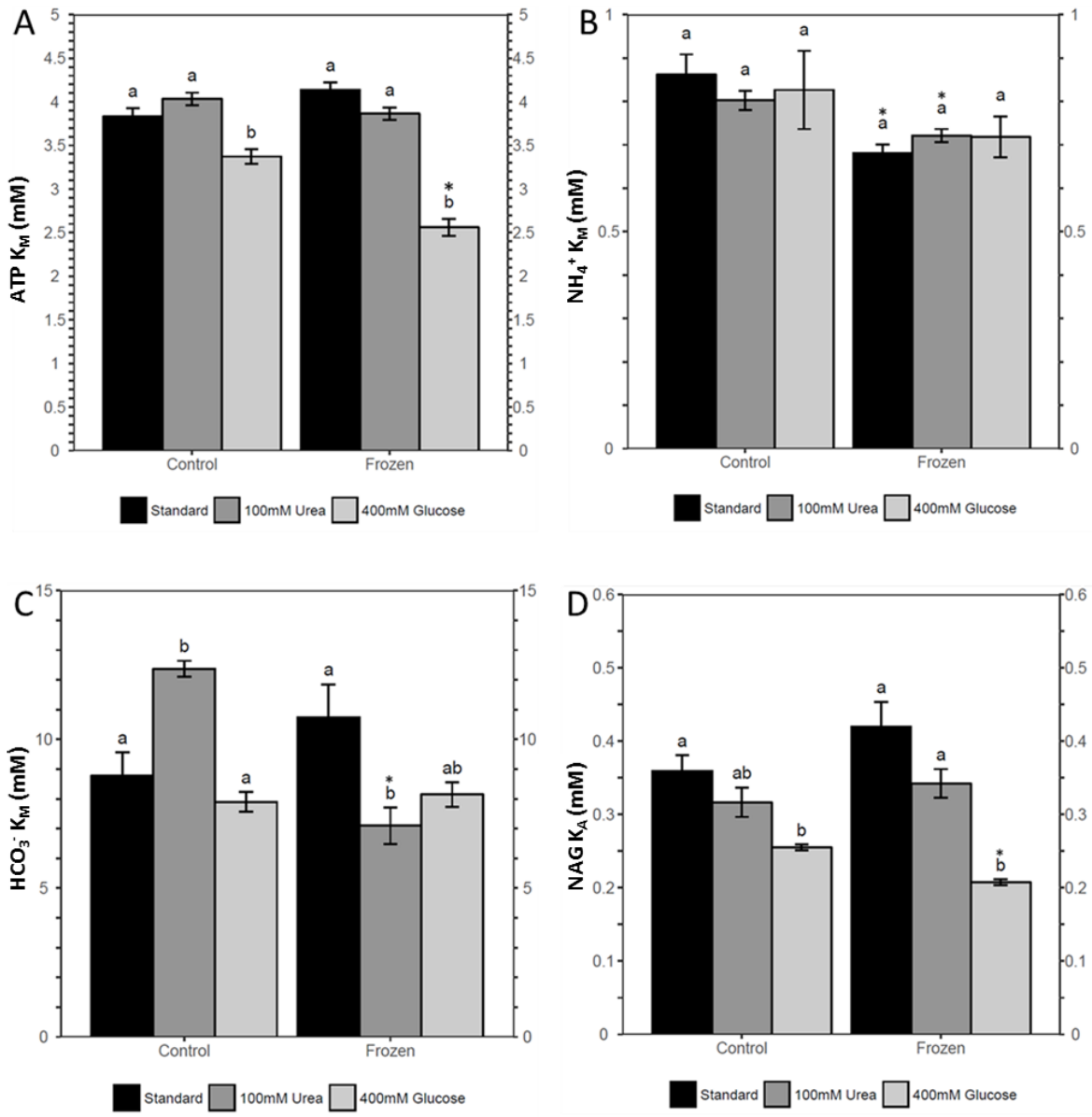

Fig. 4.2. The effects of 100 mM urea and 400 mM glucose on the *R. sylvatica* liver control and frozen CPS1 affinities for A) ATP K_M, B) NH_4^+ K_M, C) HCO_3 K_M and D) NAG K_A. Data represent means n=4 ± SEM. '*' denotes a difference between the control and respective frozen parameter determined by Student's t-test $p<0.05$. One way ANOVA analyses were run to determine significant differences due to the addition of 100 mM urea and 400 mM glucose, differences are represented by the letters (a, b) above the bars deemed to be different with a Tukey's post hoc test $p<0.05$. All assays were performed at 22°C in pH 7.4 50 mM imidazole buffer.

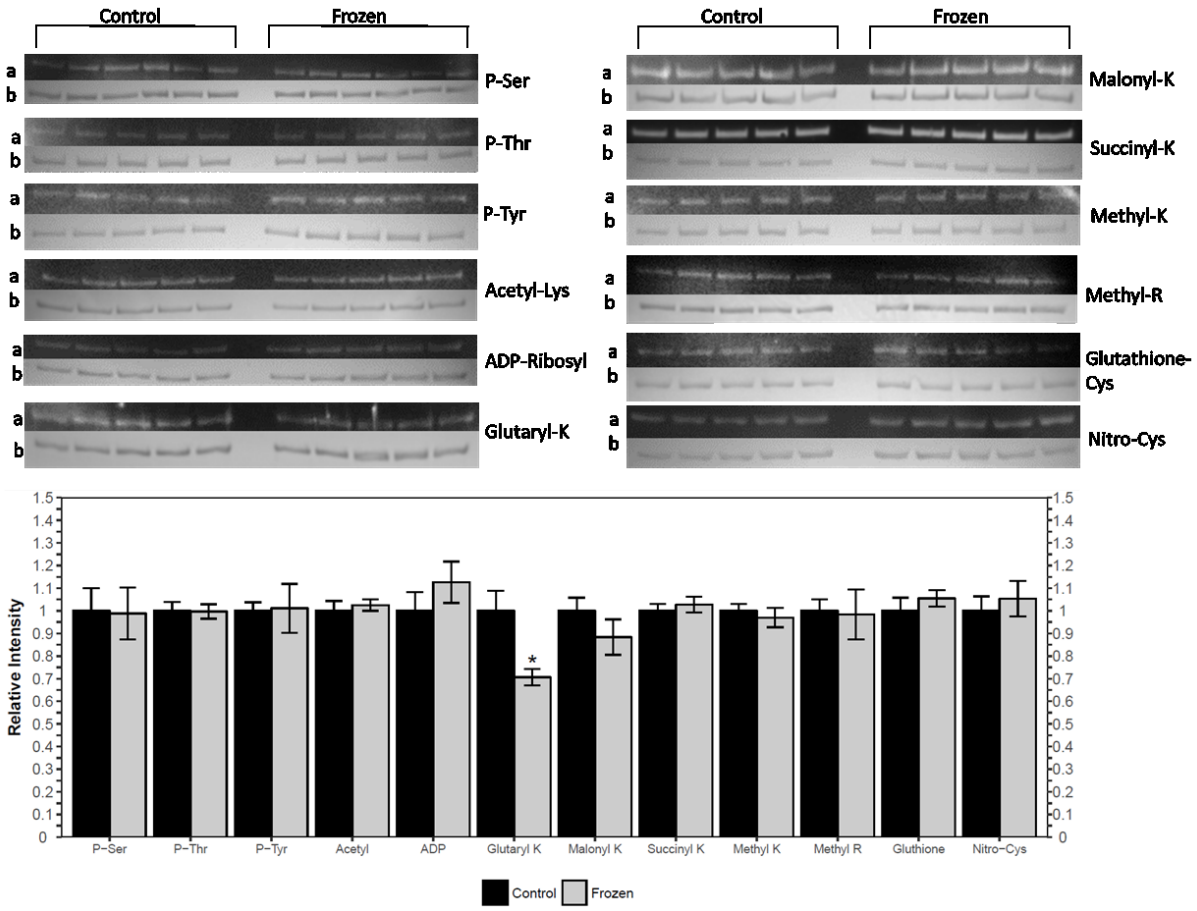

Fig. 4.3. Summary of the western blots performed to ascertain the differences in posttranslational modifications of purified CPS1 from control and frozen *R. sylvatica* liver. 'a' demonstrates the ECL signal for a particular PTM quantified and 'b' represents the Coomassie stained CPS1 bands.'*' indicates that the frozen is significantly different from the control for a given PTM, Student's t-test $p<0.05$.

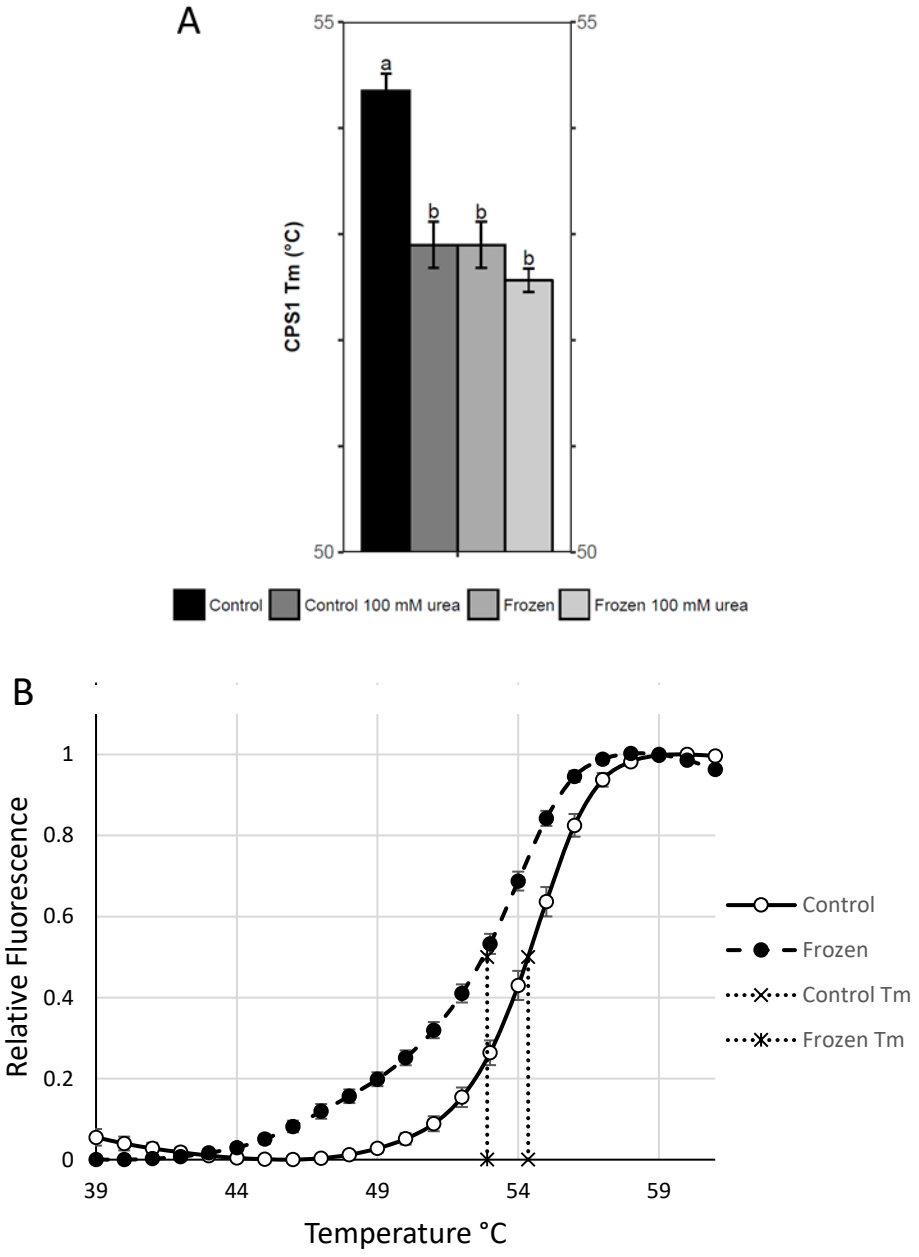

Fig. 4.4. A) The melting point (T_m) in °C for purified CPS1 from control and frozen *Rana sylvatica* liver with and without 100 mM urea at pH 7.4 determined by differential scanning fluorimetry (DSF). Letters above the bars represent the results of a one-way ANOVA used to compare the data with a Tukey's post hoc test to determine significant differences in the data ($p<0.05$). Data represents means n=6 ± SEM. **B)** Demonstrating relative fluorescence due to CPS1 unfolding with increasing temperature during DSF in the control and frozen purified enzyme with the relationship to T_m shown.

Discussion

The urea cycle is an important metabolic pathway that is well understood, but its regulatory importance to the wood frog in regard to the physiological changes accompanying freezing has not yet been explored. CPS1 represents a crucial control point through the urea cycle in the liver as it mediates an energetically expensive reaction that consumes two ATP and is therefore essentially irreversible. The ATP requirement and CPS1 mediating the rate limiting step of the urea cycle make CPS1 a likely site for metabolic regulation in response to freezing (Summar et al., 2004).

Analysis of the kinetic parameters of purified CPS1 demonstrated that the frozen enzyme had slightly higher affinity for ammonium than the control enzyme. This pattern held true when 100 mM urea was added to the well (Fig. 4.2). A similar pattern was seen when 400 mM glucose was added to the well, however the difference was not statistically significant. This increased affinity for ammonium indicates that there are two distinct forms of CPS1. This was further suggested by differences between the freeze-exposed and control enzymes' affinity for HCO_3^- and ATP in the presence of urea and glucose respectively. The K_A of the obligate activator NAG was similar between the control and freeze-exposed CPS1 except for the results obtained with the addition of 400 mM glucose in which the freeze-exposed CPS1 K_A was lower. The increased affinity for its substrates in the freeze-exposed form of the enzyme in response to the presence of cryoprotectants, notably glucose, suggests that the freeze-exposed CPS1 is being modified to function at higher a rate than the control even if substrate levels become lower. The V_{max} seen in the frozen also suggests the enzyme is being activated by some modification to its structure in response to freezing (Table 4.1). Glucose seems to have caused a pronounced increase

in the affinity for both ATP and NAG in both control and freeze-exposed CPS1 despite the change being more noticeable in the frozen. This demonstrates the importance that the high concentrations of glucose during freezing play in regulating flux through the urea cycle. The importance of physiologically relevant metabolites in response to metabolic stress on the functioning of enzymes has been noted before in the African clawed frog *Xenopus laevis.* This frog is known to produce large quantities of urea during periods of dehydration and physiological concentrations of urea have been shown to play an important role in regulating the estivated liver lactate dehydrogenase affinity for its substrates (Katzenback et al., 2014). The increase in I_{50} for succinate and malate in the freeze-exposed CPS1 suggests that these TCA cycle intermediates inhibit the activity of the urea cycle less during freezing. This may be important in the wood frog since freezing often accompanies reduced oxygen availability to the tissues that can result in accumulation of succinate (Solaini et al., 2010).

The increase in affinity for NAG due to the presence of 400 mM glucose may be necessary to maintain activity of CPS1 during freezing as NAG levels may be depleted. NAG is a small molecule generated from glutamate and acetyl-CoA by NAGS. Due to the increase in activity of GDH to supply ammonium ion needed to enter the urea cycle in the liver glutamate and by extension NAG may be limited during periods of freezing. Indeed glutamate levels are known to be reduced in the liver as a result of freezing by about 2.4 fold (Storey and Storey, 1986). Presumably, acetyl-CoA levels would also be greatly diminished during freezing due to cessation of aerobic glycolysis. As a result, elevated concentrations of glucose accompanying freezing may play a role in sensitizing CPS1 to NAG to maintain urea cycle activity during the winter.

Urea is a chaotropic agent at high concentrations and therefore sufficient concentrations of this metabolite will denature CPS1. The concentration required to reduce the activity by half was less for the freeze-exposed variant of the enzyme than for the control (Table 4.2). However, the concentrations were considerably higher than what would ever be found in the animal so these differences do not likely represent an *in vivo* functional effect of urea on the CPS1 activity in the liver of the frog. Instead, they provide information about the relative stability of the control compared to the freeze-exposed CPS1 since the mechanism of action on the activity at these concentrations is likely destabilization of the protein structure itself. This suggests that the freeze-exposed variant of the enzyme is less stable than the control. This observation was further supported by the DSF data, which demonstrated that the frozen had a decreased thermal unfolding point by 1.46°C (Fig. 4.4). The lowered stability of the freeze-exposed enzyme might suggest that the enzyme is optimized for functioning at lower temperatures that would be present during bouts of freezing. It is well known the thermal stability of an organism's enzymes is largely dependent upon pressures of thermal denaturation. Animals accustomed to life at cold temperatures, psychrophiles, have low stability enzymes as this helps to maintain their function to counteract the activity-lowering effects of frigid temperatures (Struvay and Feller, 2012). Conversely, hyperthermophiles have very stable enzymes and cellular components to prevent denaturation and resultant cellular death (Vieille and Zeikus, 2001). For the wood frog, which endures a wide range of change to its ambient temperature and has no means of controlling internal body temperature, it is possible that the ability of modifying enzymes critical for basic

metabolic processes to adapt to temperature could be helpful in ensuring survival during winter freezing.

The differences in kinetic parameters and the changes in stability suggest that CPS1 in *Rana sylvatica* liver is post-translationally modified in order to regulate the activity of the urea cycle. Western blot analysis suggested that control over lysine glutarylation might be linked to the two distinct sets of enzymatic and structural properties seen between control and freeze-exposed CPS1. It has been seen before that glutarylation on lysine residues plays a role in the regulation of CPS1 activity in mammalian models and cell lines (Tan et al., 2014). This is consistent with what was demonstrated in the present study since lower maximal activity as well as reduced affinity for ATP and NAG in the presence of 400 mM glucose and a reduced affinity for ammonium ion in all conditions were noted in the more highly glutarylated form. Glutarylation is reversible by the mitochondrial deacetylase sirtuin 5 and therefore glutarylation may serve as an important regulatory aspect of urea cycle control during freezing for the wood frog as it is rapidly reversible (Tan et al., 2014).

The results discussed here suggest that CPS1 is regulated by PTM in response to freezing in the liver of the wood frog. Improvements in affinity for ammonium in the freeze-exposed CPS1 and increased affinity for ATP and NAG in the presence of physiological levels of glucose in both the control and frozen CPS1 suggest that its regulation is related to both changes in the enzyme itself as well as responding to relevant concentrations of metabolites associated with the entrance into freezing.

Chapter 5

General Discussion

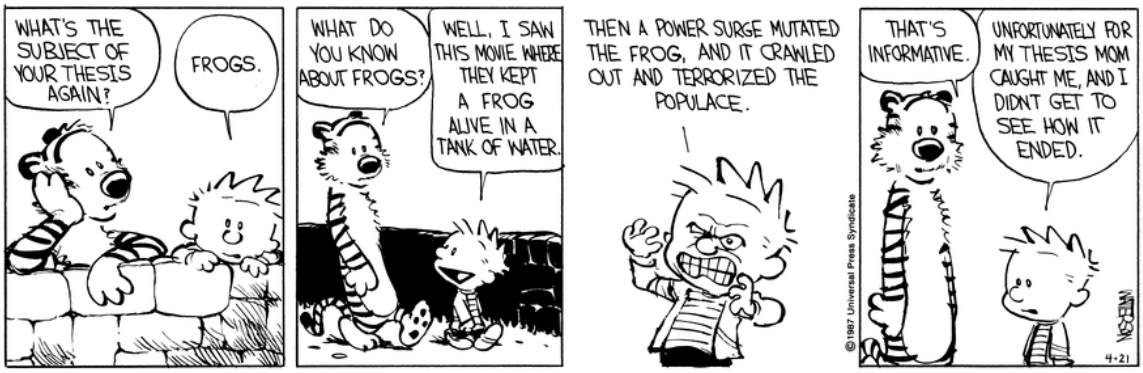

General Discussion

Freeze tolerance is one of the most extreme ectothermic survival strategies employed in nature and is limited to only a handful of known species of vertebrates. Freezing presents a host of physiological problems that the animal must be properly equipped to endure including managing osmotic balance of cells, preventing intracellular ice formation, controlling formation of extracellular ice, avoiding tissue damage due to ice recrystallization, reducing metabolic expenditures, surviving ischemia due to freezing of blood, and avoiding reperfusion injury post-thaw (Storey and Storey, 1988). Most ectothermic vertebrates avoid such extensive physiological obstacles by avoiding freezing entirely during winter through options including seeking shelter under water (e.g. many species of turtles and frogs) or retreating to a well-insulated hibernaculum deep underground where the temperature is more moderate. Freezing of the wood frog however enables them to emerge from winter dormancy earlier than other species allowing them to utilize temporary vernal ponds formed by melt water for early breeding. This permits them to occupy a distinct ecological niche and give their offspring more time to develop into mature frogs before the next winter.

The existence of freeze tolerance mechanisms in several frog species may be related to a broader amphibian ability to survive dehydration and anoxia stresses. These stress responses are highly developed since anurans have very permeable skin that is prone to water loss (Churchill and Storey, 1995) and also many species spend much of their lives underwater where they may lose access to oxygen (Currie and Boutilier, 2001). Freeze-tolerance requires a strong ability to cope with both of these stresses since

dehydration of cells is needed to quickly lower the freezing point of the cytoplasm and thereby avoid intracellular freezing and anoxia is inevitable when the blood freezes (Gerber et al., 2016). The production of urea as an osmoprotectant is well understood in many amphibian species as a way to cope with dehydration stress and also represents an important cryoprotectant in the wood frog (Costanzo et al., 2013). The aim of this thesis was to understand the enzymatic regulation behind the production of urea in response to freezing in the wood frog liver.

The use of urea to supplement glucose as a cryoprotectant to can be important in helping the liver avoid freeze damage as it has been noted that urea functions as a cryoprotectant during freezing and the production of urea increases in liver tissue during freezing (Costanzo et al., 2015). Urea is somewhat unstable in aqueous solutions since it undergoes 2 sequential hydrolysis reactions to reform ammonium and bicarbonate (Raab, 1991). Under normal physiological conditions, this is not an issue since urea is usually a metabolic waste and is regularly excreted faster than ammonia can form, but due to the high concentration of urea in the frog's liver and other tissues and the extended period spent between thaws it is a possible source of cellular ammonium ion accumulation (in addition to that produced from degradation of nitrogenous wastes). The maintenance of high quantities of urea over extended periods might then result in increased risk of elevated ammonium ion concentrations unless the activity of the urea cycle is maintained at relatively high levels during freezing. Indeed, it is known that ammonium concentrations are elevated during freezing in the wood frog liver; this is possibly due to continued consumption of glutamate and amino acids during freezing which in turn can supply more substrate for the urea cycle (Storey and Storey, 1986). Since the

concentration of urea is greatly increased and the wood frog cannot excrete urea due to its blood being frozen, it is possible that increased urea cycle activity is important in removing excessively toxic levels of ammonium that may be generated through processes such as GDH activity or hydrolysis of urea, thereby maintaining higher concentrations of cellular urea.

The role of urea as a cryoprotectant may become more important during prolonged bouts of freezing since the tissue would primarily rely on anaerobic glycolysis to provide its energy needs because oxygen supply is cut off from the liver tissue. Lowered glucose levels over the course of prolonged freezing due to anaerobic glycolysis may also necessitate rising urea levels to compensate for a reduction in concentration of this important cryoprotectant. Experimental evidence also suggests that transport of urea from the liver to other tissues prior to freezing and during periods of thawing is limited, whereas large quantities of glucose are generated rapidly from glycogenolysis and transported to all other tissues during the early hours post-nucleation to act as a cryoprotectant (Costanzo et al., 2015). The increase in liver urea concentrations may help to offset any decrease in liver glucose cryoprotection related to subsequent freeze-thaw cycles in the liver due to transport of glucose from the liver to other organs in the body.

To investigate the regulation of urea production in the wood frog liver, the functional parameters of three enzymes involved in the production of urea were analyzed. Urea is produced in the liver through the action of the urea cycle. The studies contained herein investigated the functionality of two urea cycle enzymes, OTC and CPS1, and of GDH since this latter enzyme has an important role in deaminating amino acids and thereby controlling the availability of ammonium ion substrate for the urea cycle. Many

enzymes are regulated by means of PTMs. While other forms of regulation exist, PTMs offer considerable advantages over regulation at the level of transcription or translation. In cases of reduced metabolic activity it is not desirable to regulate metabolic pathways by producing more protein or degrading existing protein since this is energetically wasteful. This is particularly true of enzymes involved in high flux metabolic pathways that make bulk quantities of metabolites such as the urea cycle since cellular concentrations of these proteins tends to be quite high (Oliveira and Sauer, 2012). This is contrasted to signaling kinases or transcription factors that are found at lower concentrations and therefore small changes in their expression can elicit large downstream physiological changes. Exploiting small reversible molecular covalent modifications to enzymes allows for control of metabolic pathways by directly manipulating the activities of the enzymes and is therefore more energetically efficient. For these reasons, it was hypothesized that regulation over the production of urea would occur via modification of key enzymes to maintain urea cycle activity in the wood frog liver despite overall reductions in metabolism at temperatures near or below 0°C.

Glutamate Dehydrogenase Regulation in Freezing

GDH is an important enzyme in many organisms from a regulatory perspective owing to its role in bridging amino acid metabolism and TCA cycle. Following proteolysis, amino acids can be mobilized as a fuel source for cellular energy production through catabolism of their carbon backbones via the TCA cycle. The production of ammonium due to the action of GDH in the oxidative deamination reaction is therefore typically thought to represent a waste product. Ammonium in many terrestrial vertebrates is incorporated quickly into urea through the urea cycle (and moved to the kidneys for

excretion from the body) and therefore GDH (with high activities in liver) represents an important regulatory step. The results of this study demonstrated an increase in the activity of both directions of the GDH reaction, although the glutamate consuming direction is more physiologically relevant under most conditions owing to the very high K_M for ammonium in the opposite direction of the reaction (Li et al., 2009). This suggests that an increase in the consumption of cellular glutamate will occur during freezing. At first, this may seem counterintuitive since the TCA is reliant upon oxygen that is in low availability during freezing and the wood frog is known to generate most of its cellular energy during freezing from glycolysis as noted by increased lactic acid concentrations in all tissues (Storey and Storey, 1984). However, it has been noted that urea concentrations in the wood frog liver increase over the course of freezing (Costanzo et al., 2013). GDH may play an important role in allowing continued production of urea during freezing by supplying ammonium for the urea cycle (Lee et al., 1982). Urea helps to act as a cryoprotectant in the wood frog as well as being important in ameliorating freeze induced dehydration wood frog, thereby suggesting that increases in GDH activity as well as the affinity for its substrates are important in the freeze response of the wood frog liver (Costanzo and Lee, 2005; Muir et al., 2008).

OTC

OTC is the second of two urea cycle enzymes located within mitochondria. Research into the role of OTC in regulating the urea cycle has been limited. However, one study has demonstrated that acetylation on a specific lysine residue in OTC inactivates the enzyme in response higher glucose levels in mammals (Yu et al., 2009).

The results from this study demonstrated an increased affinity for ornithine in the freeze-exposed form of the enzyme relative to the control. Despite the increase in affinity for this substrate, levels of OTC activity in the liver relative to the total amount of protein in crude extracts remained similar. This suggests a maintenance of urea cycle activity throughout freezing. The increased affinity of OTC for ornithine by the freeze-exposed form of the enzyme could function to encourage flux through the urea cycle while reducing access of ornithine to competitive pathways. Ornithine is also consumed by ornithine aminotransferase in the production of the amino acids proline and glutamate (Morris, 2002). Due to restriction on protein translation during freezing, it seems unlikely that amino acids would continue to be synthesized, thus by increasing OTC affinity for ornithine this may prevent unnecessary production of proline or glutamate for protein synthesis. Ornithine decarboxylase (ODC) catalyzes the first committed and rate-limiting step of polyamine synthesis by producing putrescine from ornithine. The roles of polyamines are diverse and not completely understood, however, the principal role of polyamine biochemistry is their ability to promote DNA replication and cell growth and division (Landau et al., 2010; Soda, 2011). Cell growth and division is undesirable during periods of metabolic rate depression, therefore, the increase of OTC affinity for ornithine during freezing may serve as a way to reduce production of polyamines by limiting the polyamine synthetic pathway access to its initial substrate. Alaskan populations of the wood frog are known to accumulate high concentrations of amino acids in the plasma through catabolism of skeletal muscle in preparation for freezing to help build glucose and urea stores (Costanzo et al., 2015). Although the degree that this occurs in wood frogs from further south regions such as Ottawa like those used in the study is unknown,

a rise in amino acid concentration would require the wood frog to have metabolic strategies to prevent flux through the polyamine pathway despite increases in amino acid concentrations. Reduction in flux through the competitive polyamine synthesis pathway would also help to encourage production of urea. The results suggest that OTC is modified to encourage production of urea during freezing in the wood frog liver.

CPS1

CPS1 represents the rate-limiting step of the urea cycle and is essentially irreversible due to the highly energetically favourable consumption of two ATP in producing CP (Nakagawa and Guarente, 2009). For these reasons, CPS1 is considered a major regulatory point for the urea cycle. Regulation over CPS1 activity is often in the form of the activator NAG that is necessary for activity. NAG acts as a sort of indicator of abundance of free amino acids as it is derived from glutamate, a common intermediate in the catabolism of proteins (Caldovic and Tuchman, 2003). For this reason, when considering the regulation of CPS1, it is critical to analyze the affinity of CPS1 for NAG as well as its substrates.

Improved affinity for the obligate activator NAG in the presence of 400 mM glucose as seen in the Chapter 4 would help to improve the activity of the enzyme during freezing. This is especially important because GDH activity was noted to be increased which could lead to lower levels of NAG since this metabolite is derived from glutamate through N-acetyl glutamate synthase. The increased affinity for NAG of freeze-exposed relative to control CPS1 in the presence of glucose further emphasizes the importance of CPS1 activity for freeze-survival. Glucose was also found to improve the affinity for ATP in both the freeze-exposed and control enzyme, with the freeze-exposed enzyme

demonstrating an improved affinity for ATP relative to the control. Lowered concentrations of ATP might be expected during freezing owing to the hypoxic/anoxic state placed on the tissues. Therefore, the heighted affinity for ATP of CPS1 resulting from increases in glucose cryoprotectant concentrations is likely important in ensuring that the urea cycle continues to function in the liver during freezing despite reduced ATP levels (Storey and Storey, 1984). Improvement in the CPS1 affinity for ammonia was another conspicuous difference between the control and freeze-exposed forms of the enzyme. This along with the decrease of ammonium ion affinity for the frozen form of GDH in the presence of glucose would help to prevent GDH from consuming ammonium back into glutamate and, thereby, facilitate flux of ammonium through the urea cycle. Overall, the results suggest that wood frog liver CPS1 is regulated to improve flux through the urea cycle during freezing by both innate responses to glucose concentrations that increase greatly during freezing but also by changes to protein structure.

Enzymatic Regulation by Protein Modification

The three enzymes examined in this thesis are all located within the mitochondrial matrix of wood frog liver. Because of this it was postulated that similar regulatory mechanisms might exist for all three. However, whereas there were documented changes in the post-translational modifications in comparisons of the control and freeze-exposed forms of each of the enzymes, no common regulatory mechanism was found between these three. GDH was noted to display a decreased level of ADP-ribosylation and lysine acetylation in its frozen form (Herrero-Yraola et al., 2001; Schlicker et al., 2008). This is suspected to be related to the increased activity of the freeze-exposed form of the enzyme since these changes have also been documented to lead to increased GDH activity in

other vertebrates in relation to starvation stress. The increase in lysine methylation of freeze-exposed GDH relative to control is of unknown significance since this modification has only previously been documented for GDH of thermophilic archaea (Maras et al., 1992). Lysine acetylation in humans is known to be a negative regulator of OTC activity (Yu et al., 2009). No change in the acetylation of OTC lysine residues was noted in this study and this is somewhat surprising given that acetylation is commonly used as a way to regulate activities of mitochondrial proteins including OTC and was shown to play a similar role in GDH control in this study (Ghanta et al., 2013; Hallows et al., 2011). The lack of change in the acetylation patterns of CPS1 might also suggest that this PTM might not play as important a role in urea cycle function in this species as it does in mammalian models (Nakagawa et al., 2009).

The significance of lysine glutarylation is not widely understood as a PTM in enzymatic regulation, however it has been noted in prior to studies to play a role in suppressing the activity of CPS1 (Tan et al., 2014). This modification has been associated with proteins that are also noted to be modified via acetylation and succinylation (Xie et al., 2016). Glutarylation of proteins is believed to occur through a non-enzymatic process that is similar in function to other acylation (acetyl, succinyl, malonyl) events through the transfer of glutarate via glutaryl-CoA (Hirschey and Zhao, 2015). Glutaryl-CoA is an intermediate in lysine metabolism in the mitochondria related to production of acetoacetyl-CoA that has multiple metabolic fates. Interestingly, levels of lysine are elevated in the frozen frog liver compared to controls (Storey and Storey, 1986), perhaps explaining the reduction in glutarylation in frozen frogs owing to a decrease in the flux through this pathway and a resulting decrease in the availability of glutaryl-CoA.

Glutaryl lysine modifications can be removed from proteins through the action of sirtuin 5, which serves as a deacetylase/deacylase in the mitochondria. In this regard the decrease in GDH acetylation levels may be related to the decrease in CPS1 glutarylation levels since both of these modifications can be removed through the action of sirtuin 5 (Nakagawa and Guarente, 2009; Tan et al., 2014).

Phosphorylation is a well-documented PTM that has been long associated with regulation of metabolic pathways. Understanding of protein phosphorylation is complicated by a plethora of different kinases and phosphatases affecting different amino acids. Whereas many kinases have consensus sequences that are known, predicting phosphorylation based sequence information can be hampered by the influence of many different factors such as the activity of relevant phosphatases, tertiary or quaternary structure of the protein, and subcellular compartmentalization separating kinases and potential targets. The best-characterized kinases are the serine/threonine kinases with tyrosine kinases being less common. In addition to these O-phosphorylated residues, there are rarer phosphorylation events whose regulatory roles are not well characterized such as phosphorylation of histidine, arginine, lysine, aspartate, glutamate and cysteine (Buchowiecka, 2014; Fuhrmann et al., 2013; Fuhs et al., 2015). OTC was noted to have increased phosphorylation on serine residues in response to freezing; suggesting that this enzyme could be regulated through phosphorylation to increase the affinity for ornithine as discussed earlier.

Thermal Stability

The thermal stability of a protein is a measurement indicating the temperature at which a protein will unfold. The unfolding temperature was determined using DSF for

GDH and CPS1. In both cases, the control enzyme demonstrated increased thermal stability relative to the freeze-exposed form of the enzyme. These results not only demonstrate a stable structural difference exists between the different forms of the enzyme but also may suggest functional relevance. Lowered thermal stability at first may seem undesirable to animals in reduced metabolic conditions since they are more prone to loss of function due to unfolding. However, adoption of a more flexible conformation can help to promote activity of the enzyme and offset the effects of low temperatures that typically increase the structural rigidity of an enzyme .

Conclusion

The research conducted demonstrates the importance of nitrogen metabolism during freezing in the wood frog. Improvements in the affinity of the urea cycle enzymes OTC and CPS1 as well as GDH for their substrates demonstrates that during freezing the wood frog is likely able to maintain activity and control over key reactions in urea production. Greater maximal activity of CPS1 and GDH in the freeze-exposed form of the enzyme also supports this idea. Taken together these results highlight the importance of urea as a metabolite of interest in anuran freezing survival where it can act as an important agent in regulating cell volume during osmotic stress accompanying freezing by helping to prevent cell volume from shrinking below a critical minimum during extracellular ice formation. Differences in PTM profiles between control and frozen enzymes suggests that these slight alterations to protein structure provide an important regulatory aspect governing the metabolic alterations associated with hypometabolism and the freeze response in the wood frog that lead to changes in nitrogen metabolism.

Future Directions

Several other urea cycle enzymes exist that could be studied in the future. Arginase catalyzes the final step of the urea cycle by regenerating ornithine from arginine and releasing urea into the cytosol and may be important in determining the overall regulation of the urea cycle. Arginine is an important metabolic intermediate involved in several other pathways in the liver, including protein, nitric oxide, and creatine biosynthesis (Morris, 2007). Therefore, understanding the functional parameters of arginase may be important in fully ascertaining the regulatory features that control the production of urea. Little is known about arginase regulation in other organisms at the post-translational level, although regulation at a transcriptional level has been demonstrated in macrophages to play an important role in regulating nitric oxide production via competition with nitric oxide synthase for the substrate arginine (Morris et al., 1998). To date no work has been completed on the regulation of arginase activity in animals undergoing reversible hyperuremia such as the wood frog. Arginase activity may be assayed via a coupled enzyme system involving urease and GDH with monitoring of the oxidation NADH by GDH (Ozer, 1985). In this assay urease generates 2 moles of ammonium ion for every mole of CO_2 made and then GDH can oxidize NADH through reductive amination of α-KG.

The activity of pathways branching from the urea cycle might also be of relevance in understanding the physiological role of the urea cycle in freezing survival. One such pathway is the polyamine biosynthesis pathway. This pathway intersects with the urea cycle by competing with OTC through the actions of ornithine decarboxylase (ODC). ODC removes the carboxyl group from ornithine to generate putrescine, the first committed and rate limiting step of polyamine synthesis. Polyamines are a class of

compounds that have varied and unclear roles, but generally their most established roles are in encouraging protein synthesis, cell growth and division (Igarashi and Kashiwagi, 2010; Miller-Fleming et al., 2015). As such, it is likely that ODC and polyamine biosynthesis have lower activities in reduced metabolic states such as freezing. Analysis of total polyamine levels has not been performed in the wood frog in response to freezing and could be investigated. ODC activity is often related to the level of the ODC antizyme that targets it for degradation. Measuring the ratio of ODC and the ODC antizyme through western blots may therefore give a good indication of the relative rate of polyamine synthesis between control and stress states (Gandre et al., 2002).

Similar studies to the ones currently performed could be used to investigate wood frog enzymatic responses with regards to other common environmental stresses faced in nature such as dehydration or anoxia. This could help add to the understanding of the interplay between freeze tolerance and other stresses that amphibians survive since anoxia and dehydration are also important components of freeze survival. This could also lead to studies in other anurans like the African clawed frog, *Xenopus laevis*, that uses urea to help maintain osmotic balance during bouts of dehydration (Katzenback et al., 2014). The role of nitrogen metabolism in allowing for survival of hypometabolic states represents an ongoing area of research that could be explored in diverse organisms.

References

Abboud, J. and Storey, K. B. (2013). Novel control of lactate dehydrogenase from the freeze tolerant wood frog: role of posttranslational modifications. *PeerJ* **1**, e12.

Baeza, J., Smallegan, M. J. and Denu, J. M. (2016). Mechanisms and dynamics of protein acetylation in mitochondria. *Trends Biochem. Sci.* **41**, 231–244.

Bakhach, J. (2009). The cryopreservation of composite tissues: Principles and recent advancement on cryopreservation of different type of tissues. *Organogenesis* **5**, 119–126.

Balinsky, J. B. (1981). Adaptation of nitrogen metabolism to hyperosmotic environment in amphibia. *J. Exp. Zool.* **215**, 335–350.

Banerjee, S., Schmidt, T., Fang, J., Stanley, C. A. and Smith, T. J. (2003). Structural studies on ADP activation of mammalian glutamate dehydrogenase and the evolution of regulation. *Biochemistry* **42**, 3446–3456.

Beliveau Carey, G., Cheung, C. W., Cohen, N. S., Brusilow, S. and Raijman, L. (1993). Regulation of urea and citrulline synthesis under physiological conditions. *Biochem. J.* **292 (Pt 1)**, 241–247.

Bell, R. A. V and Storey, K. B. (2010). Regulation of liver glutamate dehydrogenase by reversible phosphorylation in a hibernating mammal. *Comp. Biochem. Physiol. - B Biochem. Mol. Biol.* **157**, 310–316.

Bell, R. A. V, Dawson, N. J. and Storey, K. B. (2012). Insights into the in vivo regulation of glutamate dehydrogenase from the foot muscle of an estivating land snail. *Enzyme Res.* **2012**,.

Ben-Sahra, I., Howell, J. J., Asara, J. M. and Manning, B. D. (2013). Stimulation of de novo pyrimidine synthesis by growth signaling through mTOR and S6K1. *Science* **339**, 1323–8.

Berman, D. I. and Meshcheryakova, E. N. (2012). Is the western boundary of the Siberian salamander (*Salamandrella keyserlingii*, Amphibia, Caudata, Hynobiidae) range determined by the specific features of its wintering? *Dokl. Biol. Sci. Orig. Russ. Text © Dokl. Akad. Nauk* **443**, 97–100.

Berman, D. I., Lerikh, A. N. and Mikhailova, E. I. (1984). Winter hibernation of the Siberian salamander, Hynobius keyserlingi. *J. Evol. Biochem. Physiol.* **20**, 323–327.

Berman, D. I., Leirikh, A. N. and Meshcheryakova, E. N. (2010). The Schrenck newt (*Salamandrella schrenckii*, Amphibia, Caudata, Hynobiidae) is the second amphibian that withstands extremely low temperatures. *Dokl. Biol. Sci.* **431**, 131–134.

Biggar, K. K., Dawson, N. J. and Storey, K. B. (2012). Real-time protein unfolding: A method for determining the kinetics of native protein denaturation using a quantitative real-time thermocycler. *Biotechniques* **53**, 231–238.

Biggar, K. K., Kotani, E., Furusawa, T. and Storey, K. B. (2013). Expression of freeze-responsive proteins, Fr10 and Li16, from freeze-tolerant frogs enhances freezing survival of BmN insect cells. *FASEB J.* **27**, 3376–83.

Brooks, S. P. (1992). A simple computer program with statistical tests for the analysis of enzyme kinetics. *Biotechniques* **13**, 906–11.

Brooks, S. P. (1994). A program for analyzing enzyme rate data obtained from a microplate reader. *Biotechniques* **17**, 1154–1161.

Brosnan, J. T. (2000). Glutamate, at the interface between amino acid and carbohydrate metabolism. *J. Nutr.* **130**, 988S–90S.

Brosnan, J. T. and Brosnan, M. E. (2002). Hepatic glutaminase--a special role in urea synthesis? *Nutrition* **18**, 455–457.

Buchowiecka, A. K. (2014). Puzzling over protein cysteine phosphorylation – assessment of proteomic tools for S- phosphorylation profiling. *Analyst* **139**, 4118–4123.

Caldovic, L. and Tuchman, M. (2003). N-Acetylglutamate and its changing role through evolution. *Biochem. J.* **372**, 279–290.

Carilla-Latorre, S., Gallardo, M. E., Annesley, S. J., Calvo-Garrido, J., Graña, O., Accari, S. L., Smith, P. K., Valencia, A., Garesse, R., Fisher, P. R., et al. (2010). MidA is a putative methyltransferase that is required for mitochondrial complex I function. *J. Cell Sci.* **123**, 1674–1683.

Chew, S. F., Ong, T. F., Ho, L., Tam, W. L., Loong, A. M., Hiong, K. C., Wong, W. P. and Ip, Y. K. (2003). Urea synthesis in the African lungfish *Protopterus dolloi*--hepatic carbamoyl phosphate synthetase III and glutamine synthetase are upregulated by 6 days of aerial exposure. *J. Exp. Biol.* **206**, 3615–3624.

Chung, D. J., Szyszka, B., Brown, J. C. L., Hüner, N. P. a and Staples, J. F. (2013). Changes in the mitochondrial phosphoproteome during mammalian hibernation. *Physiol. Genomics* **45**, 389–99.

Churchill, T. A. and Storey, K. B. (1993). Dehydration tolerance in wood frogs: a new perspective on development of amphibian freeze tolerance. *Am. J. Physiol. Integr. Comp. Physiol.* **265**, R1324–R1332.

Churchill, T. A. and Storey, K. B. (1995). Metabolic effects of dehydration on an aquatic frog, *Rana pipiens*. *J. Exp. Biol.* **198**, 147–154.

Cohen, P. (2000). The regulation of protein function by multisite phosphorylation--a 25 year update. *Trends Biochem. Sci.* **25**, 596–601.

Cohen, N. S., Cheung, C. W., Sijuwade, E. and Raijman, L. (1992). Kinetic properties of carbamoyl-phosphate synthase (ammonia) and ornithine carbamoyltransferase in permeabilized mitochondria. *Biochem. J.* **282 (Pt 1**, 173–80.

Corvi, M. M., Soltys, C. L. M. and Berthiaume, L. G. (2001). Regulation of mitochondrial carbamoyl-phosphate synthetase 1 activity by active site fatty acylation. *J. Biol. Chem.* **276**, 45704–45712.

Costanzo, J. P. and Lee, R. E. (2005). Cryoprotection by urea in a terrestrially hibernating frog. *J. Exp. Biol.* **208**, 4079–4089.

Costanzo, J. P. and Lee, R. E. (2008). Urea loading enhances freezing survival and postfreeze recovery in a terrestrially hibernating frog. *J. Exp. Biol.* **211**, 2969–2975.

Costanzo, J. P., Lee, R. E. and Lortz, P. H. (1993). Glucose concentration regulates freeze tolerance in the wood frog *Rana sylvatica*. *J. Exp. Biol.* **181**, 245–55.

Costanzo, J. P., do Amaral, M. C. F., Rosendale, A. J. and Lee, R. E. (2013). Hibernation physiology, freezing adaptation and extreme freeze tolerance in a northern population of the wood frog. *J. Exp. Biol.* **216**, 3461–73.

Costanzo, J. P., Reynolds, A. M., do Amaral, M. C. F., Rosendale, A. J. and Lee, R. E. (2015). Cryoprotectants and extreme freeze tolerance in a subarctic population of the wood frog. *PLoS One* **10**, e0117234.

Currie, S. and Boutilier, R. (2001). Strategies of hypoxia and anoxia tolerance in cardiomyocytes from the overwintering strategies of hypoxia and anoxia tolerance in cardiomyocytes from the overwintering common frog, *Rana temporaria*. *Physiol. Biochem. Zool.* **74**, 420–428.

De Cima, S., Polo, L. M., Díez-Fernández, C., Martínez, A. I., Cervera, J., Fita, I. and Rubio, V. (2015). Structure of human carbamoyl phosphate synthetase: deciphering the on/off switch of human ureagenesis. *Sci. Rep.* **5**, 16950.

Dephoure, N., Gould, K. L., Gygi, S. P. and Kellogg, D. R. (2013). Mapping and analysis of phosphorylation sites: a quick guide for cell biologists. *Mol. Biol. Cell* **24**, 535–42.

Dieni, C. A. and Storey, K. B. (2014). Protein kinase C in the wood frog, *Rana sylvatica*: reassessing the tissue-specific regulation of PKC isozymes during freezing. *PeerJ* **2**, e558.

Dieni, C. A., Bouffard, M. C. and Storey, K. B. (2012). Glycogen synthase kinase-3: cryoprotection and glycogen metabolism in the freeze-tolerant wood frog. *J. Exp. Biol.* **215**, 543–551.

Do Amaral, M. C. F., Lee, R. E. and Costanzo, J. P. (2013). Enzymatic regulation of glycogenolysis in a subarctic population of the wood frog: implications for extreme freeze tolerance. *PLoS One* **8**, 1–10.

Du, J., Zhou, Y., Su, X., Yu, J. J., Khan, S., Jiang, H., Kim, J., Woo, J., Kim, J. H., Choi, B. H., et al. (2011). Sirt5 is a NAD-dependent protein lysine demalonylase and desuccinylase. *Science (80-.).* **334**, 806–809.

Duman, J. G. (2001). Antifreeze and ice nucleator proteins in terrestrial arthropods. *Annu. Rev. Physiol.* **63**, 327–357.

Emmerson, D. A., Turner, K. A., Foster, D. N., Anthony, N. B. and Nestor, K. E. (1997). Ornithine decarboxylase activity in muscle, liver, and intestinal tissue of turkeys during a short-term feed withdrawal and following refeeding. *Poult. Sci.* **76**, 1563–1568.

Fang, J., Hsu, B. Y. L., MacMullen, C. M., Poncz, M., Smith, T. J. and Stanley, C. A. (2002). Expression, purification and characterization of human glutamate dehydrogenase (GDH) allosteric regulatory mutations. *Biochem J* **363**, 81–87.

Felipo, V., Kosenko, E., Miñana, M. D., Marcaida, G. and Grisolía, S. (1994). Molecular mechanism of acute ammonia toxicity and of its prevention by L-carnitine. *Adv. Exp. Med. Biol.* **368**, 65–77.

Feller, G. (2010). Protein stability and enzyme activity at extreme biological temperatures. *J. Phys. Condens. Matter* **22**, 323101.

Fuhrmann, J., Mierzwa, B., Trentini, D. B., Spiess, S., Lehner, A., Charpentier, E. and Clausen, T. (2013). Structural basis for recognizing phosphoarginine and evolving residue-specific protein phosphatases in gram-positive bacteria. *Cell Rep.* **3**, 1832–1839.

Fuhs, S. R., Meisenhelder, J., Aslanian, A., Ma, L., Zagorska, A., Stankova, M., Binnie, A., Al-Obeidi, F., Mauger, J., Lemke, G., et al. (2015). Monoclonal 1- and 3-phosphohistidine antibodies: new tools to study histidine phosphorylation. *Cell* **162**, 198–210.

Gandre, S., Bercovich, Z. and Kahana, C. (2002). Ornithine decarboxylase-antizyme is rapidly degraded through a mechanism that requires functional ubiquitin-dependent proteolytic activity. *Eur. J. Biochem.* **269**, 1316–1322.

Gerber, V. E. M., Wijenayake, S. and Storey, K. B. (2016). Anti-apoptotic response during anoxia and recovery in a freeze-tolerant wood frog (*Rana sylvatica)*. *PeerJ* **4**, e1834.

Ghanta, S., Grossmann, R. E. and Brenner, C. (2013). Mitochondrial protein acetylation as a cell-intrinsic, evolutionary driver of fat storage: chemical and metabolic logic of acetyl-lysine modifications. *Crit. Rev. Biochem. Mol. Biol.* **48**, 561–74.

Gromova, I. and Celis, J. E. (2006). Protein detection in gels by silver staining: a procedure compatible with mass spectrometry. In *Cell Biology, A Laboratory Handbook*, pp. 219–223. Elsevier Science.

Guan, K. L. and Xiong, Y. (2011). Regulation of intermediary metabolism by protein acetylation. *Trends Biochem. Sci.* **36**, 108–116.

Gupta, R. and Deswal, R. (2014). Antifreeze proteins enable plants to survive in freezing conditions. *J. Biosci.* **39**, 931–944.

Haigis, M. C., Mostoslavsky, R., Haigis, K. M., Fahie, K., Christodoulou, D. C., Murphy, A. J., Valenzuela, D. M., Yancopoulos, G. D., Karow, M., Blander, G., et al. (2006). SIRT4 inhibits glutamate dehydrogenase and opposes the effects of calorie restriction in pancreatic b cells. *Cell* **126**, 941–954.

Hallows, W. C., Yu, W., Smith, B. C., Devires, M. K., Ellinger, J. J., Someya, S., Shortreed, M. R., Prolla, T., Markley, J. L., Smith, L. M., et al. (2011). Sirt3 promotes the urea cycle and fatty acid oxidation during dietary restriction. *Mol. Cell* **41**, 139–149.

Helbing, C., Gergely, G. and Atkinson, B. G. (1992). Sequential up-regulation of thyroid hormone beta receptor, ornithine transcarbamylase, and carbamyl phosphate synthetase mRNAs in the liver of *Rana catesbeiana* tadpoles during spontaneous and thyroid hormone-induced metamorphosis. *Dev. Genet.* **13**, 289–301.

Herrero-Yraola, A., Bakhit, S. M. A., Franke, P., Weise, C., Schweiger, M., Jorcke, D. and Ziegler, M. (2001). Regulation of glutamate dehydrogenase by reversible ADP-ribosylation in mitochondria. *EMBO J.* **20**, 2404–2412.

Hirschey, M. D. and Zhao, Y. (2015). Metabolic regulation by lysine malonylation, succinylation, and glutarylation. *Mol. Cell. Proteomics* **14**, 2308–2315.

Hofer, A. and Wenz, T. (2014). Post-translational modification of mitochondria as a novel mode of regulation. *Exp. Gerontol.* **56**, 202–220.

Horbinski, C. and Chu, C. T. (2005). Kinase signaling cascades in the mitochondrion: a matter of life or death. *Free Radic. Biol. Med.* **38**, 2–11.

Igarashi, K. and Kashiwagi, K. (2010). Modulation of cellular function by polyamines. *Int. J. Biochem. Cell Biol.* **42**, 39–51.

Iwahana, H., Fujimura, M., Ii, S., Kondo, M., Moritani, M., Takahashi, Y., Yamaoka, T., Yoshimoto, K. and Itakura, M. (1996). Molecular cloning of a human cDNA encoding a trifunctional enzyme of carbamoyl-phosphate synthetase-aspartate transcarbamoylase-dihydroorotase in de novo pyrimidine synthesis. *Biochem. Biophys. Res. Commun.* **219**, 249–55.

Jackson, M. J., Beaudet, A. L. and O'Brien, W. E. (1986). Mammalian urea cycle enzymes. *Annu. Rev. Genet.* 431–464.

Jones, M. E. (1985). Conversion of glutamate to ornithine and proline: pyrroline-5-carboxylate, a possible modulator of arginine requirements. *J. Nutr.* **115**, 509–15.

Jørgensen, C. B. (1997). Urea and amphibian water economy. *Comp. Biochem. Physiol. - A Physiol.* **117**, 161–170.

Kamau Machua, S., Mukuria, J. C., Ngure, R. M. and Gitu, P. M. (2014). Modulation of partially purified rat liver mitochondrial carbamoyl phosphate synthetase I using two glutamic acid analogues. *Unique Res. J. Biochem. Biotechnol.* **1**, 1–10.

Karve, T. M. and Cheema, A. K. (2011). Small changes huge impact: the role of protein posttranslational modifications in cellular homeostasis and disease. *J. Amino Acids* **2011**, Article ID: 207691.

Katunuma, N., Okada, M. and Nishii, Y. (1966). Regulation of the urea cycle and TCA cycle by ammonia. *Adv. Enzyme Regul.* **4**, 317–335.

Katzenback, B. A., Dawson, N. J. and Storey, K. B. (2014). Purification and characterization of a urea sensitive lactate dehydrogenase from the liver of the African clawed frog, *Xenopus laevis*. *J. Comp. Physiol. B* **184**, 601–611.

Kelleher, M. J., Rickards, J. and Storey, K. B. (1987). Strategies of freeze avoidance in larvae of the goldenrod gall moth, *Epiblema scudderiana*: Laboratory investigations of temperature cues in the regulation of cold hardiness. *J. Insect Physiol.* **33**, 581–586.

Khater, S. and Mohanty, D. (2015). novPTMenzy: a database for enzymes involved in novel post-translational modifications. *Database (Oxford).* **2015**, 1–12.

Kim, E. A., Yang, S. J., Choi, S. Y., Lee, W. J. and Cho, S. W. (2012). Inhibition of glutamate dehydrogenase and insulin secretion by KHG26377 does not involve ADP-ribosylation by SIRT4 or deacetylation by SIRT3. *BMB Rep.* **45**, 458–463.

Kiss, A. J., Muir, T. J., Lee, R. E. and Costanzo, J. P. (2011). Seasonal variation in the hepatoproteome of the dehydration and freeze-tolerant wood frog, *Rana sylvatica*. *Int. J. Mol. Sci.* **12**, 8406–8414.

Knipp, M. and Vasák, M. (2000). A colorimetric 96-well microtiter plate assay for the determination of enzymatically formed citrulline. *Anal. Biochem.* **286**, 257–64.

Kratzer, J. T., Lanaspa, M. A., Murphy, M. N., Cicerchi, C., Graves, C. L., Tipton, P. a, Ortlund, E. A., Johnson, R. J. and Gaucher, E. A. (2014). Evolutionary history and metabolic insights of ancient mammalian uricases. *Proc. Natl. Acad. Sci. U. S. A.* **111**, 3763–3768.

Landau, G., Bercovich, Z., Park, M. H. and Kahana, C. (2010). The role of polyamines in supporting growth of mammalian cells is mediated through their requirement for translation initiation and elongation. *J. Biol. Chem.* **285**, 12474–81.

Lant, B. and Storey, K. B. (2010). An overview of stress response and hypometabolic strategies in *Caenorhabditis elegans*: Conserved and contrasting signals with the mammalian system. *Int. J. Biol. Sci.* **6**, 9–50.

Larson, D. J. and Barnes, B. M. (2016). Cryoprotectant production in freeze-tolerant wood frogs is augmented by multiple freeze-thaw cycles. *Physiol. Biochem. Zool.* **89**, 340–346.

Layne, J. R. and Jones, A. L. (2001). Freeze tolerance in the gray treefrog: Cryoprotectant mobilization and organ dehydration. *J. Exp. Zool.* **290**, 1–5.

Lee, A. R., Silove, M., Katz, U. and Balinsky, J. B. (1982). Urea cycle enzymes and glutamate dehydrogenase in *Xenopus laevis* and *Bufo viridis* adapted to high salinity. *J. Exp. Zool.* **221**, 169–172.

Li, M., Smith, C. J., Walker, M. T. and Smith, T. J. (2009). Novel inhibitors complexed with glutamate dehydrogenase: allosteric regulation by control of protein dynamics. *J. Biol. Chem.* **284**, 22988–3000.

Lin, H., Su, X. and He, B. (2012). Protein lysine acylation and cysteine succination by intermediates of energy metabolism. *ACS Chem. Biol.* **7**, 947–960.

Linton, S. N. and Campbell, J. W. (1962). Studies on urea cycle enzymes in the terrestrial snail, *Otala lactea*. *Arch. Biochem. Biophys.* **97**, 360–369.

Lusty, C. J., Jilka, R. L. and Nietsch, E. H. (1979). Ornithine transcarbamylase of rat liver. Kinetic, physical, and chemical properties. *J. Biol. Chem.* **254**, 10030–10036.

Małecki, J., Ho, A. Y. Y., Moen, A., Dahl, H.-A. and Falnes, P. Ø. (2015). Human METTL20 is a mitochondrial lysine methyltransferase that targets the β subunit of electron transfer flavoprotein (ETFβ) and modulates its activity. *J. Biol. Chem.* **290**, 423–34.

Maras, B., Consalvi, V., Chiaraluce, R., Politi, L., De Rosa, M., Bossa, F., Scandurra, R. and Barra, D. (1992). The protein sequence of glutamate dehydrogenase from *Sulfolobus solfataricus*, a thermoacidophilic archaebacterium: Is the presence of N-epsilon-methyllysine related to thermostability? *Eur. J. Biochem.* **203**, 81–87.

Marshall, M. and Cohen, P. P. (1972). Ornithine transcarbamylase from *Streptococcus faecalis* and bovine: II. Multiple binding sites for carbamyl-P and L-norvaline, correlations with steady state kinetics. *J. Biol. Chem.* **247**, 1654–1668.

Martinelle, K. and Häggström, L. (1993). Mechanisms of ammonia and ammonium ion toxicity in animal cells: transport across cell membranes. *J. Biotechnol.* **30**, 339–350.

Martino, M. N. and Zaritzky, N. E. (1989). Ice recrystallization in a model system and in frozen muscle tissue. *Cryobiology* **26**, 138–148.

Miller-Fleming, L., Olin-Sandoval, V., Campbell, K. and Ralser, M. (2015). Remaining mysteries of molecular biology: The role of polyamines in the cell. *J. Mol. Biol.* **427**, 3389–3406.

Morris, S. M. (2002). Regulation of enzymes of the urea cycle and arginine metabolism. *Annu. Rev. Nutr.* **22**, 87–105.

Morris, S. M. (2007). Arginine metabolism: boundaries of our knowledge. *J. Nutr.* **137**, 1602S–1609S.

Morris, S. M., Kepka-Lenhart, D. and Chen, L. C. (1998). Differential regulation of arginases and inducible nitric oxide synthase in murine macrophage cells. *Am. J. Physiol.* **275**, E740–7.

Muir, T. J., Costanzo, J. P. and Lee, R. E. (2008). Metabolic depression induced by urea in organs of the wood frog, *Rana sylvatica*: Effects of season and temperature. *J. Exp. Zool. Part A Ecol. Genet. Physiol.* **309**, 111–116.

Nakagawa, T. and Guarente, L. (2009). Urea cycle regulation by mitochondrial sirtuin, SIRT5. *Aging (Albany. NY).* **1**, 578–81.

Nakagawa, T., Lomb, D. J., Haigis, M. C. and Guarente, L. (2009). SIRT5 deacetylates carbamoyl phosphate synthetase 1 and regulates the urea cycle. *Cell* **137**, 560–570.

Nesvizhskii, A. I., Keller, A., Kolker, E. and Aebersold, R. (2003). A statistical model for identifying proteins by tandem mass spectrometry. *Anal. Chem.* **75**, 4646–4658.

Niesen, F. H., Berglund, H. and Vedadi, M. (2007). The use of differential scanning fluorimetry to detect ligand interactions that promote protein stability. *Nat. Protoc.* **2**, 2212–2221.

Ogura, M., Nakamura, Y., Tanaka, D., Zhuang, X., Fujita, Y., Obara, A., Hamasaki, A., Hosokawa, M. and Inagaki, N. (2010). Overexpression of SIRT5 confirms its involvement in deacetylation and activation of carbamoyl phosphate synthetase 1. *Biochem. Biophys. Res. Commun.* **393**, 73–78.

Olijve, L. L. C., Meister, K., DeVries, A. L., Duman, J. G., Guo, S., Bakker, H. J. and Voets, I. K. (2016). Blocking rapid ice crystal growth through nonbasal plane adsorption of antifreeze proteins. *Proc. Natl. Acad. Sci.* **113**, 3740–3745.

Oliveira, A. P. and Sauer, U. (2012). The importance of post-translational modifications in regulating *Saccharomyces cerevisiae* metabolism. *FEMS Yeast Res.* **12**, 104–117.

Ozer, N. (1985). A new enzyme-coupled spectrophotometric method for the determination of arginase activity. *Biochem. Med.* **33**, 367–371.

Pincheira-Donoso, D., Bauer, A. M., Meiri, S. and Uetz, P. (2013). Global taxonomic diversity of living reptiles. *PLoS One* **8**, 1–10.

Prabakaran, S., Lippens, G., Steen, H. and Gunawardena, J. (2012). Post-translational modification: nature's escape from genetic imprisonment and the basis for dynamic information encoding. *Wiley Interdiscip Rev Syst Biol Med* **4**, 565–583.

Raab, R. P. (1991). Urea from the chemist's point of view. *J. Appl. Cosmetol.* **9**, 9–13.

Regnault, M. (1987). Nitrogen excretion in marine and fresh-water crustacea. *Biol. Rev.* **62**, 1–24.

Regunathan, S. and Reis, D. J. (2000). Characterization of arginine decarboxylase in rat brain and liver: Distinction from ornithine decarboxylase. *J. Neurochem.* **74**, 2201–2208.

Russell, E. L. and Storey, K. B. (1995). Glycogen-synthetase and the control of cryoprotectant clearance after thawing in the freeze-tolerant wood frog. *Cryo-Letters* **16**, 263–266.

Russo, D. (2007). The impact of kosmotropes and chaotropes on bulk and hydration shell water dynamics in a model peptide solution.

Schiller, T. M., Costanzo, J. P. and Lee, R. E. (2008). Urea production capacity in the wood frog (*Rana sylvatica*) varies with season and experimentally induced hyperuremia. *J. Exp. Zool. Part A Ecol. Genet. Physiol.* **309A**, 484–493.

Schlicker, C., Gertz, M., Papatheodorou, P., Kachholz, B., Becker, C. F. W. and Steegborn, C. (2008). Substrates and regulation mechanisms for the human mitochondrial sirtuins sirt3 and sirt5. *J. Mol. Biol.* **382**, 790–801.

Smith, T. J., Schmidt, T., Fang, J., Wu, J., Siuzdak, G. and Stanley, C. A. (2002). The structure of apo human glutamate dehydrogenase details subunit communication and allostery. *J. Mol. Biol.* **318**, 765–777.

Soda, K. (2011). The mechanisms by which polyamines accelerate tumor spread. *J. Exp. Clin. Cancer Res.* **30**, 95.

Solaini, G., Baracca, A., Lenaz, G. and Sgarbi, G. (2010). Hypoxia and mitochondrial oxidative metabolism. *Biochim Biophys Acta.* **1797**, 1171–7.

Spanaki, C. and Plaitakis, A. (2012). The role of glutamate dehydrogenase in mammalian ammonia metabolism. *Neurotox. Res.* **21**, 117–127.

Storey, K. B. (1987). Glycolysis and the regulation of cryoprotectant synthesis in liver of the freeze tolerant wood frog. *J. Comp. Physiol. B* **157**, 373–380.

Storey, K. B. and Storey, J. M. (1984). Biochemical adaption for freezing tolerance in the wood frog, *Rana sylvatica*. *J. Comp. Physiol. B* **155**, 29–36.

Storey, K. B. and Storey, J. M. (1986). Freeze tolerant frogs: cryoprotectants and tissue metabolism during freeze–thaw cycles. *Can. J. Zool.* **64**, 49–56.

Storey, K. B. and Storey, J. M. (1988). Freeze tolerance in animals. *Physiol. Rev.* **68**, 27–84.

Storey, K. B. and Storey, J. M. (1992). Natural freeze tolerance in ectothermic vertebrates. *Annu. Rev. Physiol.* **54**, 619–637.

Storey, K. B. and Storey, J. M. (2017). Molecular physiology of freeze tolerance in vertebrates. *Physiol. Rev.* **97**, 623–665.

Storey, K. B., Storey, J. M., Brooks, S. P., Churchill, T. A. and Brooks, R. J. (1988). Hatchling turtles survive freezing during winter hibernation. *Proc. Natl. Acad. Sci. U. S. A.* **85**, 8350–8354.

Storey, K. B., Baust, J. G. and Wolanczyk, J. P. (1992). Biochemical modification of plasma ice nucleating activity in a freeze-tolerant frog. *Cryobiology* **29**, 374–384.

Struck, J., Uhlein, M., Morgenthaler, N. G., Fürst, W., Höflich, C., Bahrami, S., Bergmann, A., Volk, H.-D. and Redl, H. (2005). Release of the mitochondrial enzyme carbamoyl phosphate synthase under septic conditions. *Shock* **23**, 533–538.

Struvay, C. and Feller, G. (2012). Optimization to low temperature activity in psychrophilic enzymes. *Int. J. Mol. Sci.* **13**, 11643–11665.

Summar, M. L., Gainer, J. V., Pretorius, M., Malave, H., Harris, S., Hall, L. D., Weisberg, A., Vaughan, D. E., Christman, B. W. and Brown, N. J. (2004). Relationship between carbamoyl-phosphate synthetase genotype and systemic vascular function. *Hypertension* **43**, 186–191.

Tan, M., Peng, C., Anderson, K. A., Chhoy, P., Xie, Z., Dai, L., Park, J., Chen, Y., Huang, H., Zhang, Y., et al. (2014). Lysine glutarylation is a protein posttranslational modification regulated by SIRT5. *Cell Metab.* **19**, 605–617.

Tattersall, G. J. and Ultsch, G. R. (2008). Physiological ecology of aquatic overwintering in ranid frogs. *Biol. Rev.* **83**, 119–140.

Tuchman, M. and Holzknecht, R. A. (1990). N-acetylglutamate content in liver and gut of normal and fasted mice, normal human livers, and livers of individuals with carbamyl phosphate synthetase or ornithine transcarbamylase deficiency. *Pediatr Res* **27**, 408–412.

Tuchman, M., Morizono, H., Rajagopal, B. S., Plante, R. J. and Allewell, N. M. (1998). The biochemical and molecular spectrum of ornithine transcarbamylase deficiency. In *Journal of Inherited Metabolic Disease*, pp. 40–58.

Ultsch, G. R. (2006). The ecology of overwintering among turtles: where turtles overwinter and its consequences. *Biol. Rev. Camb. Philos. Soc.* **81**, 339–367.

Van Waarde, A. (1983). Aerobic and anaerobic ammonia production by fish. *Comp. Biochem. Physiol. Part B Comp. Biochem.* **74**, 675–684.

Vieille, C. and Zeikus, G. J. (2001). Hyperthermophilic enzymes: sources, uses, and molecular mechanisms for thermostability. *Microbiol. Mol. Biol. Rev.* **65**, 1–43.

Wharton, D. A., Goodall, G. and Marshall, C. J. (2003). Freezing survival and cryoprotective dehydration as cold tolerance mechanisms in the Antarctic nematode Panagrolaimus davidi. *J. Exp. Biol.* **206**, 215–221.

Wigglesworth, V. B. (1987). Histochemical studies of uric acid in some insects. 3. Excretion of uric acid by the malpighian tubules in *Calliphora vicina* and *Rhodnius prolixus*. *Tissue Cell* **19**, 275–286.

Wolanczyk, J. P., Storey, K. B. and Baust, J. G. (1990). Ice nucleating activity in the blood of the freeze-tolerant frog, *Rana sylvatica*. *Cryobiology* **27**, 328–335.

Wraight, C. and Hoogenraad, N. (1988). Dietary regulation of ornithine transcarbamylase mRNA in liver and small intestine. *Aust. J. Biol. Sci.* **41**, 435–40.

Wright, P. (1995). Review nitrogen excretion: Three end products, many physiological roles. *J. Exp. Biol.* **281**, 273–281.

Wright, P., Anderson, P., Weng, L., Frick, N., Wong, W. P. and Ip, Y. K. (2004). The crab-eating frog, *Rana cancrivora*, up-regulates hepatic carbamoyl phosphate synthetase I activity and tissue osmolyte levels in response to increased salinity. *J. Exp. Zool. A. Comp. Exp. Biol.* **301**, 559–568.

Wu, G. and Morris Jr., S. M. (1998). Arginine metabolism: nitric oxide and beyond. *Biochem. J* **336 (Pt 1**, 1–17.

Xie, L., Wang, G., Yu, Z., Zhou, M., Li, Q., Huang, H. and Xie, J. (2016). Proteome-wide lysine glutarylation profiling of the *mycobacterium tuberculosis* H37Rv. *J. Proteome Res.* **15**, 1379–1385.

Xiong, X. and Anderson, P. M. (1989). Purification and properties of ornithine carbamoyl transferase from liver of *Squalus acanthias*. *Arch. Biochem. Biophys.* **270**, 198–207.

Xiong, Z. J. and Storey, K. B. (2012). Regulation of liver lactate dehydrogenase by reversible phosphorylation in response to anoxia in a freshwater turtle. *Comp. Biochem. Physiol. - B Biochem. Mol. Biol.* **163**, 221–228.

Yu, W., Lin, Y., Yao, J., Huang, W., Lei, Q., Xiong, Y., Zhao, S. and Guan, K. L. (2009). Lysine 88 acetylation negatively regulates ornithine carbamoyltransferase activity in response to nutrient signals. *J. Biol. Chem.* **284**, 13669–13675.

Yu, S. O., Brown, A., Middleton, A. J., Tomczak, M. M., Walker, V. K. and Davies, P. L. (2010). Ice restructuring inhibition activities in antifreeze proteins with distinct differences in thermal hysteresis. *Cryobiology* **61**, 327–334.

Zeidel, J. D., Mathai, J. C., Campbell, J. D., Ruiz, W. G., Apodaca, G. L., Riordan, J. and Zeidel, M. L. (2005). Selective permeability barrier to urea in shark rectal gland. *Am J Physiol Ren. Physiol* **289**, F83–9.

Zhang, J. and Storey, K. B. (2016). RBioplot: an easy-to-use R pipeline for automated statistical analysis and data visualization in molecular biology and biochemistry. *PeerJ* **4**, e2436.

Zolles, T., Burkart, J., Häusler, T., Pummer, B., Hitzenberger, R. and Grothe, H. (2015). Identification of ice nucleation active sites on feldspar dust particles. *J. Phys. Chem. A* **119**, 2692–2700.

Appendices

Appendix I

Mass Spectrometry and Bioinformatics Data

```
1   MLHHMRTIIN ASWRYGNKCI VRQFGFSQTY SQLKGRDLLT LKNYSAEEIK
51  YLLWVAADLK YRIKEKGEYL PLLQGKSLAM IFEKRSTRTR LSTETGFALL
101 GGHPSFLTTQ DIHLGVNESL KDTARVLSGM TDAVLARVYH QSDLEVLAEE
151 ASIPIVNGLS DDYHPIQILA DYLTIQEHYG HLKGLTISWI GDGNNVLHSI
201 MMSAAKFGMH LHIATPKGYE PNSSLTEAAK QFSKECGTKL LMTNDPLEAA
251 NGANVLVTDT WVSMGQEEEK KKRLLDFKGY QITMKTAKLA APNWIFLHCL
301 PRKPEEVDDE VFYCPKSLVF QEAENRKWTI MGVMVSLLTD YSPQLLRPTF
```

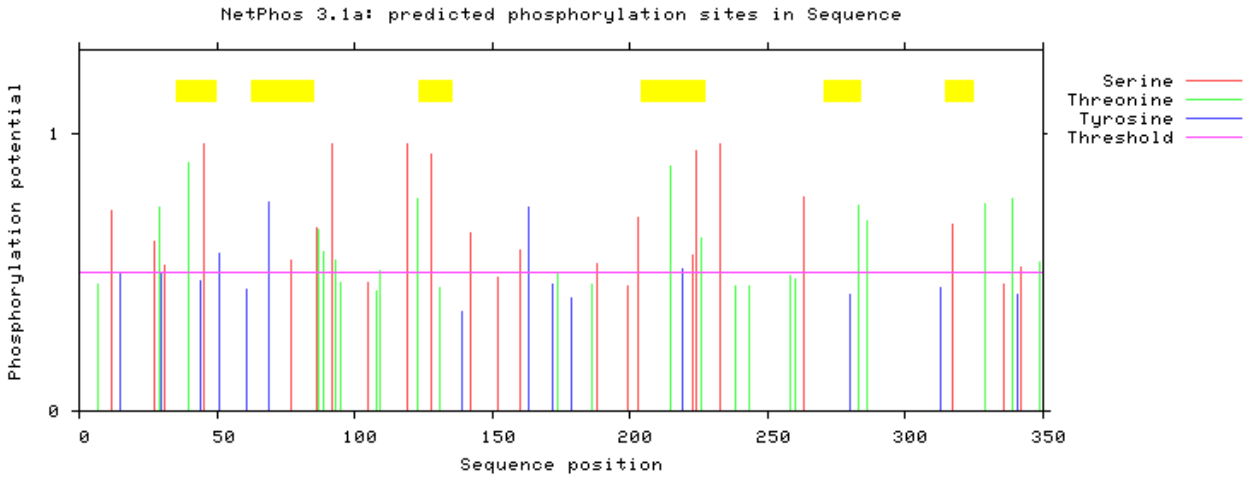

Fig. A.1.1. Ornithine transcarbamylase protein sequence from *Rana catesbeiana* (American bullfrog). Highlighted segments represent peptides that were found during mass spectrometry of the protein band in a SDS-PAGE gel from partially purified control OTC *Rana sylvatica* from liver. Peptides matched from *Rana sylvatica* constitute 28% sequence coverage. Frozen OTC was also analyzed using mass spectrometry and yielded one exclusive unique peptide fewer than control. Hydroxyl bearing amino acids predicted to be possibly phosphorylated (score greater than 0.5) using NetPhos 3.1 were underlined in the sequence and their location is shown below in the chart. The chart maps predicted phosphorylation sites based on their phosphorylation potential (scored 0 to 1) to their location in the bullfrog sequence with the bars above the chart representing the peptide sequences found in the control wood frog OTC.

Table A.1.1. Kinases associated with potential phosphorylation sites in the sequence for OTC from bullfrog (*Rana catesbeiana*) using the NetPhos 3.1. Amino acid residues predicted are given with their phosphorylation potential score in parentheses, only scores higher than 0.5 were considered.

Kinase	Predicted Phosphorylation Sites in OTC and their scores
Unspecified	12S (0.539), 27S (0.505), 45S (0.996), 51Y (0.565), 69Y (0.749), 86S (0.659), 87T (0.515), 92S (0.998), 119S (0.994), 123T (0.761), 128S (0.927), 163Y (0.734), 215T (0.882), 224S (0.939), 233S (0.986), 263S (0.772), 286T (0.686), 317S (0.670), 329T (0.746)
PKC	12S (0.720), 27S (0.555), 29T (0.735), 40T (0.894), 89T (0.575), 203S (0.696), 226T (0.624). 283T (0.740), 339T (0.767)
ATM	27S (0.612), 109T (0.503)
DNAPK	27S (0.539), 31S (0.522), 224S (0.562)
CKII	45S (0.545), 142S (0.643), 160S (0.577), 223S (0.552)
INSR	69Y (0.528), 163Y (0.516), 219Y (0.510)
PKA	77S (0.542), 87T (0.655), 92S (0.654), 128S (0.676), 329T (0.708)
RSK	93T (0.541)
Cdc2	188S (0.527)
CKI	233S (0.524)
PKG	286T (0.533), 349T (0.536)
P38 MAPK	339T (0.526)
Cdk5	342S (0.518)

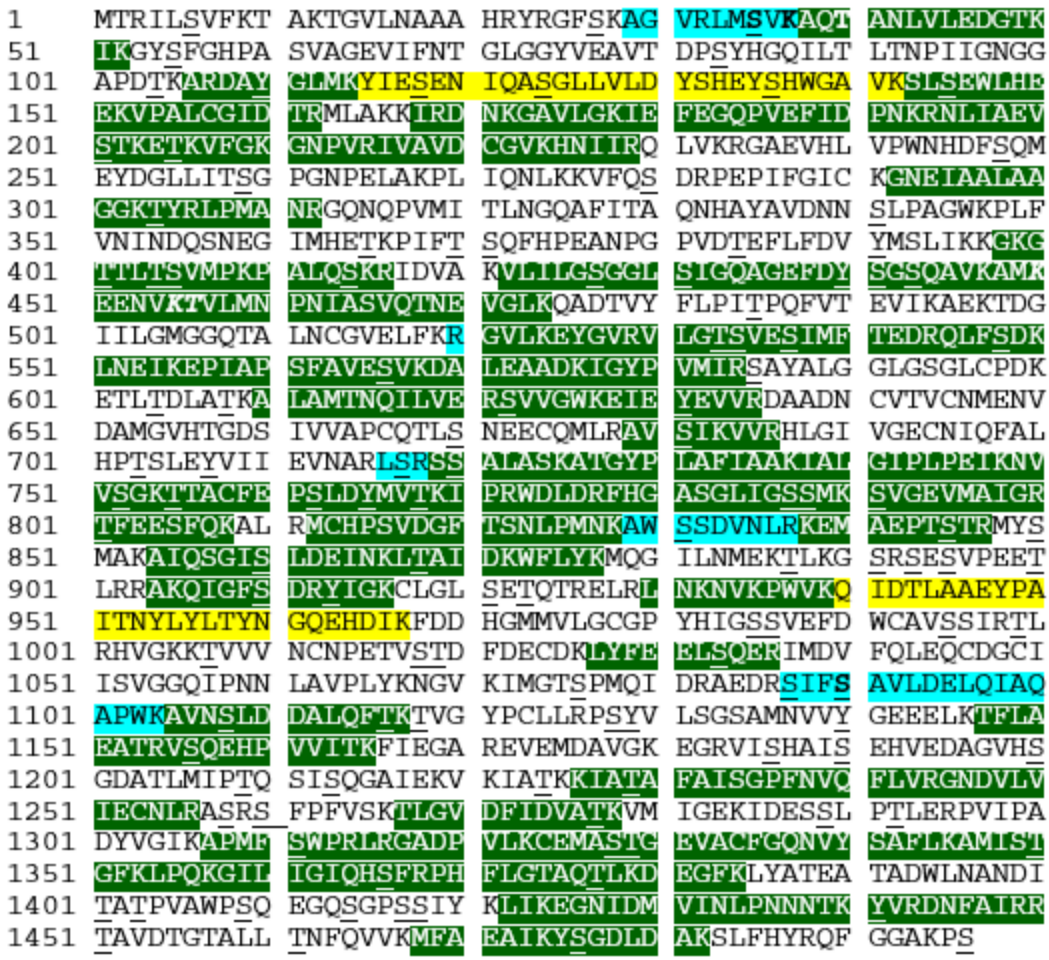

Fig. A.1.2. CPS1 sequence from *Rana catesbeiana* compared to peptides matched using mass spectrometry from trypsin digest of wood frog CPS1. Highlighted sequences represent peptides as follows: found in control and frozen, found in control only, found in frozen only. Residues in bold font were found to be modified to varying degrees in frozen. Italic letters indicate that the residue was found to be modified in control. Bold or italics for S, T, Y amino acids indicate phosphorylation but for K this indicates acetylation. Underlined amino acids were predicted to have phosphorylation by NetPhos 3.1 (score higher than threshold of 0.5).

Appendix II

Supplementary Enzymatic Assay Information

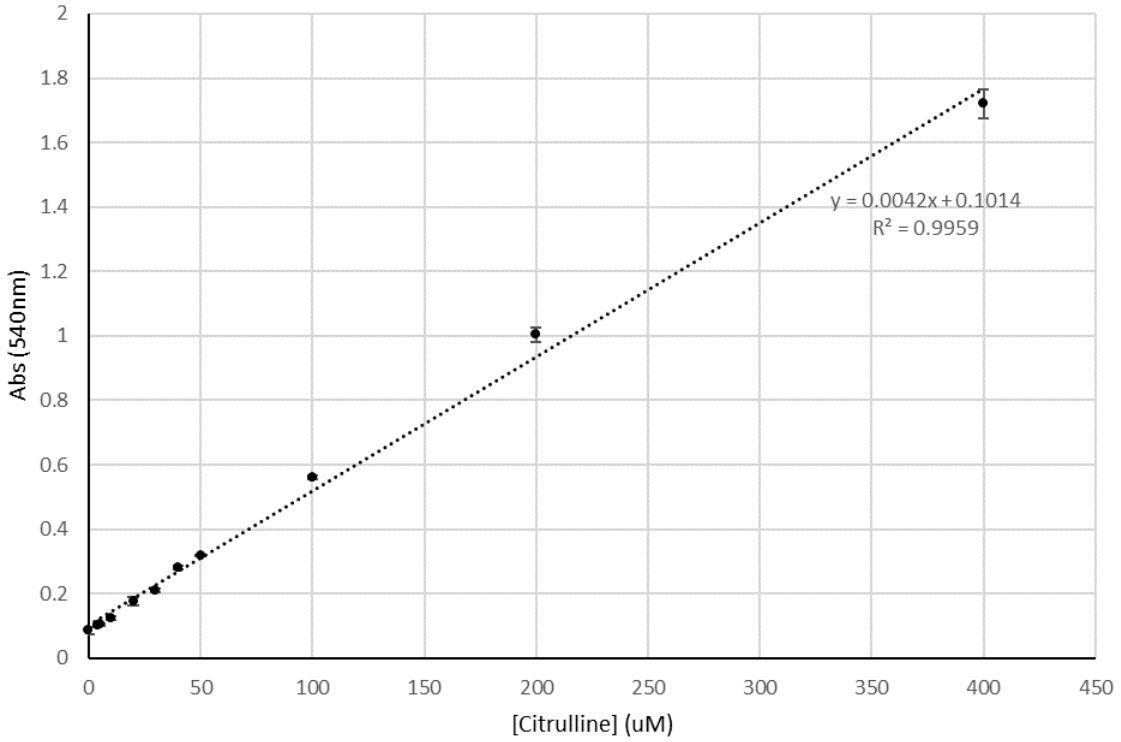

Fig. A.2.1. Standard curve relating citrulline concentration to absorbance at 540 nm. This was used to determine OTC activities in *Rana sylvatica* liver.

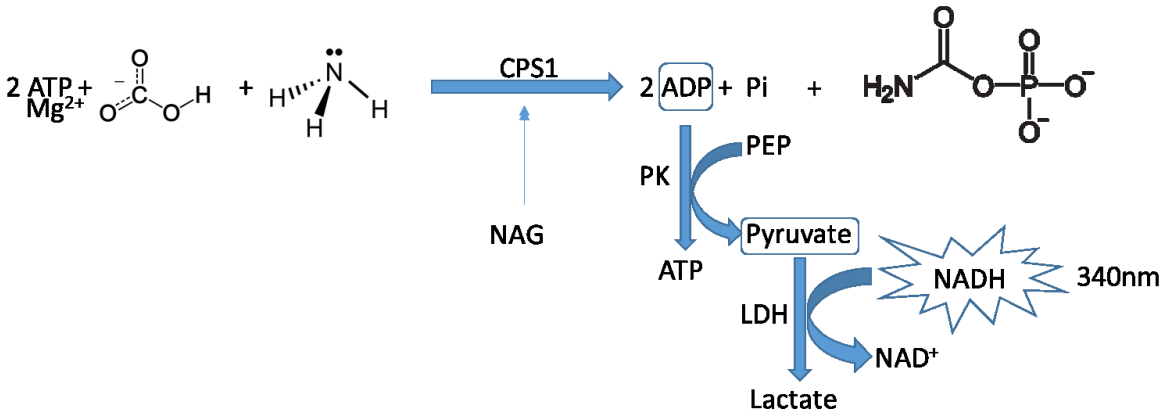

Fig. A.2.2. Visual depiction of the assay used to determine CPS1 activity from *Rana sylvatica* liver samples. NAG (N-acetylglutamate), CPS1 (carbamoyl phosphate synthetase 1), PEP (phosphoenolpyruvate), LDH (lactic acid dehydrogenase), NADH (nicotinamide adenine dinucleotide reduced).